DISCLAIMER NOTICE

THIS DOCUMENT IS BEST QUALITY PRACTICABLE. THE COPY FURNISHED TO DTIC CONTAINED A SIGNIFICANT NUMBER OF PAGES WHICH DO NOT REPRODUCE LEGIBLY.

AFCRL-71-0213

DEFINITION OF TETHERED BALLOON SYSTEMS

Philip F. Myers
Jerome J. Vojtech

Goodyear Aerospace Corporation
Akron, Ohio 44315

Contract No. F 19628-71-C-0091

Project No. 7659

Task No. 765906

Work Unit No. 76590601

Scientific Report No. 1

31 March 1971

Contract Monitors: Edward F. Young, Major, USAF and
Don E. Jackson, Captain, USAF
Aerospace Instrumentation Laboratory

Prepared
for

AIR FORCE CAMBRIDGE RESEARCH LABORATORIES
AIR FORCE SYSTEMS COMMAND
UNITED STATES AIR FORCE
BEDFORD, MASSACHUSETTS 01730

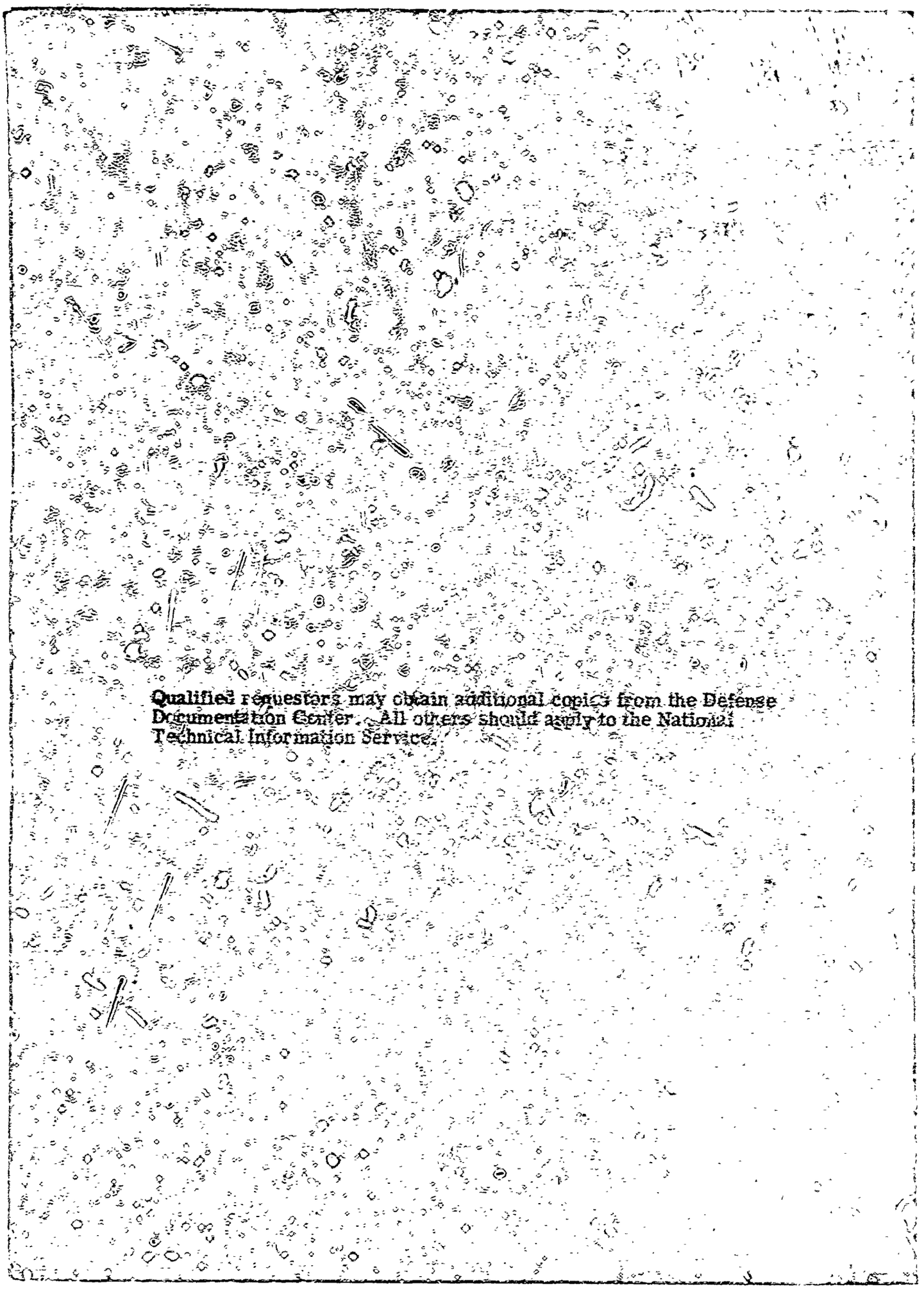

Unclassified
Security Classification

DOCUMENT CONTROL DATA - R & D

Security classification of title, body of abstract and indexing annotation must be entered when the overall report is classified)

1 ORIGINATING ACTIVITY (Corporate author) Goodyear Aerospace Corporation Akron, Ohio, 44315	2a. REPORT SECURITY CLASSIFICATION Unclassified 2b. GROUP

3 REPORT TITLE

DEFINITION OF TETHERED BALLOON SYSTEMS

4 DESCRIPTIVE NOTES (Type of report and inclusive dates)
Scientific - Interim

5 AUTHOR(S) (First name, middle initial, last name)
Philip F. Myers
Jerome J. Vorachek

6 REPORT DATE	7a. TOTAL NO. OF PAGES	7b. NO. OF REFS
31 March 1971		22

8a. CONTRACT OR GRANT NO	9a. ORIGINATOR'S REPORT NUMBER(S)
F19628-71-C-0091	GER-15246
b. PROJECT NO Task, Work Unit Nos. 7659-06-01	Scientific Report No. 1
c DoD Element: 62101F	9b. OTHER REPORT NO(S) (Any other numbers that may be assigned this report) AFCRL-71-0213
d DoD Subelement: 687659	

10 DISTRIBUTION STATEMENT

This document has been approved for public release and sale, its distribution is unlimited.

11 SUPPLEMENTARY NOTES	12 SPONSORING MILITARY ACTIVITY
TECH, OTHER	Air Force Cambridge Research Laboratories (LC) L. G. Hanscom Field Bedford, Massachusetts 01730

13 ABSTRACT

An analytical investigation of the behavior of tethered balloons is in progress. This report, the first of three scientific reports, covers balloon system definition for three design altitudes, 5,000, 10,000, and 20,000 feet above sea level.

Three balloon shapes being considered are the Vee-Balloon, the Bateman and Jones (BJ) barrage balloon, and Goodyear Aerospace Corporation Model No. 1649 single-hull balloon. Tether constructions are Columbian Rope Company's NOLARO utilizing prestretched polyester filaments, and US Steel Corporation's Amgal-Monitor AA wire ropes.

Eight specific balloon/cable combinations are defined, covering the three design altitudes. Total cable curve, downwind displacement, etc., have been calculated by computer program and results are tabulated.

Each balloon type is sized twice at 10,000 feet; one for a NOLARO tethering, and the other for the Amgal-Monitor wire rope.

The BJ shape only is sized for the 5,000 and 20,000 foot design altitudes, and with NOLARO tether.

Aerodynamic characteristics, weight, inertias, and dynamic characteristics are developed and tabulated for use in the following phases of this program. The Characteristic Equation Stability Analyses and Dynamic Simulation Analyses will be based on the information and data of this report.

DD FORM 1 NOV 65 1473

Unclassified
Security Classification

Unclassified

Security Classification

14. KEY WORDS	LINK A		LINK B		LINK C	
	ROLE	WT	ROLE	WT	ROLE	WT
Aerostats						
Balloons						
Balloon Aerodynamics						
Balloon Dynamics						
Balloon Behavior						
Balloon Flying Qualities						
Balloon Mass Characteristics						
Balloon Stability						
Balloon Systems						
Cables						
Cable Dynamics						
Captive Balloons						
Dynamic Simulation Analysis						
Kite Balloons						
Stability Analysis						
Tethered Balloons						
Tethered LTA Vehicles						
Tethers						

Security Classification

AFCRL-71-0213

DEFINITION OF TETHERED BALLOON SYSTEMS

Philip F. Myers
Jerome J. Vorachek

Goodyear Aerospace Corporation
Akron, Ohio 44315

Contract No. F 19628-71-C-0091

Project No. 7659
Task No. 765906
Work Unit No. 76590601

Scientific Report No. 1

31 March 1971

Contract Monitors: Edward F. Young, Major, USAF and
Don E. Jackson, Captain, USAF
Aerospace Instrumentation Laboratory

Prepared
for

AIR FORCE CAMBRIDGE RESEARCH LABORATORIES
AIR FORCE SYSTEMS COMMAND
UNITED STATES AIR FORCE
BEDFORD, MASSACHUSETTS 01730

ABSTRACT

An analytical investigation of the behavior of tethered balloons is in progress. This report, the first of three scientific reports, covers balloon system definition for three design altitudes, 5,000, 10,000, and 20,000 feet above sea level.

Three balloon shapes being considered are the Vee-Balloon*, the Bateman and Jones (BJ) barrage balloon, and Goodyear Aerospace Corporation (GAC) Model No. 1649 single-hull balloon. Tether constructions are Columbian Rope Company's NOLARO utilizing prestretched polyester filaments, and US Steel Corporation's Amgal-Monitor AA wire ropes.

Eight specific balloon/cable combinations are defined, covering the three design altitudes. Total cable curve, downwind displacement, etc., have been calculated by computer program and results are tabulated.

Each balloon type is sized twice at 10,000 feet, one for a NOLARO tethering, and the other for the Amgal-Monitor wire rope.

The BJ shape only is sized for the 5,000 and 20,000 foot design altitudes, and with NOLARO tether.

Aerodynamic characteristics, weight, inertias, and dynamic characteristics are developed and tabulated for use in the following phases of this program. The Characteristic Equation Stability Analyses and Dynamic Simulation Analyses will be based on the information and data of this report.

*T.M., Goodyear Aerospace Corporation, Akron Ohio 44315

FOREWORD

This research was supported by the Air Force Systems Command, USAF, DOD and was under the technical cognizance of the Air Force Cambridge Research Laboratories under Contract No. F 19628-71-C-0091.

The project is being carried out under the direction of Major Edward Young and Captain Don Jackson as Contract Monitors for the Air Force Cambridge Research Laboratories. Mr. Jerome Vorachek is the Goodyear Aerospace Corporation Project Engineer. Technical assistance was provided by Mr. Philip Myers, Mr. Walt Stricker, Mr. Nicholas Costakos, Mr. William Ebert, Mr. George Doyle and Mr. Louis Handler.

The contractor's number for this report is GER-15246.

TABLE OF CONTENTS

LIST OF ILLUSTRATIONS

LIST OF TABLES

LIST OF SYMBOLS

b	Empennage span
b	Difference in weight densities of air and inflation gas (= 0.862 ρ_{air} g) lb/ft^3
B.S.	Breaking strength, lb
CA	Center of additional mass
CG	Center of gravity
C_D	Aerodynamic drag coefficient
C_L	Aerodynamic lift coefficient
C_m	Aerodynamic pitching moment coefficient
C_n	Aerodynamic yawing moment coefficient
C_Y	Aerodynamic side force coefficient
D	Aerodynamic drag, lb
D	Diameter, ft or in.
DC	Dynamic center
D_B	Aerodynamic drag of balloon, lb
D_N	Net drag, horizontal component of tension at the top end of the cable, lb
d	Downwind displacement or horizontal distance from the top end of cable to bottom end measured parallel to earth plane, ft.
F_x	Horizontal force, lb
F_y	Side force, lb
F_z	Vertical force, lb
f	Fineness ratio or ratio of length to max. diameter
fps	Feet/second
G	Specific gravity
g	Acceleration of gravity (32.2 ft/sec.^{2})
h	Float Altitude above mean sea level, ft.

LIST OF SYMBOLS (Continued)

IAS	Indicated air speed, knots
I_x	Mass moment of inertia in roll, slug ft^2
I_y	Mass moment of inertia in pitch, slug ft^2
I_z	Mass moment of inertia in yaw, slug ft^2
k	Various coefficients
L	Hull length
L'	Vee balloon hull length along ℄ of symmetry
L_a	Aerodynamic lift, lb
L_N	Net lift of balloon or vertical component of tension at the top end of the cable, lb
L_S	Net static lift (gross static lift - W_B - P), lb
M	Pitching moment, ft lb
M_x	Rolling moment about the X axis at zero angle of attack
MC	Mass center
MSL	Mean sea level
N	Yawing moment, ft lb
P	Payload weight, lb
p	Rolling velocity
q	Dynamic Pressure (= 1/2 ρ_{alt} v^2) lb/ft^2
r	Yawing velocity
S	Empennage area, ft^2
SL	Sea level
T	Tether tension, lb
t	Time at float altitude, hr
u	Horizontal velocity increment, fps
V	Balloon hull volume, ft^3

LIST OF SYMBOLS (Continued)

V	Wind velocity, fps
V_k	Wind velocity, knots
v	Sideslip velocity
W_B	Total balloon and suspension weight, lb
W_C	Total weight of cable segment, lb
w	Unit weight of balloon fabric, lb/ft^2
w	Vertical velocity of balloon during transient motion
x	Downwind displacement, ft (on computer printout)
Y	Side force
z	Distance vertically down from design altitude, ft.
α	Angle of attack, degrees
β	Angle of sideslip, degrees
θ	Angle between the cable and the vertical, degrees (PHI in computer printout)
ρ	Density of air, $slugs/ft^3$

Note: A variety of symbols are defined and used in Setion IV and Appendices I and II which are not necessarily listed in the tabulation above.

SECTION I

INTRODUCTION

The objective of this program is to investigate the dynamic behavior of tethered balloons and in so doing to establish design criteria for tethered balloons, tethers and payloads. The program is organized into three steps.

(1) Definition of balloon systems for dynamic analysis
(2) A study of stability characteristics of tethered balloon systems
(3) A study of dynamic response of tethered balloon systems to wind gusts.

This first scientific report presents a definition of tethered balloon systems to be investigated in subsequent dynamic studies.

For design purposes in the subject investigation the following design parameters were specified in Reference 1:

Payload and Design Altitude

Payload (lb) P	Float Altitude (ft above MSL) h
1500	5,000
1000	10,000
600	20,000

Tethers

Two specific tether constructions are to be considered, NOLARO by Columbian Rope Company, and Amgal-Monitor AA wire rope by United States Steel. A safety factor of 2.0 will be used with NOLARO; 1.5 for Amgal-Monitor. Tether design load will be based on a survival wind of 1.3 times the operational wind at balloon altitude.

Wind Profile

The wind profile as specified by Reference 1 is shown in Figure 1 and tabulated below:

Altitude (ft above MSL)	Operational Wind Speed (knots)	Survival Wind Speed (knots)
Sea Level	10	13.
5,000	31	40.3
10,000	40	52.
20,000	54	70.2

This profile of operational wind is closely approximated by the relation:

$$V_{knots} = 0.8794\ (\text{altitude} + 350)^{0.415}$$

The 1962 U. S. Standard Atmosphere is used as the source for atmospheric data (see Table I).

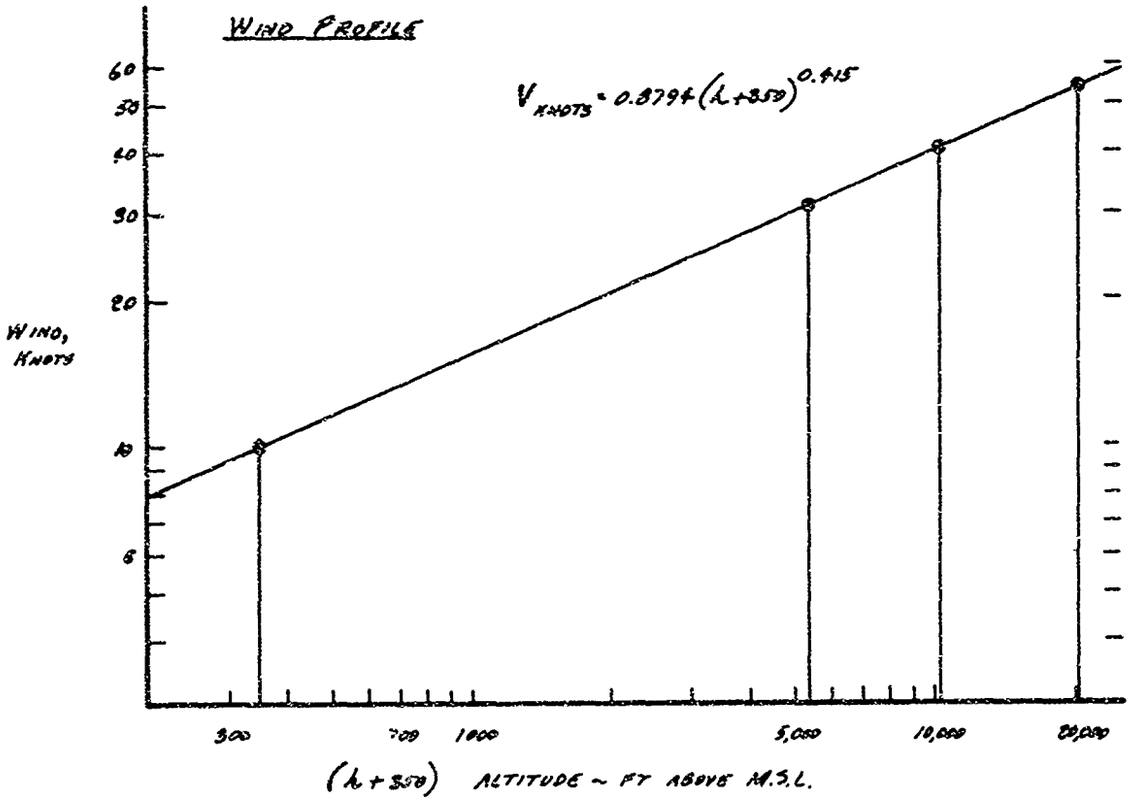

Figure 1. Wind Profile

Table I. Standard Altitude and Unit Helium Lift

Altitude (Ft.)	Density (Slug/ft^3)	Density Ratio (Alt./Zero Alt.)	Pressure (Lb/ft^2)	Buoyancy Given For Different Purities of Helium	
				100% (Lb/ft^3)	97% (Lb/ft^3)
0.	0.0023769	1.0000000	2116.2170410	0.0659	0.0639
1000.	0.0023081	0.9710660	2040.8571777	0.0640	0.0621
2000.	0.0022409	0.9427790	1967.6914062	0.0621	0.0603
3000.	0.0021751	0.9151295	1896.6716309	0.0603	0.0585
4000.	0.0021109	0.8881069	1827.7478027	0.0585	0.0568
5000.	0.0020482	0.8617023	1760.8730469	0.0568	0.0551
6000.	0.0019868	0.8359040	1695.9997559	0.0551	0.0534
7000.	0.0019269	0.8107038	1633.0812988	0.0534	0.0518
8000.	0.0018684	0.7860914	1572.0712891	0.0518	0.0503
9000.	0.0018113	0.7620566	1512.9265137	0.0502	0.0487
10000.	0.0017555	0.7385901	1455.6020508	0.0487	0.0472
11000.	0.0017011	0.7156832	1400.0544434	0.0472	0.0458
12000.	0.0016479	0.6933257	1346.2407227	0.0457	0.0443
13000.	0.0015961	0.6715091	1294.1193848	0.0443	0.0429
14000.	0.0015455	0.6502230	1243.6489258	0.0429	0.0416
15000.	0.0014961	0.6294589	1194.7880859	0.0415	0.0402
16000.	0.0014480	0.6092079	1147.4982910	0.0402	0.0389
17000.	0.0014011	0.5894610	1101.7407227	0.0388	0.0377
18000.	0.0013553	0.5702096	1057.4758301	0.0376	0.0365
19000.	0.0013107	0.5514442	1014.6652832	0.0363	0.0353
20000.	0.0012672	0.5331573	973.2741699	0.0351	0.0341

SECTION II

BALLOON TYPES AND CHARACTERISTICS

1. BALLOONS SELECTED FOR STUDY

For this study of dynamic behavior of tethered balloon, four aerodynamically shaped balloons were investigated. The balloons investigated were Vee-Balloon, a GAC model single hull (No. 1649) with "thin" or "thick" fins, and the BJ British barrage balloon. These shapes were selected for investigation because a wide range of physical and functional characteristics such as aerodynamic lift, drag, fineness ratio, volume per surface area, fin size, etc., is encompassed. In addition, wind tunnel test data is available for all of the balloons and full-scale vehicles of each except the GAC No. 1649 balloon have been flown. Realistic size and weight scale factors can therefore be obtained for analyzing balloons designed for many wind velocities and altitudes.

2. BALLOON DESCRIPTION

a. General

A ballonet system for accommodating volume change and maintaining pressure for all aerodynamically-shaped balloons was assumed. A blower and battery type were assumed for all ballonet systems except the BJ. For this type, it was assumed that dynamic pressure alone, such as in the barrage balloons, was sufficient to retain pressurization.

In order to give relative size of each balloon with respect to a different shape of comparable volume, Table II lists the basic dimensions and areas for the various shapes, each with a hull volume of 100,000 cubic feet.

b. Vee-Balloon Configuration

The Vee-Balloon (Figure 2) was chosen because it represents the high aerodynamic lift-type tethered balloon. The configuration consists of two streamlined hulls joined at the nose to form a "V". A horizontal tail is connected between the hulls with the two vertical fins mounted on the aft end of each hull. The balloon exhibits one of the highest aerodynamic lift coefficients and the highest drag coefficient of any of the aerodynamically-shaped balloons selected for the evaluation. The empennage is helium-inflated.

c. BJ (Bateman and Jones)

The BJ configuration (Figure 3) was chosen because it represents a typical single-hull, streamlined shape, tethered balloon. The basic shape

Table II. Physical Dimensions of Various Balloon Configurations for Hull Volumes of 100,000 Cubic Feet

Balloon Type	Reference Hull Volume (ft^3)	Hull Length (ft)	Max. Dia. (ft)	Wetted Area (ft^2)	Fineness Ratio	No. of Horizontal Fins	Each Horizontal Fin			No. of Vertical Fins	Each Vertical Fin			Total Wetted Area (ft^2)	Total Volume (ft^3)
							Projected Area (ft^2)	Wetted Area (ft^2)	Volume (ft^3)		Projected Area (ft^2)	Wetted Area (ft^2)	Volume (ft^3)		
Vee-Balloon	100,000	118.8 (113.30)	29.7	15,016	4.0	1	1523	3366	6242	2	169	392	231	19,166	106,704
BJ	100,000	109.1	43.8	11,660	2.5	2	496	1155	4125	1	776	1807	8078	15,777	116,329
No. 1649 with Thin Fins	100,000	123.9	41.3	12,485	3.0	2	797	1722	3669	1	797	1722	3669	17,651	111,006
No. 1649 with Thick Fins	100,000	123.9	41.3	12,485	3.0	2	797	1945	9723	1	797	1945	9723	18,320	129,168

(113.30) = L' = L (cos 17-1/2°) where hull included angle of intersection is 35°

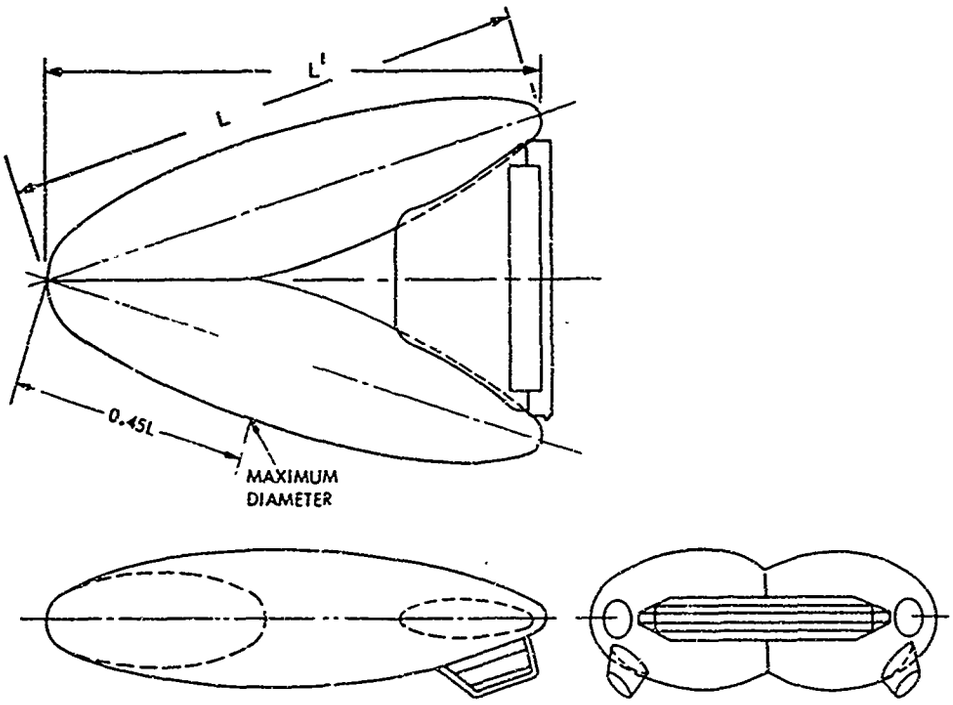

Figure 2 . Vee-Balloon Configuration

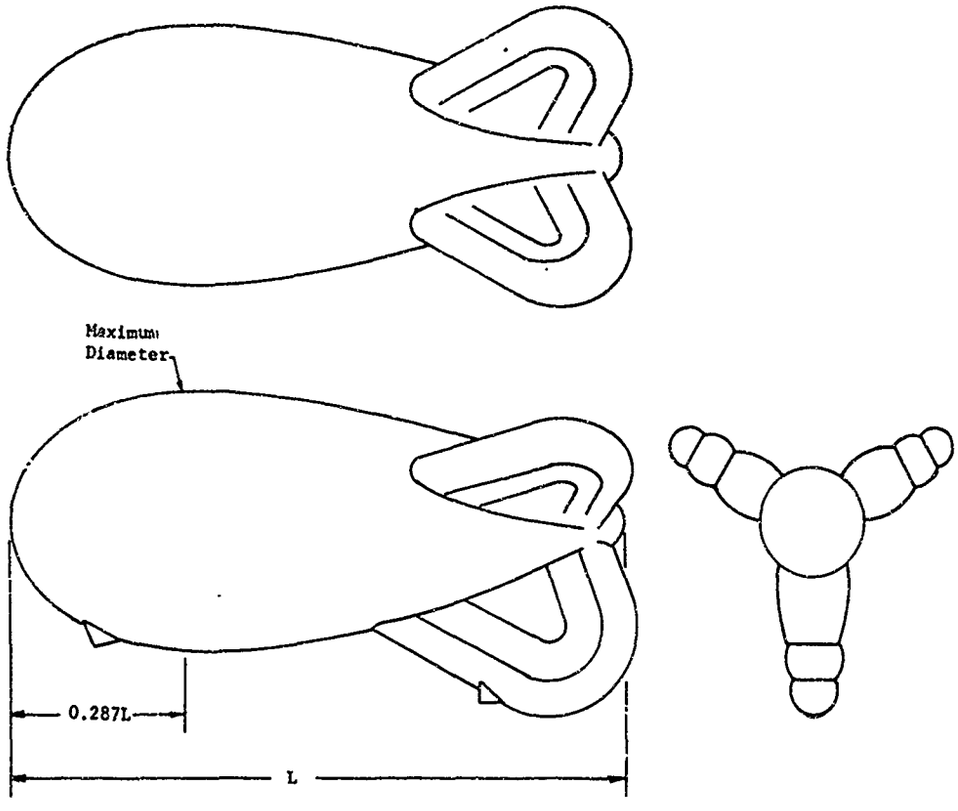

Figure 3. BJ Configuration

consists of a streamlined hull with a Y-type tail. The balloon exhibits the lowest aerodynamic lift coefficient and almost the lowest drag coefficient of any of the aerodynamically-shaped balloons selected for evaluation.

d. GAC No. 1649 Balloon With Thin Fins

This body (Figure 4) represents an appreciable aerodynamic improvement over the BJ or the frequently used Class "C" shape. Its aerodynamic L/D ratio is best of those considered.

e. GAC No. 1649 Balloon With Thick Fins

This is the same body-of-revolution as in (d) above, but fitted with much thicker empennage and has aerodynamic performance comparable to the BJ balloon. This body will not be carried on in the dynamic study.

3. AERODYNAMIC CHARACTERISTICS

Aerodynamic lift coefficients, drag coefficients, and lift-to-drag ratio versus angle of attack for the aerodynamically-shaped balloons are given in Figures 5 through 7. The hull volume to the two-thirds power is used as a reference area. Aerodynamic side force, yawing moment and pitching moment coefficients are given in Figures 8 through 18.

Aerodynamic data was taken from References 2 through 9.

The aerodynamic coefficients are defined as follows:

Lift Coefficient, $C_L = \frac{L_a}{q \forall^{2/3}}$

Drag Coefficient, $C_D = \frac{D_a}{q \forall^{2/3}}$

Side Force Coefficient, $C_Y = \frac{F_Y}{q \forall^{2/3}}$

Pitching Moment Coefficient, $C_m = \frac{M}{q \forall}$

Yawing Moment Coefficient, $C_n = \frac{N}{q \forall}$

where $\forall$ is the hull volume for the single hull balloons and the volume of the two hulls for the Vee-Balloon.

The axis for measurement of moments is located along the longitudinal axis measured from the nose of the balloon. For the Vee-balloon the fractional

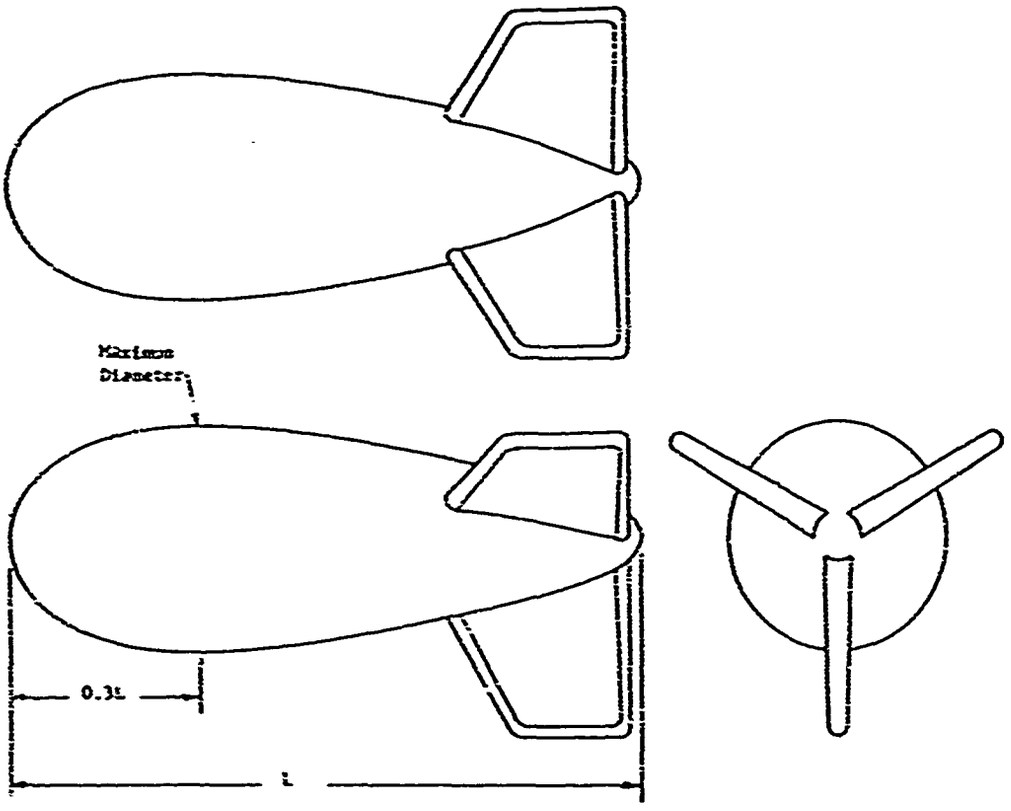

Figure 4. GAC No. 1649 Balloon Configuration

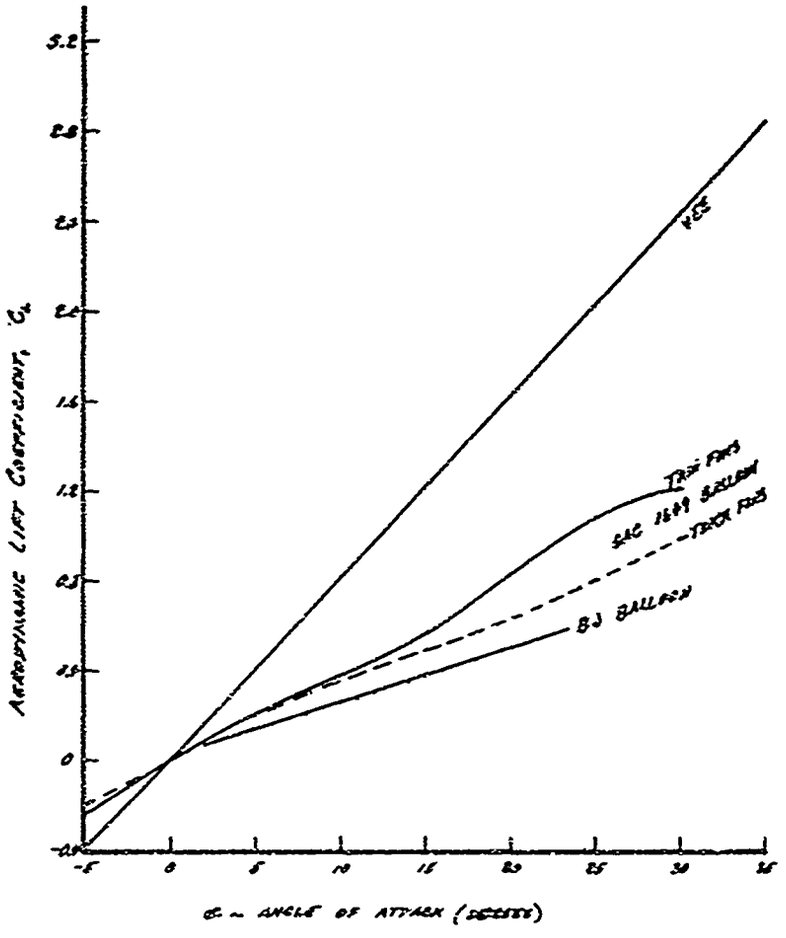

Figure 5. Aerodynamic Lift Coefficient for Various Balloon Configurations

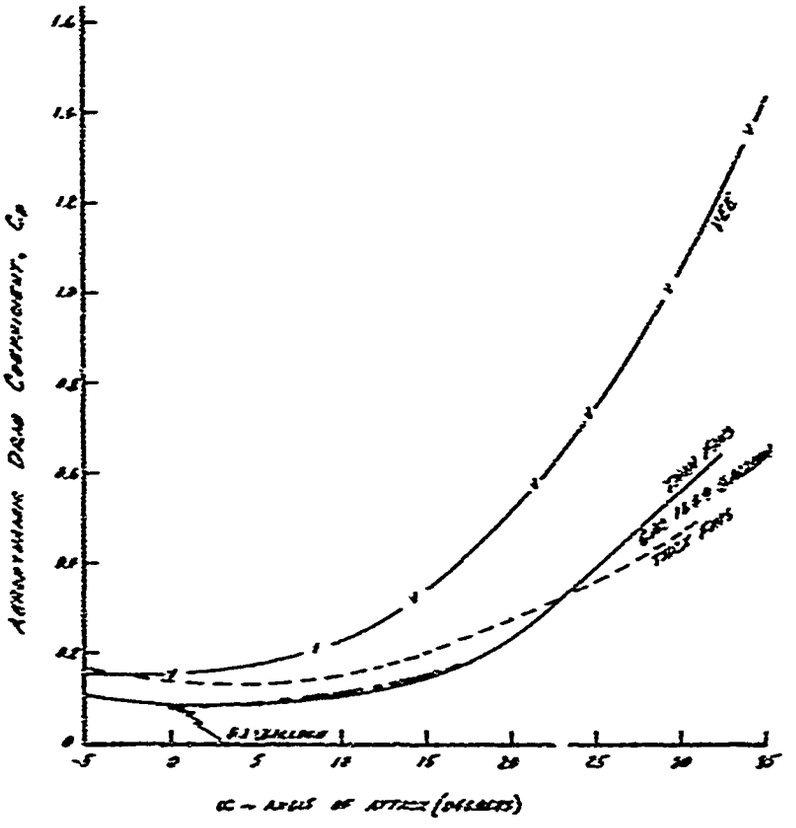

Figure 6. Aerodynamic Drag Coefficient for Various Balloon Configurations

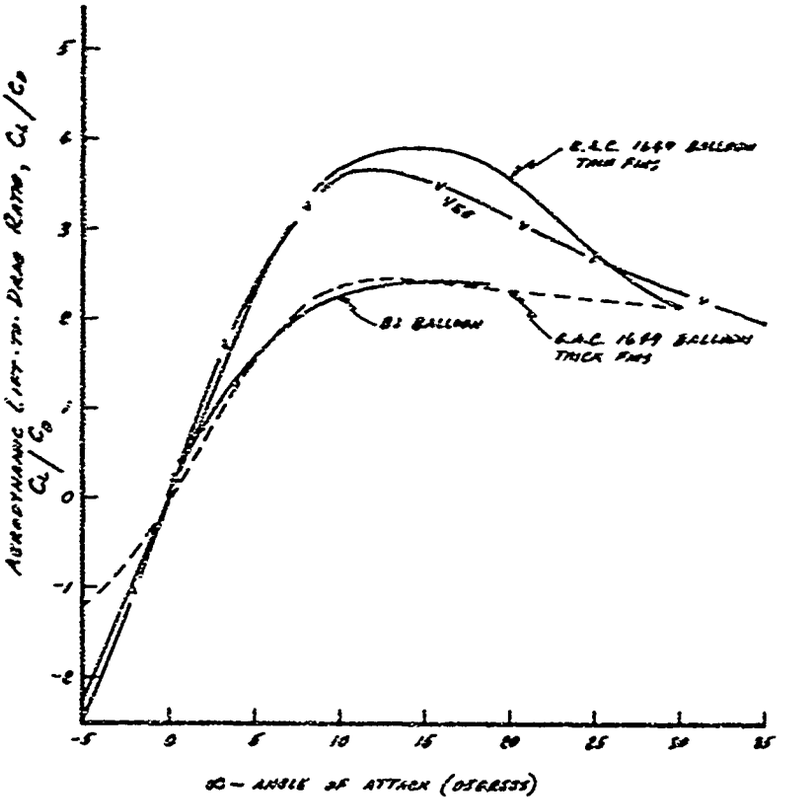

Figure 7. Aerodynamic Lift-Drag Ratio for Various Balloon Configurations

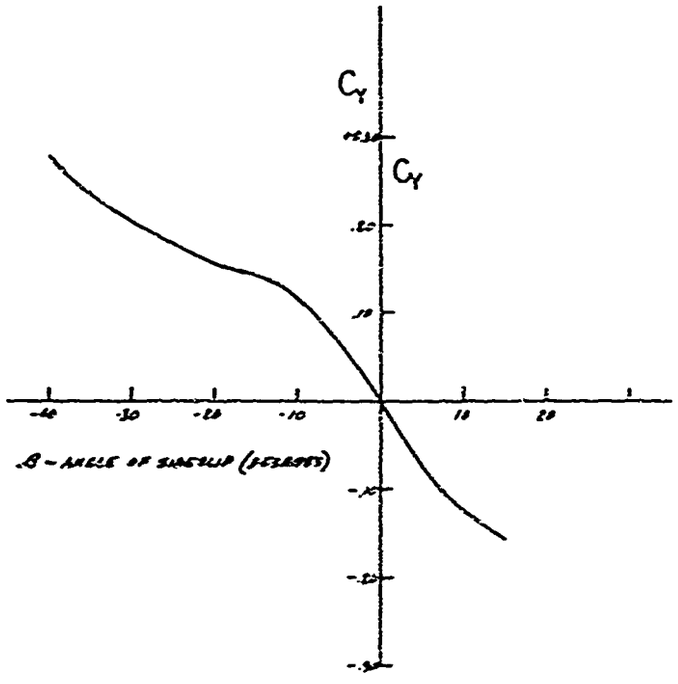

Figure 8. Aerodynamic Side Force Coefficient, Vee-Balloon

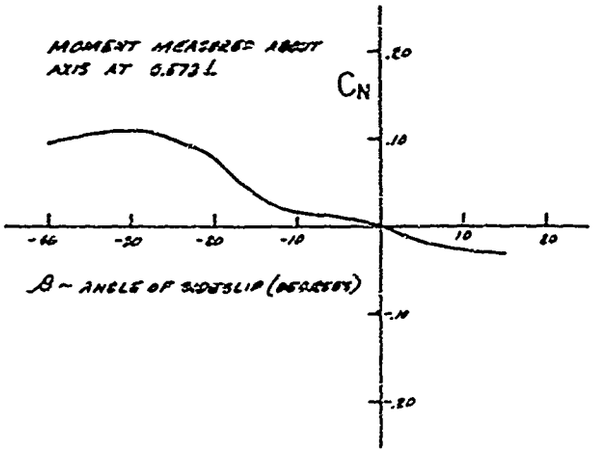

Figure 9. Aerodynamic Yawing Moment Coefficient, Vee-Balloon

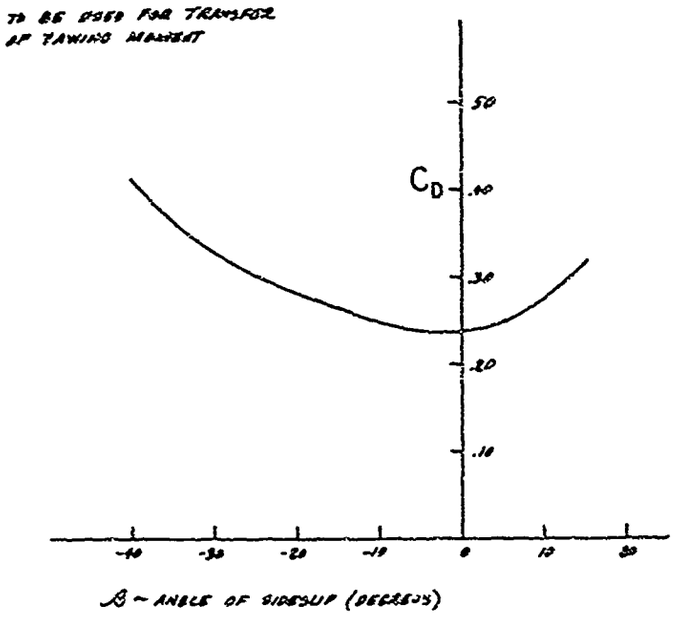

Figure 10. Aerodynamic Drag Coefficient as a Function of Sideslip Angle - Vee-Balloon

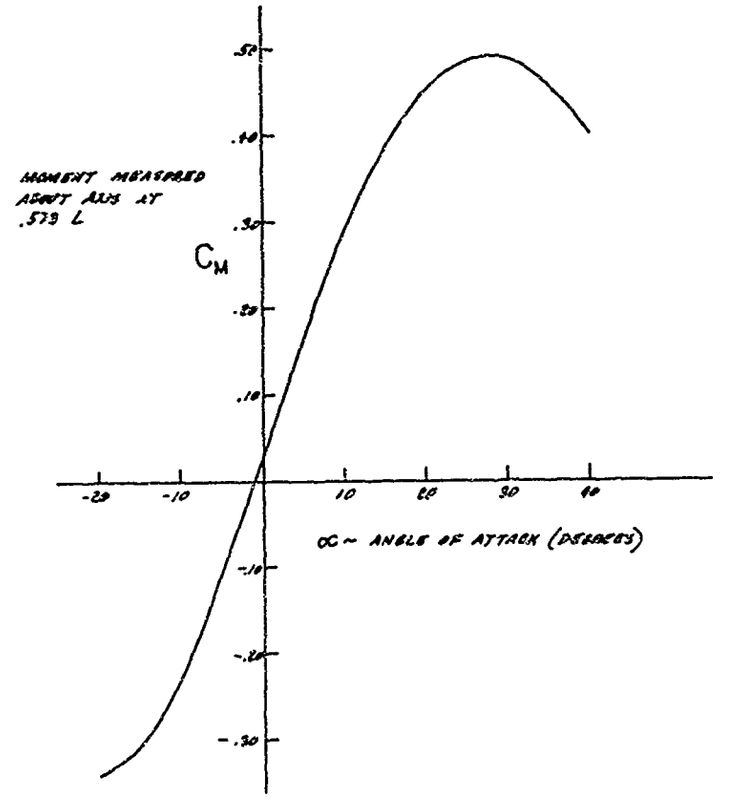

Figure 11. Aerodynamic Pitching Moment Coefficient, Vee-Balloon

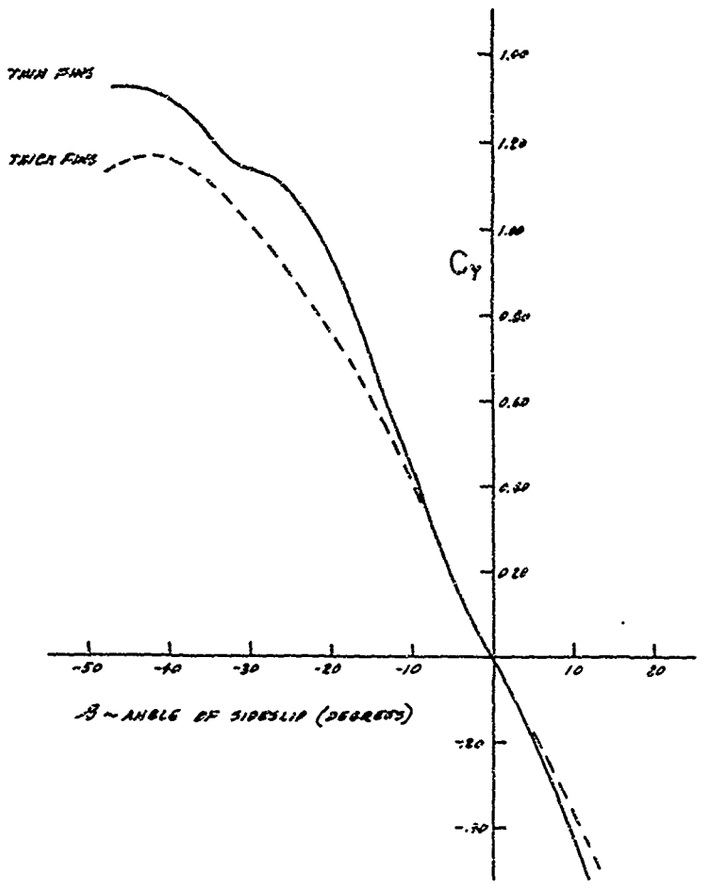

Figure 12. Aerodynamic Side Force Coefficient, GAC No. 1649 Balloon

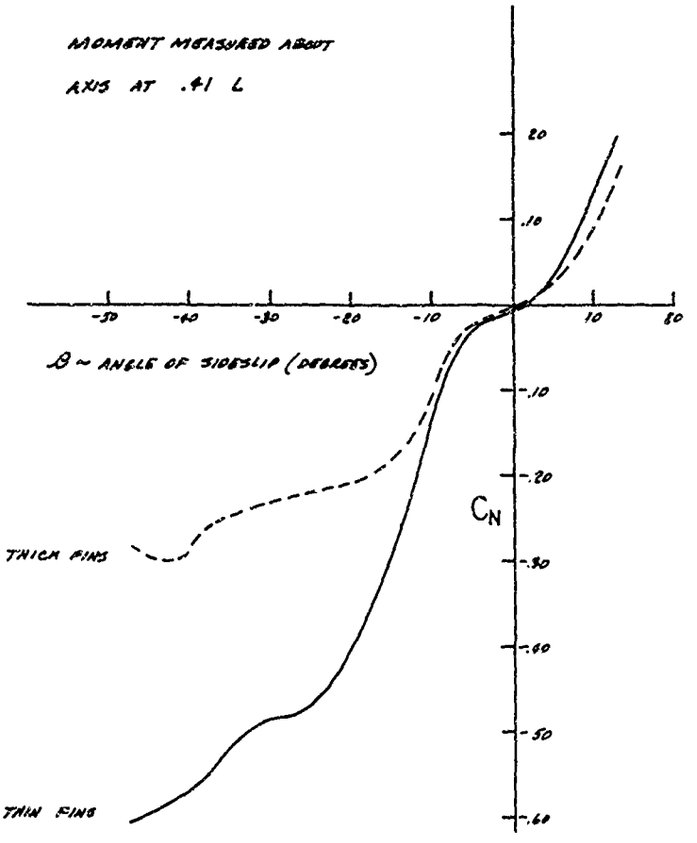

Figure 13. Aerodynamic Yawing Moment Coefficient, GAC No. 1649 Balloon

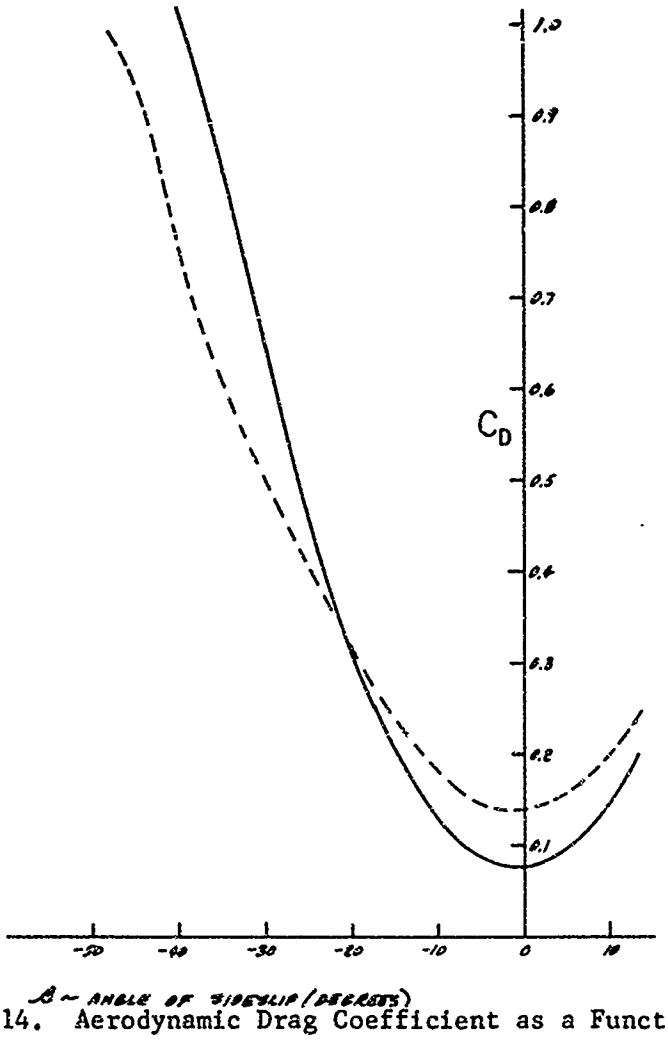

Figure 14. Aerodynamic Drag Coefficient as a Function of Sideslip Angle GAC No. 1649 Balloon

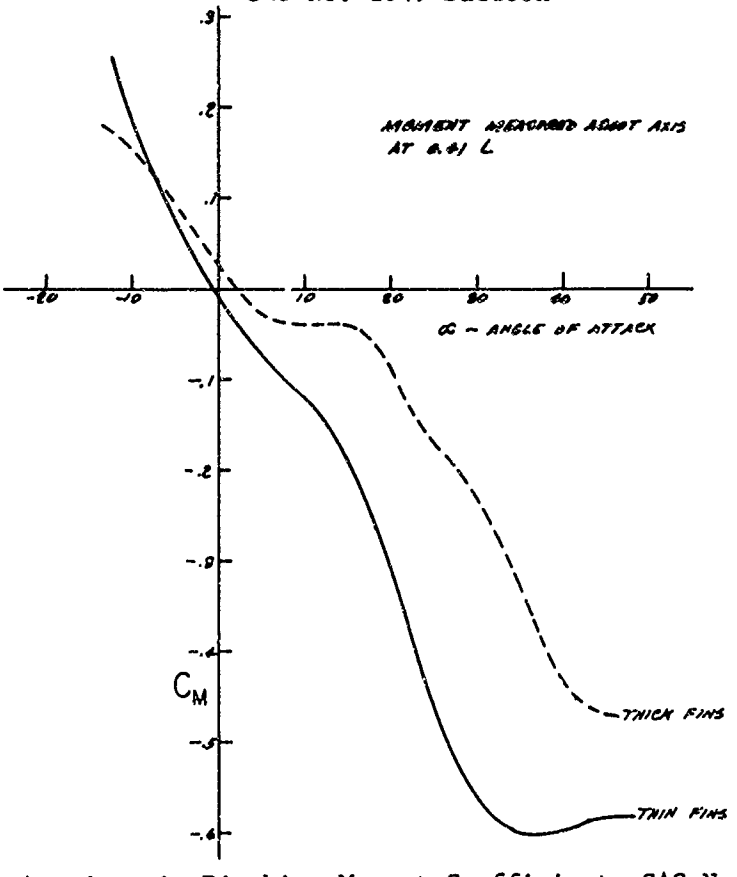

Figure 15. Aerodynamic Pitching Moment Coefficient, GAC No. 1649 Balloon

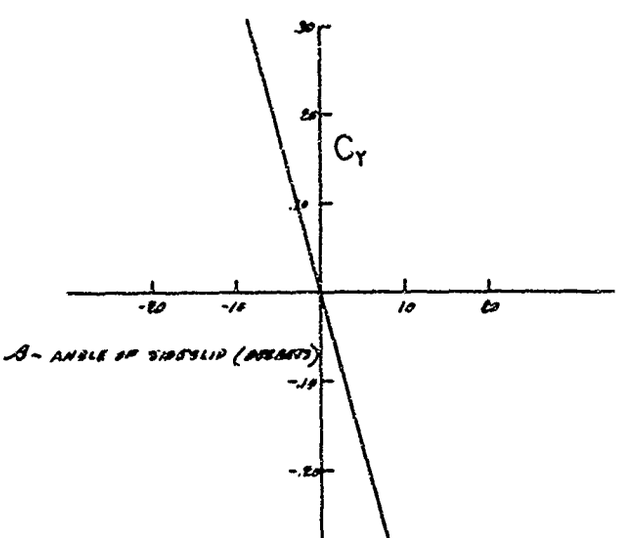

Figure 16. Aerodynamic Side Force Coefficient, BJ Balloon

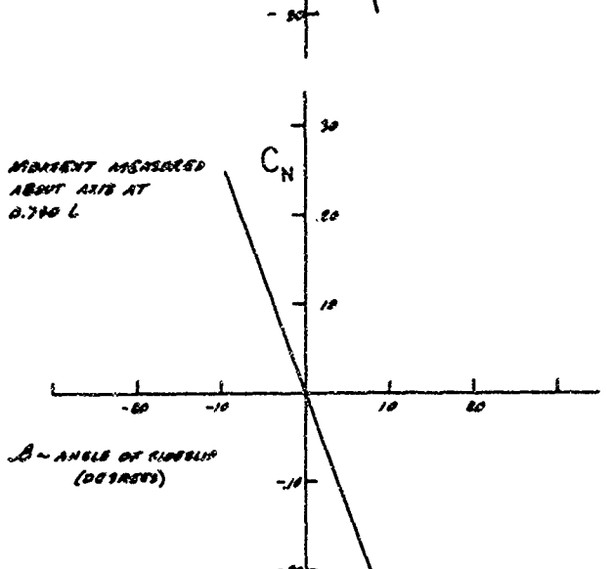

Figure 17. Aerodynamic Yawing Moment Coefficient, BJ Balloon

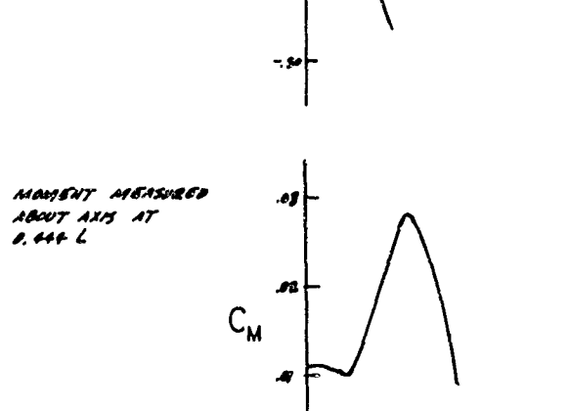

Figure 18. Aerodynamic Pitching Moment Coefficient, BJ Balloon

length from the nose is based on the projected length of the hulls on the longitudinal centerline and is measured from the nose intersection of the two hull centerlines.

The forces and moments measured in the wind tunnel are measured about a fixed axis. During dynamic maneuvers, these moments will act about the dynamic center, so that the test results must be transposed to the new center of moments. Since the dynamic center includes the added mass effects, its location will be slightly different for motions about each axis. The following pages show the method used to transpose these moments.

Figures 19 and 20 present the transfer of pitching moment or yawing moment to the dynamic center.

4. WEIGHT ANALYSIS OF AERODYNAMICALLY SHAPED BALLOONS

a. Stress Considerations

Internal pressure in the balloon at float altitude was based on the following requirements:

(1) The nose of the balloon shall not cup or dimple in the wind at altitude, as this will create a large increase in drag, and cause the balloon to lose its aerodynamic characteristics.

(2) The minimum operating pressure for a reliable pressure relief valve shall have a minimum opening pressure of approximately 1/4 in. H_2O.

Therefore, the required balloon internal pressure was selected to be 1.15 times the stagnation pressure at altitude or 1/4 in. H_2O, whichever is greater. The critical pressure required to prevent buckling of the hull was assumed to be less than that required to prevent dimpling of the nose of the balloon. In most cases, the critical pressure to prevent buckling is less than that required to prevent dimpling. However, in any further detailed design study or prototype development, the validity of this assumption must be verified. The actual stress used in the weight analysis was the sum of the stresses caused by the internal pressure, buoyant lift, aerodynamic load, and hull bending moment.

b. Balloon Material

At the present time, material for fabrication of the balloon was investigated only on a strength-to-unit-weight basis. Figure 21 is a plot of breaking strength versus unit weight for various existing materials that are used for fabrication of balloons. The curve of Figure 21 was used in the weight analysis to determine the hull material weight after the stress (allowing a factor of safety of 4) has been determined. See Table III for fabric code numbering system.

c. Balloon Weight

Once the stress is determined for a particular balloon shape, the weight can be estimated. The product of wetted area and unit weight, where

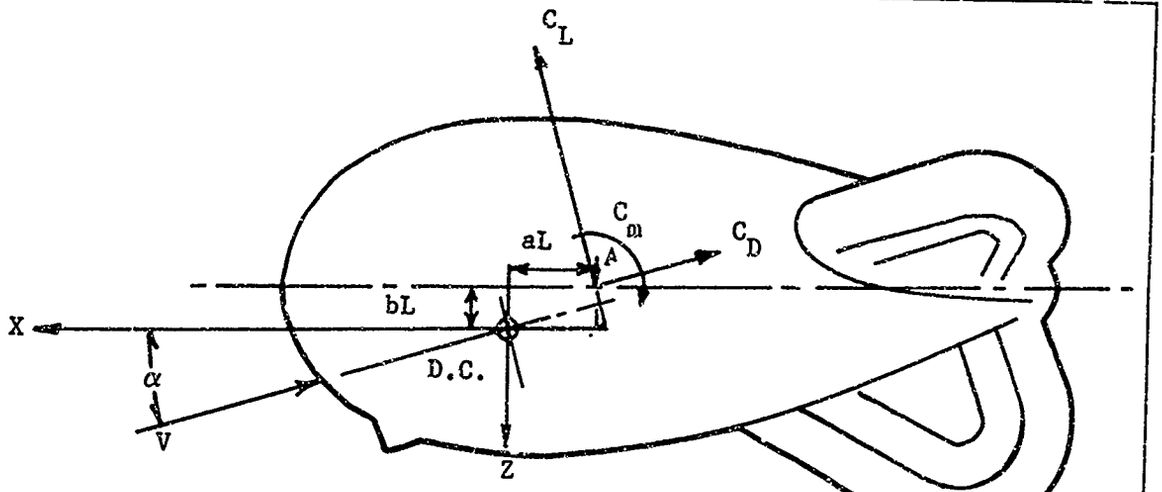

$$C_{m_{D.C.}} = C_{m_A} + C_D \frac{L}{V^{1/3}} (b \cos \alpha - a \sin \alpha)$$

$$- C_L \frac{L}{V^{1/3}} (a \cos \alpha + b \sin \alpha)$$

where a and b are expressed as a percentage of the length L

Figure 19. Transfer of Pitching Moment From Point of Measurement "A" to Dynamic Center

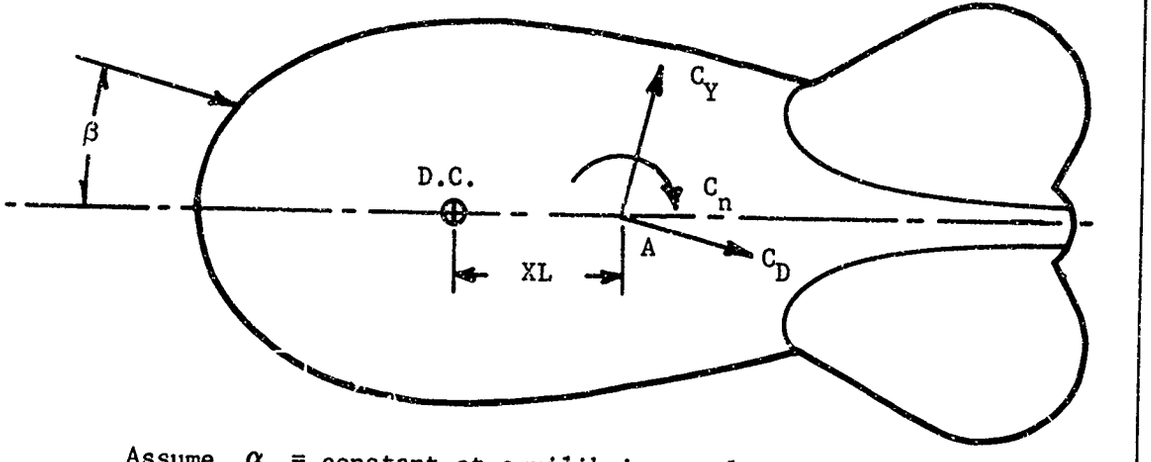

Assume α = constant at equilibrium angle at attachment

$$XL = a\,L \cos \alpha + b\,L \sin \alpha$$

$$C_{n_{D.C.}} = C_{n_A} - C_Y \frac{XL}{V^{1/3}} \cos \beta + C_D \frac{XL}{V^{1/3}} \sin \beta$$

Figure 20. Transfer of Yawing Moment from Point of Measurement "A" to Dynamic Center

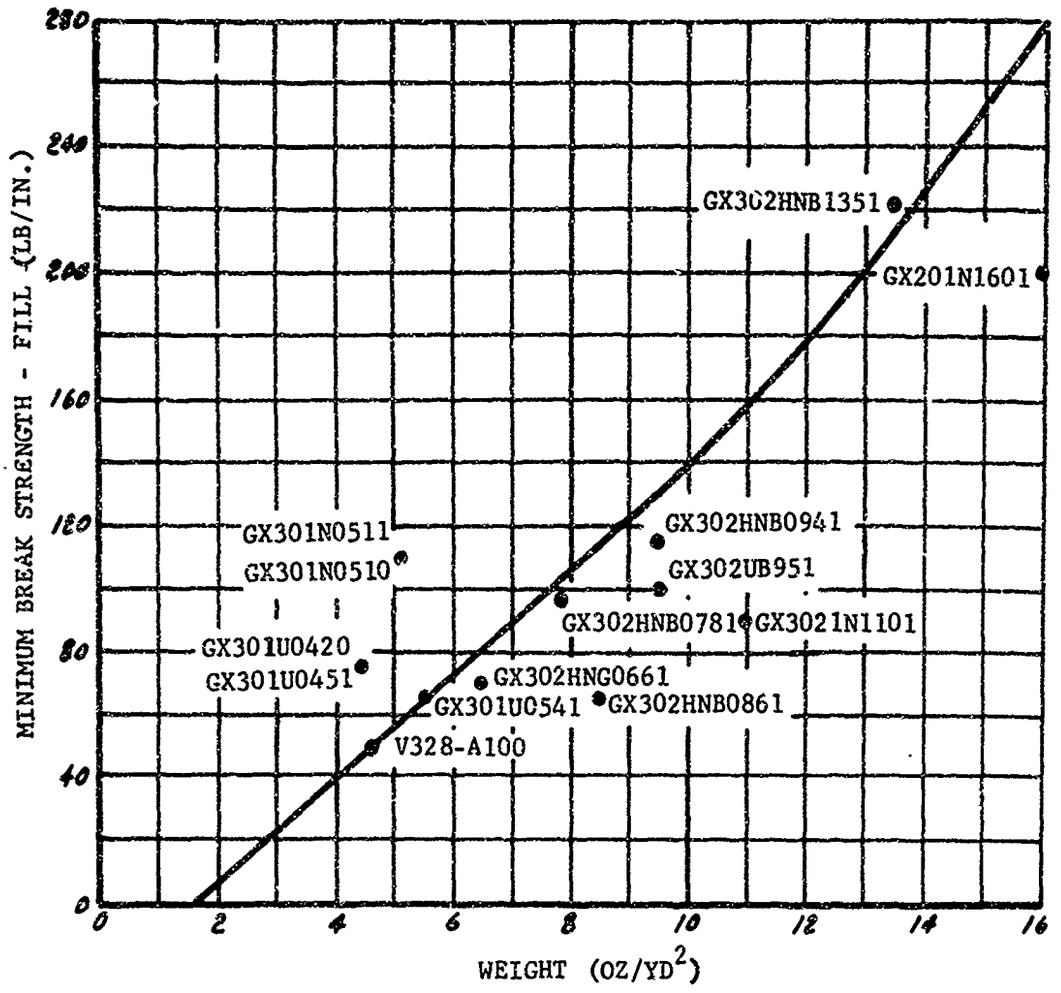

Figure 21. Quick Break Strength vs Unit Weight for Various Balloon Materials

Table III. Goodyear Aerospace Corporation Fabric Code Numbering System

Letters	Numbers	Letter	Numbers	Last Number
GX- Goodyear Aerospace Corporation	Cloth Type No. of Film Plies No. of Cloth Plies	Elastomer Type	Fabric oz/yd^2 to tenths	Type Pigment Outer Coating
	100-Cotton 200-Nylon 300-Dacron 400-Fiberglass 500-Stainless 600-NOMEX 700-Rene' 41 2nd Digit = No. Film Plies 3rd Digit = No. Cloth Plies	B-Butyl H-Hypalon N-Neoprene P-Polyurethane S-Silicone U-Uncoated		0-None 1-Aluminum 2-TiO_2

Example: GX311P0541 is identified as: GX 3 1 1 P 054 1

- GX — GAC
- 3 — Dacron Cloth
- 1 — Number of Film Plies
- 1 — Number of Cloth Plies
- P — Polyurethane Elastomer Coating
- 054 — 5.4 oz/yd^2 Fabric
- 1 — Aluminum Pigment - Outer Coating

wetted area depends on shape and unit weight depends on stress, determines the major part of balloon weight. An allowance of 10 percent was made for seam weight; i.e., hull weight, fin weight, etc., were increased by 10 percent. Wetted areas were scaled up from existing sizes, or in the case of the No. 1649 balloon, from model dimensions. Where a blower is provided for pressurization, blower and battery weight depend on design altitude, balloon volume, differential pressure, and power density of the battery. Other weight contributions and the detailed method of calculating stress and weight of aerodynamically-shaped balloons are given in Appendix II. Computer printout data for a 100,000 cu. ft. Vee-balloon configuration is given in Tables IV and V.

The balloon weights as generated by the Appendix II computer program for the payload/altitude/wind criteria of Section II are plotted in Figures 22 and 23. The four configurations are plotted in Figure 22 for the 10,000-foot design altitude, with specific sizes to be used later indicated. Figure 23 presents the BJ balloon weights for design altitudes of 5,000, 10,000 and 20,000 feet and the appropriate payloads.

5. TRIM ATTITUDE

The computer program weight analysis of Appendix II includes a stress consideration of balloon angle of attack. Table VI presents the operational and survival winds at the various design altitudes corrected to a sea-level indicated air speed. The trim attitudes are tabulated in Table VI for the BJ and the Vee-balloon, as taken from Figure 24. These curves are from Reference 7, Figure 8, and Reference 10, Figure B-3.

These angles of attack are used in the determination of balloon aerodynamic lifts and drags and thus (for survival winds) affect balloon weight and tether breaking strength and weight. The lift and drag loads for the operational wind are used in the solution of selected tethers in the operational wind profile.

The Vee-balloon angle of attack profile with wind is due to its unique suspension system, incorporating stretchable, bungee links in the aft suspension. At nine or ten knots, suspenion loads become large enough to start elongating the aft suspension, changing the suspension geometry and literally effecting a reduction in angle of attack. It is not expected that the equations of motion will be made to handle other than a rigid body balloon/suspension arrangement. Airloads used will be based on the Figure 24 angles of attack, as the Vee-balloon and tether weights quoted in this report are not achievable in the desired winds without this unique suspension.

TABLE IV.

IDENTIFICATION OF COMPUTER PRINTOUT

MAXIMUM ALTITUDE - FT

CABLE SAFETY FACTOR - DIMENSIONLESS

INPUTS: PAYLOAD - WEIGHT (LB)
ANGLE OF ATTACK - DEGREES
FOR TYPE - BALLOON TYPE
ALTITUDE - (FT)
VOLUME - FT^3
(1 - VEE, 3 - SINGLE HULL)
VELOCITY - FT/SEC
OPTIME - OPERATING TIME (HOURS)
MATERIAL FACTOR OF SAFETY - DIMENSIONLESS

UNIT FABRIC WEIGHT - LB/FT^3

Q - EXTERNAL DYNAMIC PRESSURE (LB/FT^2)
L - HULL LENGTH (FT)
APHT - PROJECTED AREA HORIZ. TAIL (FT^2)
AWHT - WETTED AREA OF HORIZ. TAIL (FT^2)
HVTA - THICKNESS OF VERT. TAIL (FT)
VTOT - TOTAL VOLUME (FT^3)
ABNT - AREA OF BALLONET (FT^2)
VLEAK - HELIUM LEAK RATE (FT^3/24 HRS)
QT - TOT.VOL.AIR PUMPED THRU BLOWERS DURING DESCENT (FT^3)
NA - AERODYNAMIC STRESS (LB/FT)

PSF - INTERNAL PRESSURE (LB/FT^2)
D - MAXIMUM DIAMETER (FT)
APVT - PROJECT AREA VERT.TAIL (FT^2)
AWVT - WETTED AREA VERT.TAIL (FT^2)
VHT - VOLUME HORIZ. TAIL (FT^3)
VBNT - VOL BALLONET (FT^3)
AINT - AREA HULL INTERSECT (FT^2)
VTEMP - VOLUME CHANGE DUE TO VARIATION IN TEMP.(FT^3)
TOPER - DESCENT BLOWER OPER.TIME(HRS)
ND - BUOYANT STRESS (LB/FT)

NDES - DESIGN STRESS (LB/FT)
AH - HULL AREA (FT^2)
LMAXD - LENGTH FROM NOSE WHERE MAX. DIAMETER OCCURS (FT)
HHTA - THICKNESS HORIZ.TAIL(FT)
VVT - VOLUME VERT.TAIL (FT^3)
DBNT - DIAMETER BALLONET (FT)
QBLO - BLOWER FLOW RATE (FT^3/HR)
VREPL - VOLUME OF HELIUM TO BE REPLACED DUE TO LEAKAGE & TEMP.CHANGE(FT^3/DAY)
NI - INTERNAL PRES.STRESS (LB/FT)

WH - WEIGHT HULL (LB)
WINTA - WEIGHT HULL INTERSECT ATTACH.(LB)
WHTP - WEIGHT HORIZ.TAIL PARTITIONS (LB)
WVTA - WEIGHT VERT.TAIL ATTACH.(LB)
WBLO - WEIGHT BLOWERS (LB)
WAVAL - WEIGHT AIR VALVE (LB)
WBUNG - WEIGHT BUNGEE (LB)
WBNTS - WEIGHT BALLONET SEAMS (LB)
WSUS - WEIGHT SUSPENSION SYSTEM (LB)

WHS - WEIGHT HULL SEAMS (LB)
WHT - WEIGHT HORIZ.TAIL (LB)
WHTS - WEIGHT HORIZ.TAIL SEAMS (LB)
WVTP - WEIGHT VERT.TAIL PARTITIONS(LB)
WBAT - WEIGHT BATTERIES (LB)
WSVAL - WEIGHT SAFETY VALVE (LB)
WSHOE - WEIGHT SHOE (LB)
WMF - WEIGHT MISC. FABRIC (LB)
WHL - WEIGHT HANDLING LINES(LB)

WINT - WEIGHT HULL INTERSECTS(LB)
WHTA - WEIGHT HORIZ.TAIL ATTACH.(LB)
WVT - WEIGHT VERT.TAIL (LB)
WVTS - WEIGHT VERT.TAIL SEAMS (LB)
WME - WEIGHT MISC.EQUIPMENT (LB)
WCHK - WEIGHT CHECK VALVE (LB)
WBNT - WEIGHT BALLONET (LB)

BUOYANT LIFT - (LB)

VOL	CD	C_L	BALLOON WT	UNIT LIFT OF HELIUM AT ALTITUDE	PAYLOAD
HULL VOLUME (FT^3)	DRAG COEFFICIENT (DIMENSIONLESS)	LIFT COEFFICIENT (DIMENSIONLESS)	TOTAL WEIGHT (LBS)	(LB/FT^3)	WEIGHT (LB)

FZ	FX	FY	D	NET LIFT	L
FORCE IN VERT DIRECTION (LB)	FORCE IN DIRECTION OF WIND (LB)	FORCE IN CROSS-WIND DIRECTION (LB)	AERODYNAMIC DRAG (LB)	BUOY.LIFT+L-HULL WT-PAYLOAD (LB)	AERODYNAMIC LIFT (LB)

Table V. Vee-Balloon Computer Printout

```
MAXIMUM ALTITUDE  1.000E 04


CABLE SAFETY FACTOR      2.0

INPUTS:     PAYLOAD =       1000.00     ALTITUDE =       10000.     VELOCITY =      89.5241
     ANGLE OF ATTACK =       6.0000       VOLUME =      150000.      OPTIME =        48.0
           FOR TYPE  1          MATERIAL FACTOR OF SAFETY =  4.00
           HELIUM PURITY =     0.970

UNIT FABRIC WEIGHT =         0.04946

D    =          7.0349                PSR  =          8.0902                NOES =       1119.1495
L    =        136.0202                D    =         34.0351                AM   =      19477.3629
APHT =       1995.9375                APVT =        221.4139                LMAXD=         61.2091
AMHT =       4411.0195                AMVT =        514.1440                MMYA =          4.0910
MVTA =          1.5831                VHT  =       9362.8750                VVT  =        346.4253
VTOT =     160055.6250                VBNT =      41841.5234                ORNT =         43.0484
APNT =       9833.3320                AIOT =        948.9642                GBLO =       2000.0000
VLEAK=        160.4935                VTEMP=      16005.5547                VROPL=      32332.3938
QT   =      40500.6367                TMPER=         14.1660                NI   =        151.6280
NA   =         35.8834                 S   =         22.1248

WH   =        973.2468                WHS  =         97.3246                WENT =         44.9109
WINTA=         46.9169                WHT  =        219.1734                WHTA =         73.9973
WHTP =        197.4420                WHTS =         21.8173                WVT  =         29.4301
WVTA =          8.3919                WHTP =         21.9225                WVTS =          2.9430
WBLO =         16.7975                WBAT =         16.0107                WHS  =          8.0093
WSVAL=          8.7321                WSWAL=          0.0                   WCNS =          8.3988
WBURG=          0.0                   WSNOE=          0.0                   WBNT =        190.7409
WBNTS=         19.0790                WHF  =         53.5285
WSUS =        931.9900                WHL  =        178.7453

BUOYANT LIFT =      7555.3477

          VOL              CD              CL          BALLOON WT          UNIT LIFT          PAYLOAD

      1.500E 05         0.10540         0.49200           2822.             0.04720          1000.0

          FZ              FX              FY              D              WBT LIFT            L

       13504.18         3692.11           0.0           3692.11          13504.18         9771.28
```

Table VI. Trim Attitudes for Operational and Survival Wind

BJ Balloon

h Altitude (Ft)	T A S (Knots)		ρ/ρ_o	$\sqrt{\rho/\rho_o}$	I A S (Knots)		α	α
	v Surv	v Oper			v Surv	v Oper	Surv	Oper
Sea-Level	13.000	10.000	1.000	1.0000	13.000	10.000	3.4°	2.8°
5,000	40.3091	31.007	0.86170	0.92828	37.418	28.783	8.7	7.0
10,000	53.0062	40.774	0.73859	0.85941	45.554	35.042	10.2	8.2
15,000	62.4260	48.020	0.62946	0.79338	49.528	38.098	10.8	8.8
20,000	70.1753	53.981	0.53316	0.73018	51.241	39.416	11.0	9.0

Vee-Balloon

h Altitude (Ft)							α Surv	α Oper
10,000	53.0062	40.774	0.73859	0.85941	45.554	35.042	5.7°	6.9°

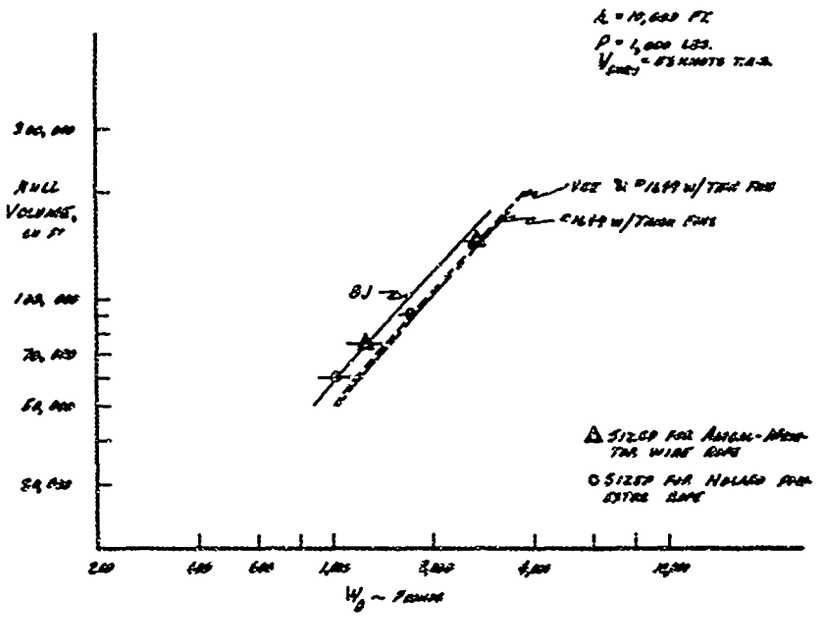

Figure 22. Balloon and Suspension Weights, All Configurations for 10,000 Feet Design Altitude

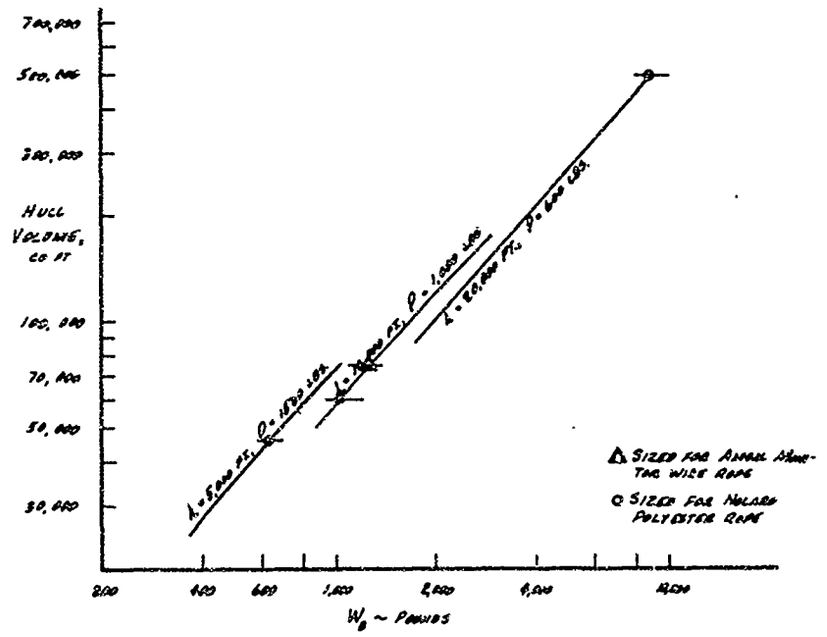

Figure 23. BJ Ballcon and Suspension Weights, Design Altitudes of 5,000, 10,000 and 20,000 Feet

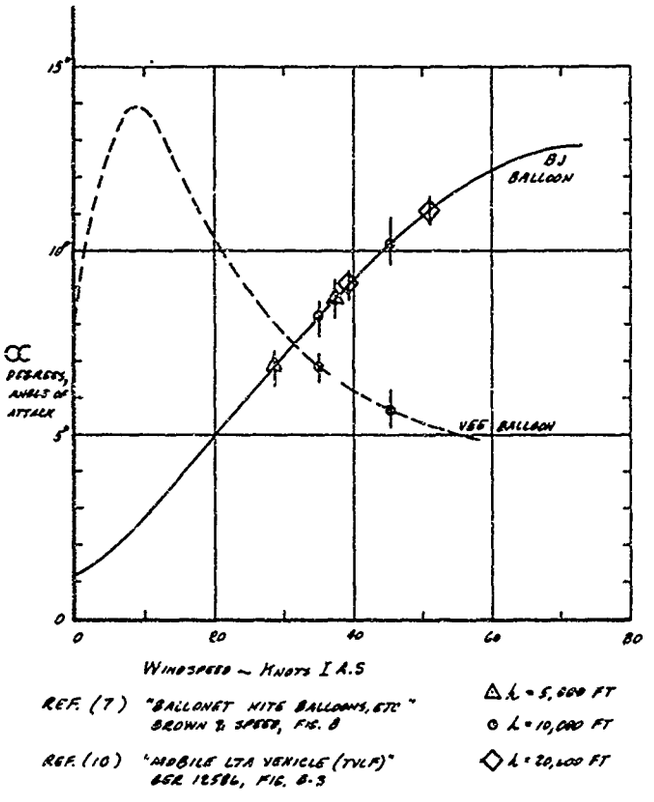

Figure 24. Equilibrium Pitch Angles for Balloons

SECTION III

BALLOON MASS CHARACTERISTICS

1. GENERAL

The balloons' physical and apparent mass characteristics, consistent with the geometries of Table II and the total weights of Figures 22 and 23 (tabulated in Tables VII and XII) are presented in this section. Figure 25, 26 and 29 present the balloons' actual physical mass characteristics (including internal gases) and Figures 25, 27, and 30 present the additional mass characteristics at the design altitudes. If a specific balloon is later studied at a lower altitude, the physical mass characteristics will have to be adjusted to represent the changed masses of either internal helium and/or air. The apparent masses will change as the air density changes. Figure 28 represents the dynamic center location.

The physical mass characteristics do not include payloads. Payloads will be added during the later work and physical mass characteristics appropriately adjusted.

Table VII lists the mass characteristics for some of the arbitrary balloon sizes run out by the computer program. The actual selected balloon sizes of Table XIV are bracketed by the sizes of Table VII.

2. ADDITIONAL MASS

The acceleration of the balloon in any of the six degrees of freedom causes aerodynamic forces in addition to the velocity and attitude changes. It has been shown by Lamb (Reference 11) that the derivatives of these acceleration forces have the dimension of mass. For all practical purposes, this additional mass term may be added to the actual mass of the balloon for purposes of calculating forces and responses of the system. References 12 and 13 were also useful in the development of this section.

The additional mass and additional moments of inertia for acceleration in a fluid have been worked out theoretically for a number of ellipsoids of revolution. Figures 31 and 32 show these coefficients plotted against fineness ratio. The added mass is obtained by multiplying these coefficients by the mass of the displaced air. It has been proposed and has become the custom to use (for airships and balloons) values based on the ellipsoid having the same volume and the same length as the hull. In addition, the theoretical longitudinal coefficient of additional mass shown on the curves will be increased 50% to allow for the boundary layer which is dragged along with the balloon.

Table VII. Balloon Mass Characteristics

Balloon Type	Design Altitude (ft)	Hull Length (ft)	Volume (ft^3)	W_B (1) (lb)	Center of Gravity Horiz. (3) (ft)	Center of Gravity Vert. (4) (ft)	Balloon Mass (2) (slugs)	Mass Center Horiz. (3) (ft)	Mass Center Vert. (4) (ft)	Additional Mass Long. (slugs)	Additional Mass Vert. (slugs)	Additional Mass Lateral (slugs)	Center of Additional Mass In Pitch Horiz. (3) (ft)	Center of Additional Mass In Pitch Vert. (4) (ft)	Center of Additional Mass In Yaw Horiz. (3) (ft)	Center of Additional Mass In Yaw Vert. (4) (ft)	Dynamic Center In Pitch Horiz. (3) (ft)	Dynamic Center In Pitch Vert. (4) (ft)	Dynamic Center In Yaw Horiz. (3) (ft)	Dynamic Center In Yaw Vert. (4) (ft)
BJ	5,000	86.57	50,000	687	49.37	4.39	54.95	53.04	2.99	15.35	107.57	111.64	45.65	0	47.07	3.07	48.15	1.01	49.04	3.05
	10,000	86.57	50,000	868	48.39	4.82	55.76	52.00	3.41	13.18	92.22	95.70	45.65	0	47.07	3.07	48.05	1.29	48.89	3.20
		99.10	75,000	1,276	54.82	5.67	82.83	59.31	3.97	19.74	138.31	143.44	52.26	0	53.87	3.55	54.90	1.49	55.86	3.70
		117.50	125,000	2,095	64.07	6.96	137.07	69.90	4.78	32.91	230.50	239.08	61.96	0	63.88	4.18	64.92	1.78	66.07	4.40
		131.45	175,000	2,939	70.78	7.88	192.08	77.77	5.42	46.09	322.96	334.90	69.35	0	71.48	4.67	72.49	2.02	73.77	4.94
	20,000	186.52	500,000	8,933	100.44	11.64	485.61	108.52	8.59	95.05	665.66	690.37	98.36	0	101.39	6.65	102.65	3.62	104.34	7.45
VEE	10,000	107.96	75,000	1,450	60.40	5.95	68.19	57.77	3.95	44.04	177.04	119.07	63.46	0	52.67	0.74	61.88	1.10	54.52	1.91
		128.00	125,000	2,364	71.34	7.45	112.05	68.28	4.91	73.41	295.11	197.71	75.23	0	62.28	0.83	73.33	1.35	64.45	2.30
		143.19	175,000	3,287	79.61	8.60	156.15	76.24	5.65	102.75	413.94	276.90	84.23	0	69.69	0.93	82.04	1.55	72.05	2.63
ϕ1649 with Thin Fins	10,000	112.60	75,000	1,457	63.36	4.94	81.43	64.93	2.75	14.73	169.36	154.44	64.96	0	61.85	2.44	64.95	0.89	62.92	2.34
		133.50	125,000	2,365	73.98	6.10	133.77	76.39	3.35	24.59	282.06	257.29	76.99	0	73.31	2.92	76.80	1.08	74.37	3.02
		149.34	175,000	3,292	82.13	6.98	186.70	85.11	3.83	34.41	395.16	360.23	86.16	0	82.02	3.25	85.83	1.23	83.08	3.44

Balloon Type	Design Altitude (ft)	Volume (ft^3)	Axis	Balloon Mass Moment of Inertia (slug ft^2)	Additional Mass Moment of Inertia (slug ft^2)
BJ	5,000	50,000	Roll	8,874	14,377
			Pitch	40,818	49,540
			Yaw	38,881	55,693
	20,000	500,000	Roll	429,311	413,194
			Pitch	1,731,251	1,423,965
			Yaw	1,639,971	1,597,608

NOTES:
(1) Balloon and suspension weight, no gas, payload or tether
(2) Total balloon mass including internal gas and air
(3) Feet aft of theoretical bow
(4) Feet below horizontal ℄

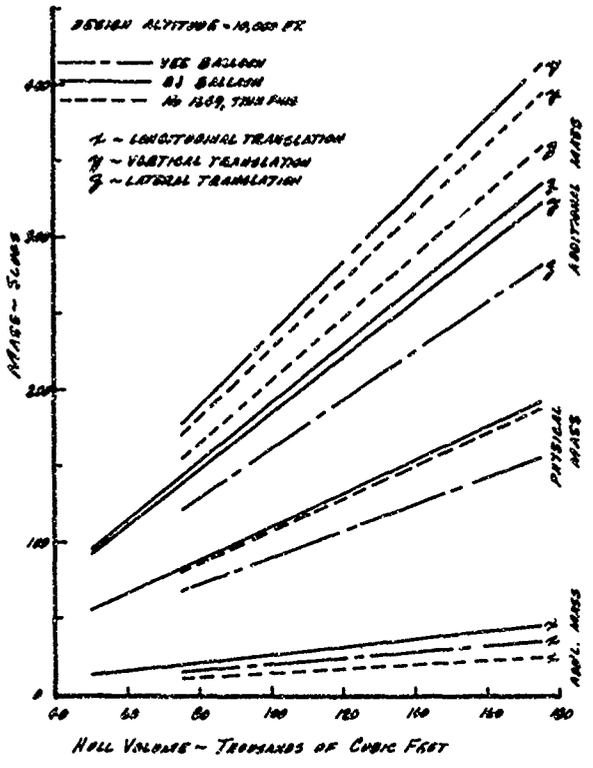

Figure 25. Balloon Total Mass and Additional Mass vs Hull Volume

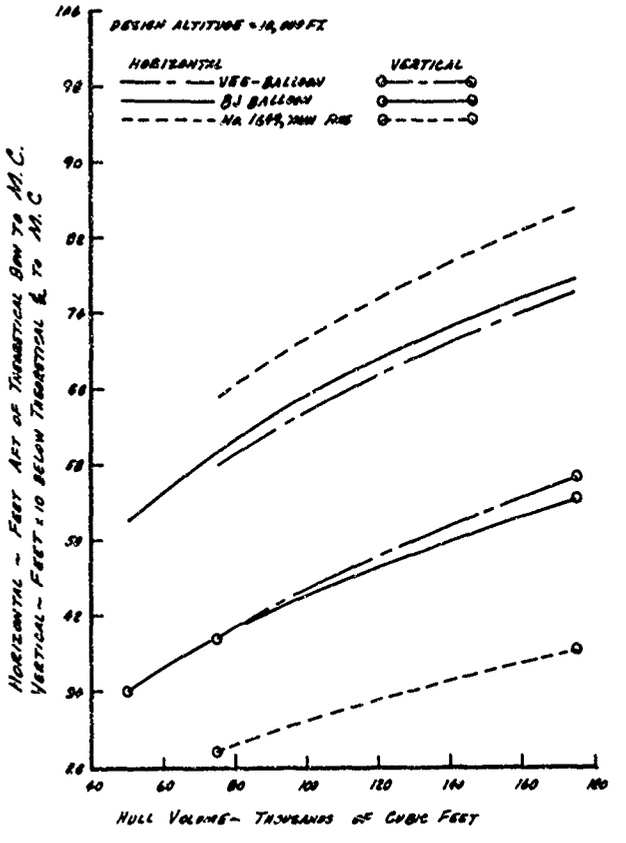

Figure 26. Balloon Mass Center

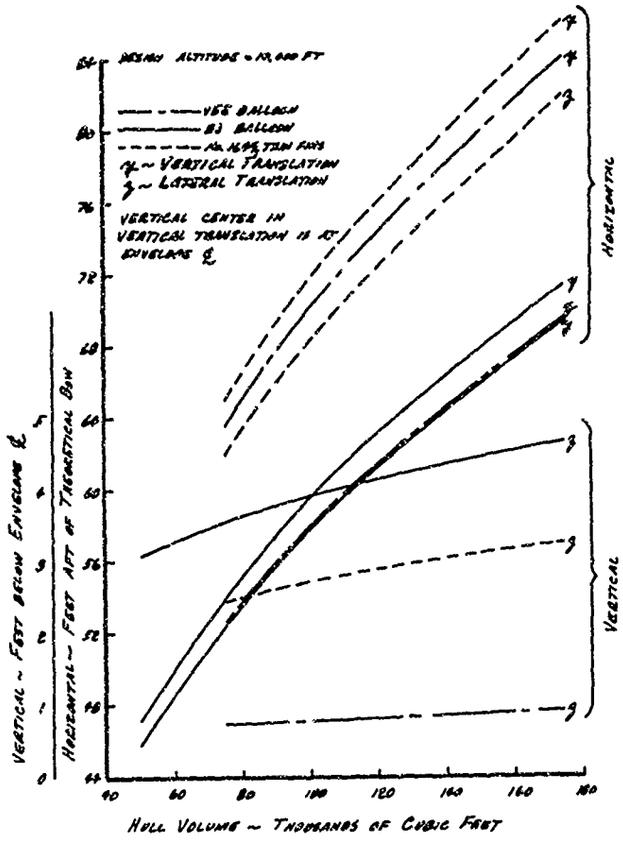

Figure 27. Center of Additional Mass

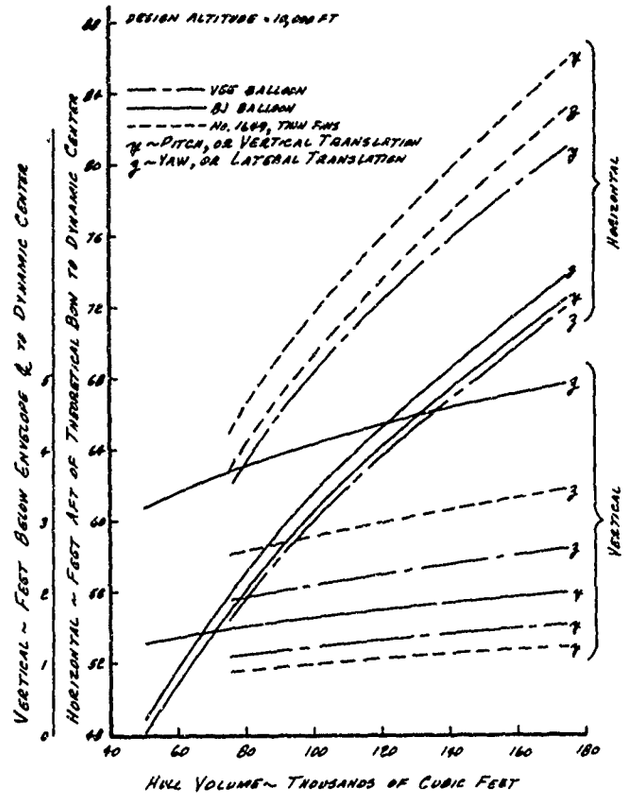

Figure 28. Dynamic Center (Pitch and Yaw)

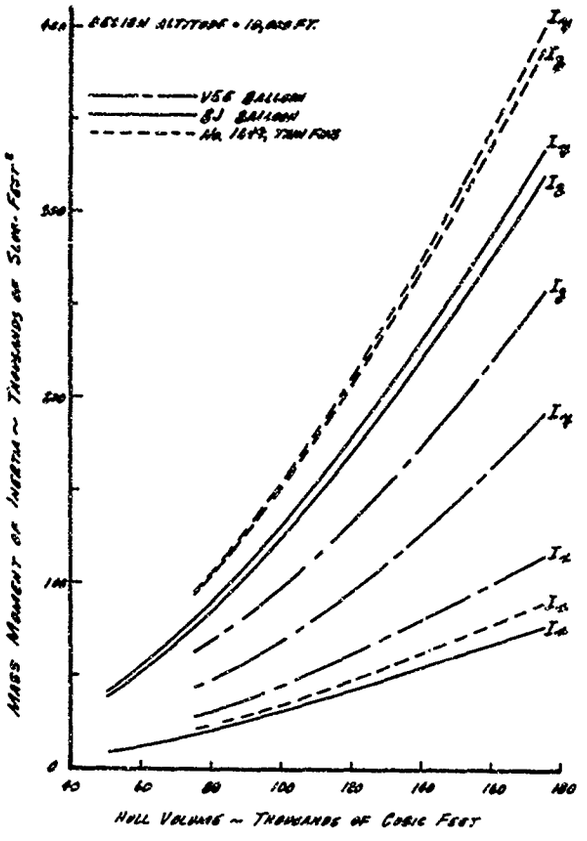

Figure 29. Mass Moment of Inertia (Pitch and Yaw)

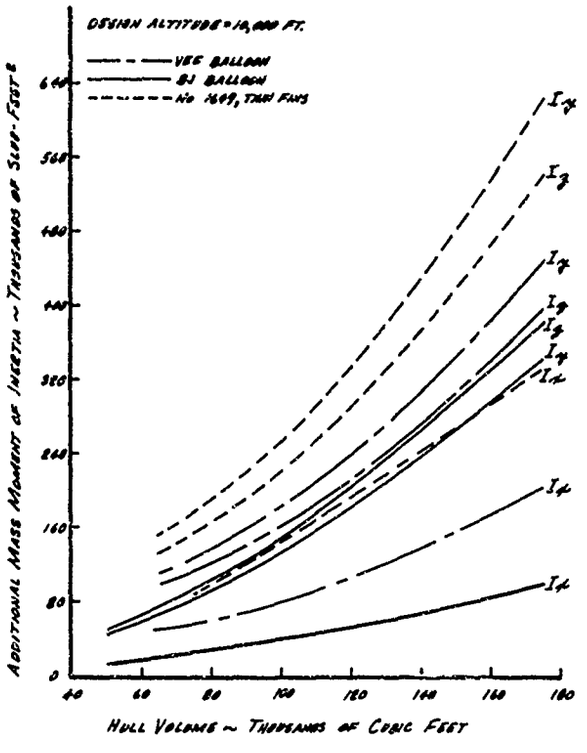

Figure 30. Additional Mass Moment of Inertia (Pitch and Yaw)

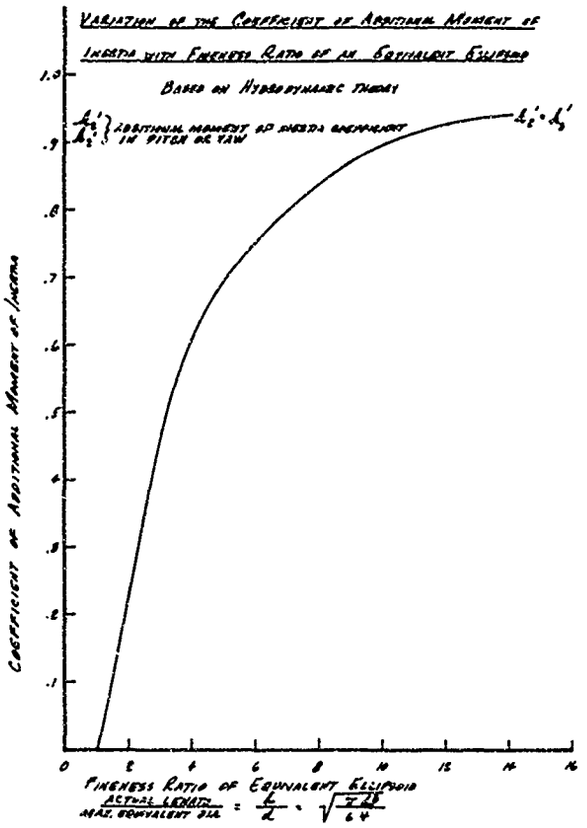

Figure 31. Variation of the Coefficient of Additional Moment of Inertia with Fineness Ratio of an Equivalent Ellipsoid

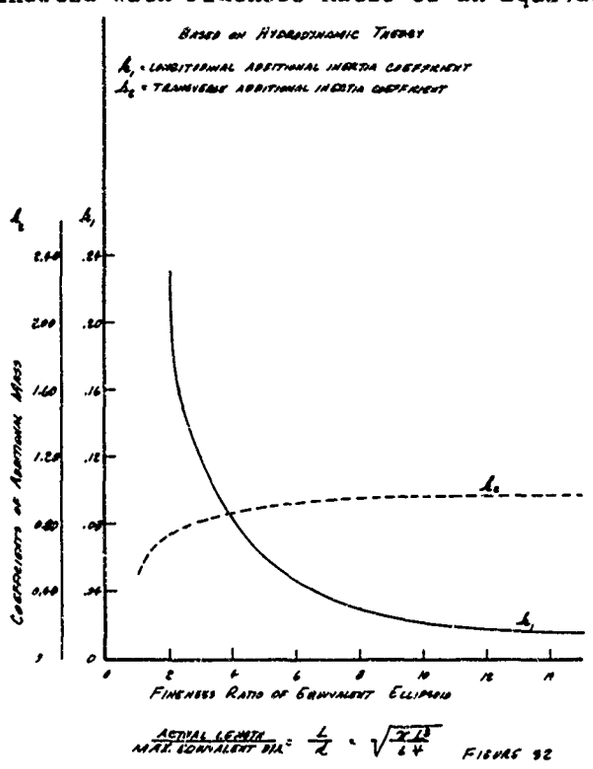

Figure 32. Variation of the Coefficient of Additional Mass with Fineness Ratio of an Equivalent Ellipsoid

The fineness ratio of the equivalent ellipsoid to the hull must be computed based on equal volumes and equal lengths.

$$V = \frac{\pi}{6} d^2 L$$

$$d = \sqrt{\frac{6V}{\pi L}}$$

$$\text{Fineness ratio} = \frac{L}{\sqrt{\frac{6V}{\pi L}}} = \sqrt{\frac{\pi L^3}{6V}}$$

The flat tail surfaces also exhibit an added mass effect when accelerated normal to their chords For large aspect ratios, the added mass is equivalent to the mass of air contained in a cylinder whose diameter is equal to the chord of the tail. Tests have provided corrections for smaller aspect ratios and for taper. The tail added mass terms can be obtained from Figure 33 and added to the hull added mass for the total added mass and moment of inertia effects of each balloon,and for determining the dynamic center.

The added mass of the tail is obtained by multiplying these coefficients of the mass of air contained in a cylinder having the length equal to the span and a diameter equivalent to the chord of a rectangular tail having the same area.

3. DYNAMIC CENTER LOCATION

Under dynamic loads the balloon will have a mass and moment of inertia which includes the additional mass and additional moment of inertia of the affected surrounding air.

It has been assumed that the axes chosen are the principal axes so that the products of inertia drop out.

The additional mass along each major axis is added directly to the mass of the balloon. The center of the additional mass, however, does not coincide with the center of gravity. The combination of these two masses will determine the dynamic center about which the complete balloon will act in air. Since the value and location of the additional mass is different for accelerations along each axis, the dynamic center will be located at different places for the lateral and vertical accelerations.

Figure 34 shows how the dynamic center is located and the combined moment of inertia is calculated.

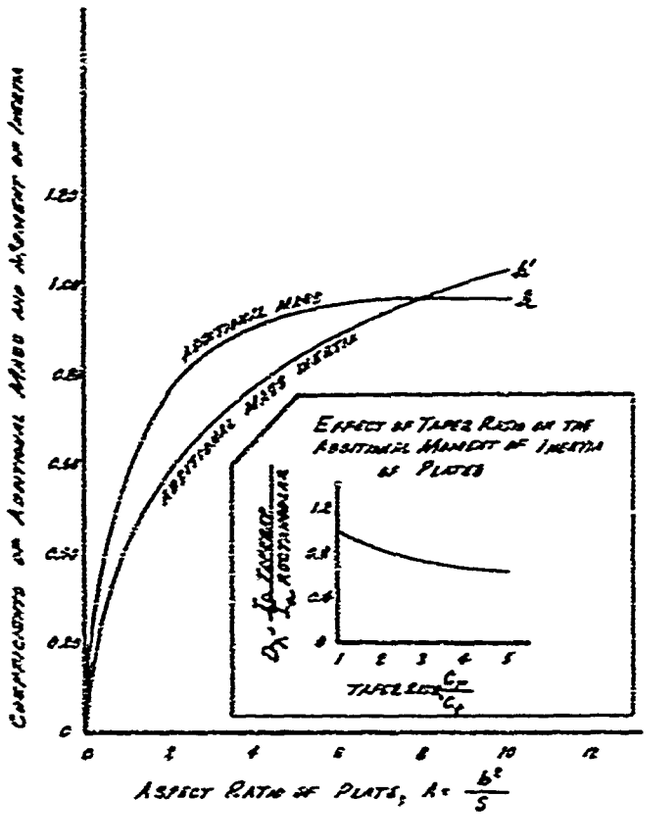

Figure 33. Variation of the Coefficients of Additional Mass and Moment of Inertia with Aspect Ratio of Rectangular Plates

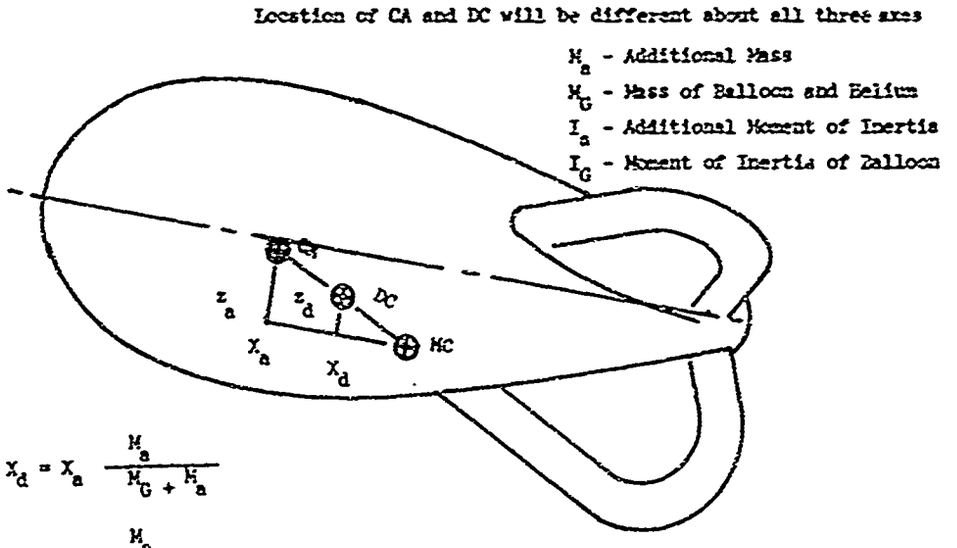

$$X_d = X_a \frac{M_a}{M_G + M_a}$$

$$z_d = z_a \frac{M_a}{M_G + M_a}$$

$$I_D = I_G + I_a + M_a \left[(X_a - X_d)^2 + (z_a - z_d)^2 \right] + M_G \left[X_d^2 + z_d^2 \right]$$

Figure 34. Location of Dynamic Center from Mass Center and Center of Additional Mass

SECTION IV

STATIC AND DYNAMIC AERODYNAMIC DERIVATIVES

1. GENERAL

The fundamental equations of motion state that the sum of the forces equals the mass times an acceleration in the fashion of Newton's Second Law of motion.

$$F = \frac{W}{g} a \text{ and } M = I \ddot{\theta}$$

where F and M are the unbalanced force and moment on the balloon of mass $\frac{W}{g}$ and moment of inertia I undergoing accelerations a and $\ddot{\theta}$.

The Force F is the unbalanced force resulting from the vector sum of all applied forces to the balloon. The applied forces include buoyancy, gravity, cable forces and aerodynamic forces. The moment M is likewise the unbalanced moment.

The aerodynamic forces are fundamentally caused by the wind and its relation to the position and attitude of the balloon. At equilibrium, all the forces are balanced and the acceleration is zero. There are secondary forces applied due to changes in attitude, velocity and acceleration when the balloon is disturbed or returning to equilibrium.

The forces and moments are resolved into components along the major axes and it is assumed that these components can be introduced into the equation as acting about or along that axis.

In order to keep the mathematics to a reasonable effort, it is assumed that the dynamics of the situation having 6 degrees of freedom can be handled as two separate problems without cross coupling of one to the other. The first occurs in the pitch plane and includes lift, drag and pitching moment. The other 3 degrees of freedom are handled as a single problem in roll, yaw and side force.

The force components are assumed to be added arithmetically and are caused by very small deviations from the equilibrium attitude. The deviations are assumed to be linear and can be expressed by the form

$$\frac{\partial y}{\partial x} \cdot \Delta x.$$

The aerodynamic partial derivatives will be evaluated for insertion into the six equations of motion representative of the six degrees of freedom of the balloon. When tests of a complete balloon are not available, it will be assumed that the effect of components, i.e., hull, tail, etc., are

additive with a minimum of interference effects. The following discussions eliminate, when they are zero, or determine coefficient forms of the aerodynamic parameters.

The space position of the balloon, i.e., displacement along any axis, has no effect on the aerodynamic parameters. There is a very small effect with vertical position because both wind velocity and air density change with altitude. In the linearized equations, however, it is assumed the displacement is so small that its effect can be neglected.

Velocity along the space axis also has no effect except where it changes the relative wind, which is assumed constant and horizontal. Since model tests and the evaluation formulas are referenced to the relative wind, the space velocity derivatives are dropped in favor of aerodynamic derivatives.

Likewise rotational attitude and velocity are referenced to the relative wind instead of the space reference coordinates.

Acceleration along an axis produces a change in the flow with resulting aerodynamic forces. Sir Horace Lamb showed that the acceleration derivatives have the dimension of mass and could be considered as an additional mass added to the mass terms on the right hand side of the equation. The additional mass terms will be handled later. The added moments of inertia are handled the same way.

2. LIFT

The uncoupled derivatives that must be evaluated for lift are related to angles of attack, and to velocities along the X and Z axis and rotation velocity about the Y axis.

$$\frac{\partial L}{\partial \alpha}, \qquad \frac{\partial L}{\partial u}, \qquad \frac{\partial L}{\partial w}, \qquad \frac{\partial L}{\partial \dot{\alpha}}$$

The effect of angle of attack change on lift, $\frac{\partial L}{\partial \alpha}$, can be determined from the lift curve. This is usually determined in wind tunnel tests and plotted as lift coefficient vs angle of attack. These curves are presented in Figure 5.

$$\frac{\partial L}{\partial \alpha} = \left(\frac{1}{2} \cdot \rho V^2 \nabla^{2/3}\right) C_{L_\alpha} \qquad (1)$$

where C_{L_α} is the slope of the lift coefficient curve measured at the equilibrium angle of attack.

The effect of small change in velocity, $\frac{\partial L}{\partial u}$, can be evaluated

$$L = \frac{1}{2} \cdot \rho V^2 \nabla^{2/3} C_L$$

Since u is a small change in V, differentiating,

$$\frac{\partial L}{\partial u} = \rho V \forall^{2/3} C_L$$

Multiply by $\frac{2V}{2V}$,

$$\frac{\partial L}{\partial u} = \left(\frac{1}{2} \cdot \rho V^2 \forall^{2/3}\right) \frac{2C_L}{V}$$

$$\frac{\partial L}{\partial u} = (\text{Lift}) \frac{2}{V}$$

The effect of vertical velocity on lift, $\frac{\partial L}{\partial w}$, can be resolved as an induced angle of attack change.

$$\frac{\partial L}{\partial w} = \frac{\partial L}{\partial \alpha} \cdot \frac{\partial \alpha}{\partial w} \qquad (2)$$

For small angles,

$$\alpha = \alpha_o + \frac{w}{V} .$$

differentiating;

$$\frac{\partial \alpha}{\partial w} = \frac{1}{V}$$

From equations (1) and (2) above,

$$\frac{\partial L}{\partial w} = \left(\frac{1}{2} \cdot \rho V^2 \forall^{2/3}\right) \frac{C_{L_\alpha}}{V}$$

This can also be expressed

$$\frac{\partial L}{\partial w} = \frac{\partial L_a}{\partial \alpha} \times \frac{1}{V}$$

The lift due to pitch rotation, $\frac{\partial L}{\partial \dot{\alpha}}$, can be measured on models in a whirling arm test facility or by oscillating curved models in a conventional wind tunnel. Curved models have also been used in a wind tunnel. These data have not been measured on models of the configuration of these balloons.

To evaluate this derivative, standard airship design practices based on model airship tests will be used. This assumes that the hull derivative can be added to the tail contribution to make up the whole. The effect of the shape of the Vee-Balloon hull is unknown.

3. DRAG

In a parallel and similar manner, the derivatives of drag are obtained.

$$\frac{\partial D}{\partial \alpha} = \left(\frac{1}{2} \rho V^2 \forall^{2/3}\right) C_{D_\alpha}$$

$$\frac{\partial D}{\partial u} = \left(\frac{1}{2} \rho V^2 \forall^{2/3}\right) \frac{2C_D}{V} \qquad \text{Also } \frac{\partial D}{\partial u} = (\text{drag}) \frac{2}{V}$$

$$\frac{\partial D}{\partial w} = \left(\frac{1}{2} \rho V^2 \forall^{2/3}\right) \frac{C_{D_\alpha}}{V} = \frac{\partial D}{\partial \alpha} \times \frac{1}{V}$$

The derivative $\frac{\partial D}{\partial \dot{\alpha}}$ has not been evaluated experimentally or theoretically and is neglected in airship dynamic analyses. If it is neglected this means the value zero is assigned to it. Rather, it is thought better to try to assign some value to it, possibly related to the lift through the induced lift-drag ratio,

$$\frac{\partial D}{\partial \dot{\alpha}} = \frac{\partial L}{\partial \dot{\alpha}} \times \frac{D}{L}$$

where, $\frac{D}{L} = \frac{C_{D_i}}{C_L} = \frac{KC_L^2}{C_L}$ where K = .9 for general airship shapes

Then $\frac{\partial D}{\partial \dot{\alpha}} = \frac{\partial L}{\partial \dot{\alpha}} \times .9\, C_L$

4. PITCHING MOMENT

Also, it is obvious that the following relationships concerning pitching moment are,

$$\frac{\partial M}{\partial \alpha} = \left(\frac{1}{2} \cdot \rho V^2 \forall\right) C_{m_\alpha}$$

$$\frac{\partial M}{\partial u} = \left(\frac{1}{2} \cdot \rho V^2 \forall\right) \frac{2C_m}{V} = (\text{Moment}) \frac{2}{V}$$

$$\frac{\partial M}{\partial w} = \left(\frac{1}{2} \cdot \rho V^2 \forall\right) \frac{C_{m_\alpha}}{V} = \frac{\partial M}{\partial \alpha} \times \frac{1}{V}$$

The rotary derivative $\frac{\partial M}{\partial \dot{\alpha}}$ can be evaluated from airship data using airship design methods for the circular balloons. The value for the Vee-balloon hull is not known due to the shape of its hull.

5. ROLLING MOMENT

Rolling moment, as with yawing moment and side force, is studied uncoupled from the pitch plane. All model tests are made at zero angle of attack. Accordingly, the derivatives will be evaluated at zero angle of attack and assumed to be independent of it. The following derivatives are assumed to have a non-zero value which can be estimated.

$$\frac{\partial M_x}{\partial \beta}, \qquad \frac{\partial M_x}{\partial p}, \qquad \frac{\partial M_x}{\partial r}, \qquad \frac{\partial M_x}{\partial v},$$

Rolling moment due to yaw, $\frac{\partial M_x}{\partial \beta}$, for symmetrical balloons would be zero about the longitudinal axis. If the center of gravity is not on the axis, then there is a rolling moment due to side force multiplied by a suitable moment arm. This term will be handled when the center of moments is shifted to the center of gravity and is not included in the aerodynamic efforts. For the unsymmetrical tail of the Vee-balloon, there is an additional moment due to the side force of the vertical tail.

$$M_x = \frac{1}{2} \rho V^2 A_v \cdot C_{L_t} \cdot z$$

Where z is the vertical distance between the longitudinal axis and the center of pressure of the vertical tail area,

$$\frac{\partial M_x}{\partial \beta} = \left(\frac{1}{2} \rho V^2 A_v z\right) C_{L_{t_\beta}}$$

Rolling moment due to rolling velocity, $\frac{\partial M_x}{\partial p}$, is caused by the damping effect of the apparent angle of attack of the tail. This is composed of the sum of the effect of all the tail surfaces, plus, in the case of the Vee-balloon, an effect of the hull. The latter effect has not been measured experimentally; however, some value should be estimated for it. The rolling moment due to the tail will be estimated in the following way.

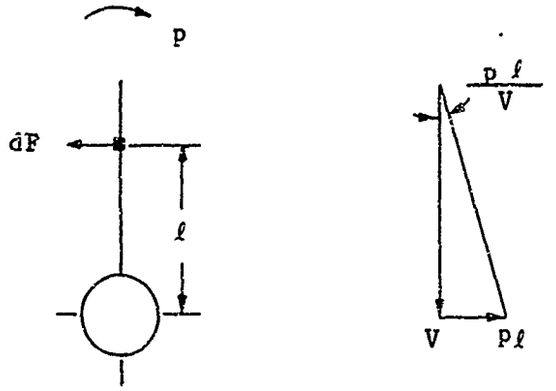

$$dM_x = \ell dF$$

$$dF = \frac{1}{2} \rho V^2 C_{L_t} c \, d\ell$$

where c is the local tail chord

$$C_{L_t} = C_{L_{t_\alpha}} \frac{p\ell}{V}$$

$$M_x = \int_{\ell_1}^{\ell_2} \frac{1}{2} \rho V p C_{L_{t_\alpha}} c\ell^2 d\ell$$

$$\frac{\partial M_x}{\partial p} = \frac{1}{2} \rho V C_{L_{t_\alpha}} \int_{\ell_1}^{\ell_2} c\ell^2 \, d\ell$$

Rolling moment due to yawing velocity, $\frac{\partial M_x}{\partial r}$, is zero for a balloon symmetrical about the X-Y plane. In the Vee-balloon the tail side force is produced by an apparent angle of attack change which is, $\frac{Xr}{V}$, where X is the longitudinal distance between the center of rotation and the center of pressure of the tail. The moment of the force about the roll axis of symmetry becomes,

$$M_x = \frac{1}{2} \rho V^2 A_V z C_{L_{t_\alpha}} \frac{Xr}{V}$$

When z is the distance between the axis and the center of pressure of the tail,

$$\frac{\partial M_x}{\partial r} = \frac{1}{2} \rho V A_v X z C_{L_{t_\alpha}}$$

Rolling moment due to sideslip velocity, $\frac{\partial M_x}{\partial v}$, only has a value for the unsymmetrical tail. Here the side slip velocity introduces an apparent angle of attack change $\frac{v}{V}$. The moment then becomes

$$M_x = \frac{1}{2} \rho V^2 A_v z C_{L_{t_\alpha}} \frac{v}{V}$$

$$\frac{\partial M_x}{\partial v} = \frac{1}{2} \rho V A_v z C_{L_{t_\alpha}} = \frac{\partial M_x}{\partial r} \times \frac{1}{X}$$

6. YAWING MOMENT

The yawing moment due to yaw, $\frac{\partial N}{\partial \beta}$, is the slope of the yawing moment curve at zero yaw obtained from wind tunnel data.

This can be expressed

$$\frac{\partial N}{\partial \beta} = (\frac{1}{2} \rho V^2 V) C_{n_\beta}$$

The yawing moment due to rolling velocity, $\frac{\partial N}{\partial p}$, is zero for a balloon with a symmetrical tail. For the Vee-balloon with an unsymmetrical tail, a net force is caused by the apparent angle of attack change of the tail caused by the following velocity which produces a moment in yaw,

$$N = XF = X \int_{\ell_1}^{\ell_2} \frac{1}{2} \rho V^2 c C_{L_{t_\alpha}} \frac{\ell p}{V} d\ell$$

$$\frac{\partial N}{\partial p} = \frac{1}{2} \rho V X C_{L_{t_\alpha}} \int_{\ell_1}^{\ell_2} c\ell \, d\ell$$

Due to symmetry, there will be no yawing moment due to rolling velocity of the hull.

The yawing moment due to yawing velocity, $\frac{\partial N}{\partial r}$, has not been measured on the balloon shapes. This rotary derivative can be estimated from airship data using standard airship design methods. When symmetry exists, it is related to the pitching moment due to pitching velocity.

The yawing moment due to side slip velocity, $\frac{\partial N}{\partial v}$, is caused by an apparent angle of yaw due to the relative wind.

$$N = \frac{1}{2} \rho V^2 \forall C_{n_\beta} \frac{v}{V}$$

$$\frac{\partial N}{\partial v} = \left(\frac{1}{2} \rho V^2 \forall\right) \frac{C_{n_\beta}}{V} = \frac{\partial N}{\partial \beta} \times \frac{1}{V}$$

7. SIDE FORCE

The side force due to yaw, $\frac{\partial Y}{\partial \beta}$, is available from wind tunnel tests.

$$Y = \frac{1}{2} \rho V^2 \forall^{2/3} C_Y$$

$$\frac{\partial Y}{\partial \beta} = \left(\frac{1}{2} \rho V^2 \forall^{2/3}\right) C_{Y_\beta}$$

A side force due to rolling velocity, $\frac{\partial Y}{\partial p}$, will occur when the balloon is not symmetrical about the longitudinal axis. The rolling velocity produces a local angle of attack of the tail with a resulting side force,

$$d Y = \frac{1}{2} \rho V^2 C_{L_{t_\alpha}} \frac{\ell p}{V} c \, d\ell$$

$$Y = \frac{1}{2} \rho V p C_{L_{t_\alpha}} \int_{\ell_1}^{\ell_2} c \ell \, d\ell$$

$$\frac{\partial Y}{\partial p} = \frac{1}{2} \rho V C_{L_{t_\alpha}} \int_{\ell_1}^{\ell_2} c \ell \, d\ell = \frac{\partial N}{\partial p} \times \frac{1}{X}$$

The side force due to yawing velocity, $\frac{\partial Y}{\partial r}$, for symmetrical balloons is related to the rotary derivatives of lift due to pitching velocity. There are very little wind tunnel data available on this derivative; however it will be combined with airship data and a value will be estimated by established techniques.

The side force due to the side slip velocity, $\frac{\partial Y}{\partial v}$, can be evaluated as an apparent angle of attack change,

$$Y = \frac{1}{2} \rho V^2 \forall^{2/3} C_{Y_\beta} \frac{v}{V}$$

$$\frac{\partial Y}{\partial v} = \left(\frac{1}{2} \rho V^2 \forall^{2/3} C_{Y_\beta}\right) \frac{1}{V} = \frac{\partial Y}{\partial \beta} \times \frac{1}{V}$$

SECTION V

TETHER CABLES

1. PHYSICAL PROPERTIES

Appropriate tethers for the systems under study are restricted to NOLARO and Amgal-Monitor AA wire ropes.

The NOLARO is an unbraided (NO-LAy-ROpe) construction of the Columbian Rope Company. Yarns may be nylon, polyester (Dacron), or polypropelene. Jackets can be of polyethylene, polyvinyl chloride, polyurethane, etc. Table VIII presents some typical polyester NOLARO line. To maximize strength/weight ratio this tabulation was refigured for a polyester jacket of 0.040 in. wall and is presented in Table IX. These values are used throughout this report in describing a system using NOLARO tether. BS/N was determined as implied by Table VIII values.

Table VIII

Columbian Rope Company
"NOLARO"

Prestretched Polyester Jacketed with Polyethylene

Nominal Size (In.-Strand)	Approx. B.S.*(Lb)	Polyester Diameter (In.)	Nominal Jacket Thickness (In.)	Weight Lbs/M Ft	Unit Weight Ft/Lb
3/16 -4	1,400	0.142	0.025	13.2	75.8
1/4 -6	2,100	0.174	0.038	20.5	48.8
5/16 -10	3,400	0.225	0.044	31.6	31.6
3/8 -16	5,300	0.284	0.045	45.7	21.9
7/16 -22	7,300	0.334	0.052	57.4	17.4
1/2 -30	10,000	0.390	0.055	81.7	12.2
5/8 -50	16,500	0.502	0.060	128.0	7.81
3/4 -80	25,000	0.635	0.060	187.0	5.35
1 -155	46,000	0.887	0.060	332.0	3.01
1-1/4 -340	60,000	1.100	0.075	527.0	1.90
1-5/8 -400	100,000	1.420	0.102	868.0	1.15

*Breaking Strength

Table IX

Prestretched Polyester Jacketed With 0.040 Polyethylene

B.S. (lb)	$\frac{B.S}{N}$ (lb)	N	d (in.)	D (in.)	Yarn wt/1000 ft (lb)	Jacket wt/1000 ft (lb)	Total wt/1000 ft (lb)
2,000	337.8	5.93	0.173	0.253	10.0	10.7	20.7
5,000	334.5	14.5	0.27	0.35	24.4	15.5	39.9
10,000	329.0	30.4	0.39	0.47	51.1	21.5	72.6
20,000	318.0	62.8	0.56	0.64	105.5	29.3	134.8
30,000	307.0	97.7	0.70	0.78	164.0	36.9	200.9
40,000	296.0	135.0	0.82	0.90	227.0	41.1	268.0
50,000	285.0	175.3	0.94	1.02	295.0	48.6	344.0
60,000	274.0	219.0	1.05	1.13	368.0	56.1	424.0
70,000	263.0	266.5	1.16	1.24	448.0	59.2	507.0
80,000	252.0	317.5	1.26	1.34	534.0	62.4	596.0
90,000	241.0	374.0	1.37	1.45	629.0	68.6	698.0
100,000	230.0	435.0	1.48	1.56	731.0	78.0	809.0

where B.S. = breaking strength, lb

N = number of prestretched yarns

d = diameter of yarn bundle (in) $\left[d = 0.071 \sqrt{N}\right]$

D = O.D. (in) $\left[D = d + 2t, \text{ where } t = 0.040\right]$

$Wt_{yarn} = 1.68\ (N)$

$Wt_{jacket} = 340\ (D^2 - d^2)\ G$

G = specific gravity of jacket [0.92 for PE; 1.25 for PVC]

PE = Polyethylene

PVC = Polyvinyl Chloride

Approximate elongation for prestretched polyester NOLARO rope is given below in Table X:

Table X

Approximate NOLARO Elongation

Load as Percent of Breaking Strength	Approximate Elongation (%)
10	1.0
20	1.8
30	2.8
50	4.3
70	5.6

Table XI presents U. S. Steel's Amgal-Monitor AA wire rope. Figures 35 and 36 present the cable weight vs breaking strength and cable weight vs diameter for the two constructions.

In combined balloon-tether solutions later the specific Amgal wire rope sizes as given in Table XI will be used, as these are the available sizes. Any desired size of NOLARO, along the curves of Figures 35 and 36 can be manufactured. Thus an infinite range of sizes is available in the NOLARO construction.

The computer solution, as presented in Appendix I, incorporates a C_D for the cable of 1.1 which is consistent with Reference 14. Both constructions are solved with this same drag factor, although NOLARO is smooth and Amgal-Monitor is a lay-up of three main elements of rough surface. However, Reference 14 indicates that a surface roughness in the appropriate Reynold's number regime provides a reduction in C_D. The reference diameter for the Amgal-Monitor is that of a circumscribing circle, which is 115% of the sum of the diameters of any two main rope elements

$$\left(\frac{1}{\sin 60^\circ} = 1.15\right).$$

Comparative solutions of cables for the 10,000 foot altitude balloons resulted in 1-2% more tether out and 5-8% more downwind displacement for C_D = 1.5 as against C_D = 1.1.

Results for both constructions in this report are based on C_D = 1.1.

2. AERODYNAMIC FORCES ON THE CABLE

The drag coefficient on cylinders and cables which represent the tether cable may be found in Reference 14. This cable will be operating at a Reynold's number of 10^4 which is well below the critical number for cylinders and is in an area where the C_D value is essentially constant at 1.1.

Table XI

UNITED STATES STEEL TETHERS
Amgal-Monitor AA Wire Rope

Minimum Breaking Strength (lb)	Diameter (in.)	Design Construction	Weight per 1000 Feet (lb)
2,800	0.156 (5/32)	3 x 7	40.2
3,500	0.172 (11/64)	3 x 19	50.7
4,000	0.187 (3/16)	3 x 19	58.6
5,400	0.218 (7/32)	3 x 19	79.5
6,750	0.250 (1/4)	3 x 19	99.7
10,300	0.312 (5/16)	3 x 19	153.0
14,800	0.375 (3/8)	3 x 19	220.0
20,000	0.437 (7/16)	3 x 19	304.0
25,700	0.500 (1/2)	3 x 19	392.0
32,500	0.562 (9/16)	3 x 19	492.0
40,300	0.625 (5/8)	3 x 19	602.0
57,800	0.750 (3/4)	3 x 19	879.0
78,000	0.875 (7/8)	3 x 19	1210.0
100,600	1.000 (1)	3 x 19	1560.0

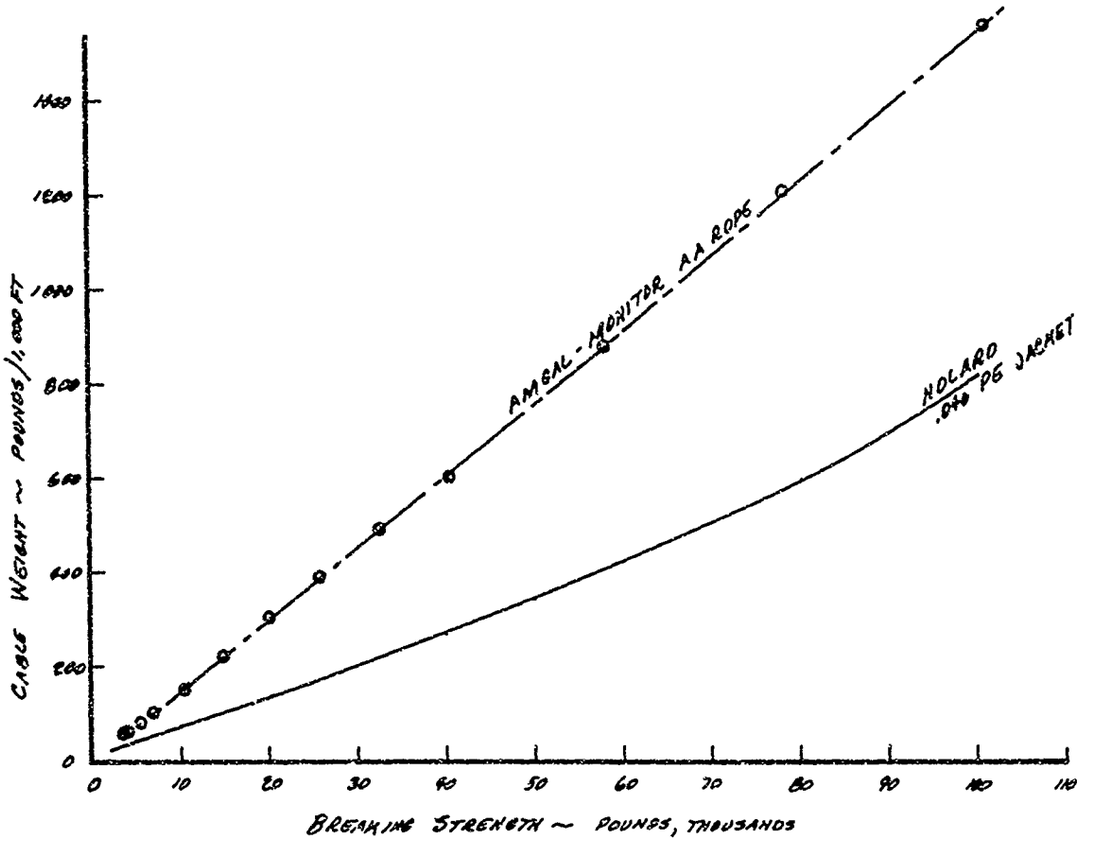

Figure 35. Cable Weight vs Breaking Strength

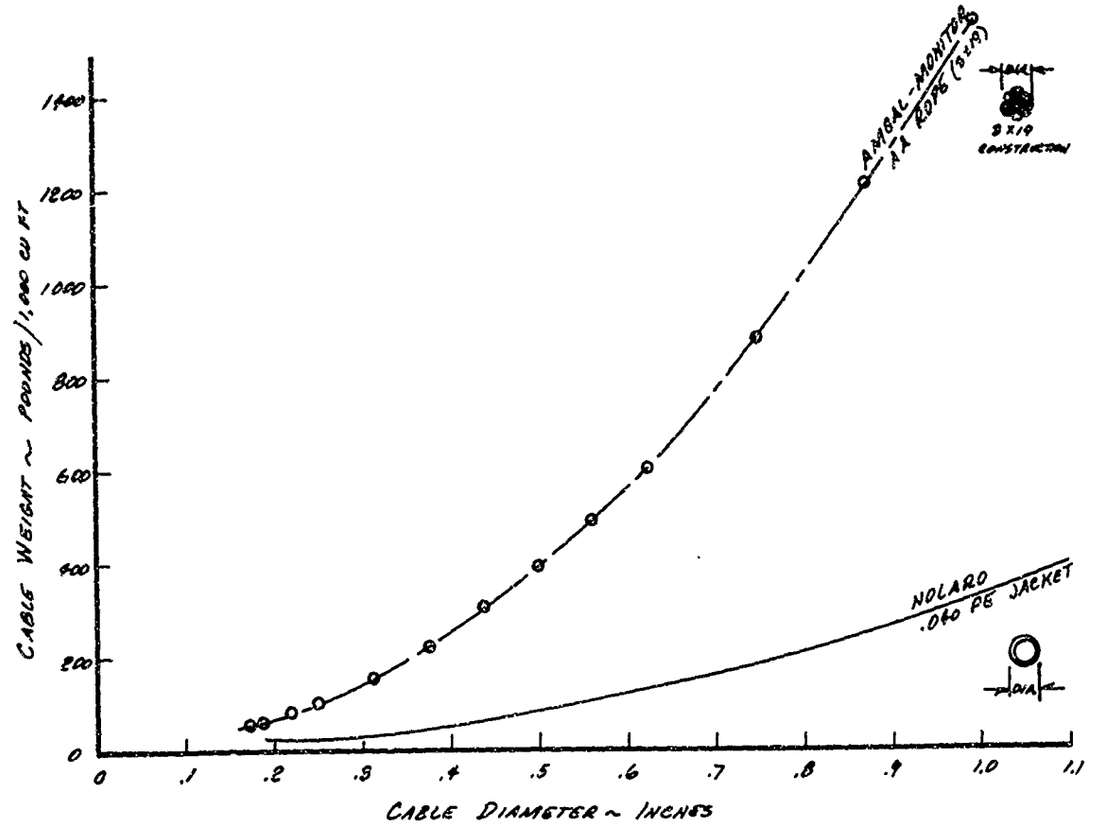

Figure 36. Cable Weight vs Diameter

In a cable such as this where the pressure drag is very large compared to the friction drag, the latter may be ignored in the calculations. Also it is assumed that the cable force per unit of length always acts normal to it and has a value varying as the $\cos^2 \theta$.

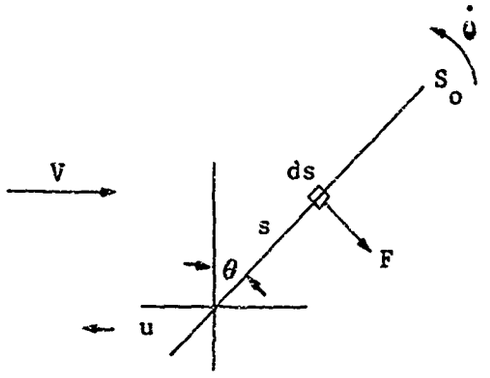

Since the equations are written as moments about the base

$$M = Fs = \int_o^{S_o} \frac{1}{2} \rho V^2 \times 1.1 \cos^2 \theta \; t \; s \; ds$$

$$M = 0.55 \; t \cos^2 \theta \int_o^{S_o} \rho V^2 \; s \; ds$$

where ρ and V are functions of altitude and thus s.

The cable also has a damping moment due to rotation and translation velocities, the latter caused by movement of the upper end of the link below. The moment equation thus becomes

$$M = 0.55 \; t \cos^2 \theta \int_o^{S_o} \rho \; (V + u + s \dot{\theta} \cos \theta)^2 \; s \; ds$$

The vertical component of the velocity is small and has a secondary effect only changing θ a small amount. Accordingly, it was not included in the damping equation.

For convenience in handling this mathematically and to arrive at a damping number, it is assumed temporarily that V and ρ are not significant functions of s.

$$M = 0.55\ \rho\ t\ \cos^2\theta \left|_{o}^{s_o} \frac{(V + u + s\ \dot{\theta}\ \cos\theta)^4}{4\ \dot{\theta}^2\ \cos^2\theta}\right.$$

$$- \frac{(V + u)\ (V + u + s\ \dot{\theta}\ \cos\theta)^3}{3\ \dot{\theta}^2\ \cos^2\theta}$$

$$M = \frac{0.55\ \rho\ t\ s^2\ \cos^2\theta}{12}\ (8\ Vs\ \dot{\theta}\ \cos\theta + 6\ V^2 + 12\ Vu + 8\ u\ s\ \dot{\theta}$$

$$\cos\theta + 6u^2 + 3\ s^2\dot{\theta}^2\ \cos^2\theta)$$

Differentiating,

$$\frac{\partial M}{\partial \dot{\theta}} = \frac{0.55\ \rho\ t\ s^2\ \cos^2\theta}{12}(8\ Vs\ \cos\theta + 8\ u\ s\ \cos\theta + 6\ s^2\ \dot{\theta}\ \cos^2\theta)$$

Allow u and $\dot{\phi} \longrightarrow 0$

$$\frac{\partial M}{\partial \dot{\theta}} = 0.366\ \rho V\ t\ s^3\ \cos^3\theta$$

Motions of the link below this one also introduces a damping force on this link. This can be resolved by differentiating the moment with respect to this velocity u.

$$\frac{\partial M}{\partial u} = \frac{0.55\ \rho\ t\ s^2\ \cos^2\theta}{12}\ (12\ v + 8\ s\ \dot{\theta}\ \cos\theta + 12\ u)$$

Allow u and $\dot{\phi} \longrightarrow 0$.

$$\frac{\partial M}{\partial u} = 0.55\ \rho V\ t\ s^2\ \cos^2\theta$$

SECTION VI

BALLOON/CABLE SYSTEMS

1. STATIC SOLUTIONS

The balloon aerostatic lift capability in no wind, and tether weight for the proper strength tether as determined by survival wind, are plotted in Figures 37 through 41 for the several balloon configurations and payload/altitude criteria. Net static lift, L_S, is gross aerostatic lift less balloon weight and payload weight. Tether weight for lengths from sea-level vertically to design altitude (of breaking strength appropriate to the survival loads x factor of safety) is plotted as a function of balloon volume. The intersection of the two curves indicates the minimum balloon size which is aerostatically adequate. A given balloon/cable combination which is statically adequate may not be operationally adequate; the balloon total lift and drag under the operational wind profile may be inadequate to support the greater length (and weight) of tether which must be paid out under the wind condition, and the system may not be able to maintain design altitude.

The cable solutions for the various balloon/cable systems shown in this section have been solved by the Appendix I program for the operational wind profile, and provide satisfactory solutions both in operational as well as no wind. Results are tabulated in the following section.

Initially, it was intended to size balloons with approximately a 10 percent excess of buoyant lift for static conditions. One of the parameters to be varied during the study of dynamic behavior is "free" lift. However a number of practical problems interfere with this goal.

Since the wire rope must be used in specific sizes available, the weight curves for this tether have a typical stair-step shape. Balloon sizes usable are not smoothly variable but must be selected in jumps. A considerable increase in balloon size may be involved in moving from one rope size to the next. For the wire rope, the largest balloon with the smallest cable which provided a positive static solution was always chosen. For instance a BJ balloon at 10,000 feet was sized at 75,000 cubic feet with a 1/4-inch wire rope. The minimum size possible with a 1/4-inch rope would be 65,000 cubic feet with no "free" lift. A larger size than 75,000 cubic feet necessitates a 5/16-inch wire rope, and sizes of 85,000 to 117,000 cubic feet. To keep balloon sizes minimal within these constraints, it was not always possible to achieve 10 percent excess buoyancy.

At 20,000 feet, static solutions are not possible with the wire rope (see Figure 41). For the BJ balloon the minimum static solution is with a 320,000 cubic feet volume for NOLARO tether. A 500,000 cubic foot size has been selected and this size provides approximately a 6 percent excess static buoyancy. Ten percent excess buoyancy requires a 700,000 cubic foot size.

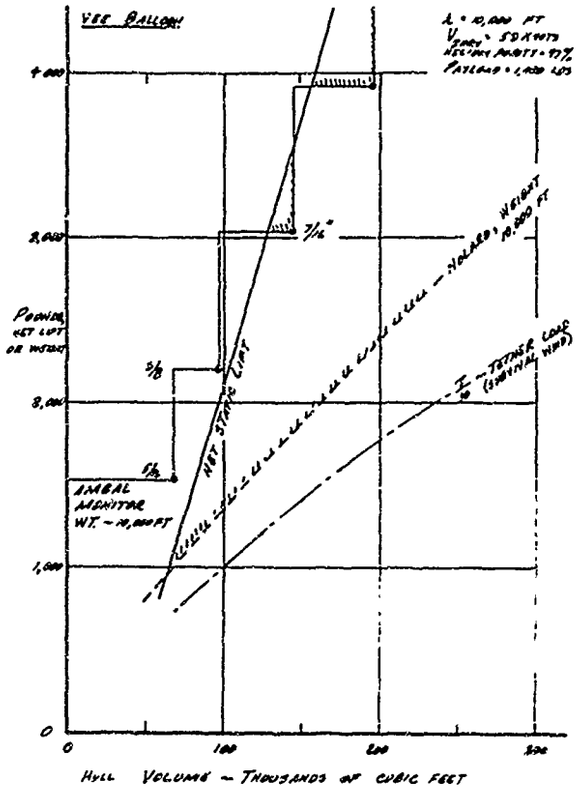

Figure 37. Vee Balloon System, Static Solution for 10,000 Feet Altitude

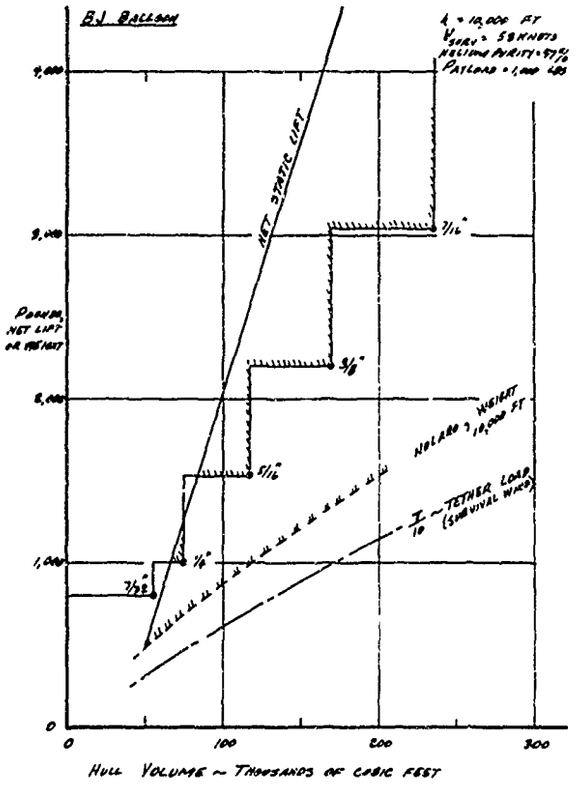

Figure 38. BJ Balloon System, Static Solution for 10,000 Feet Altitude

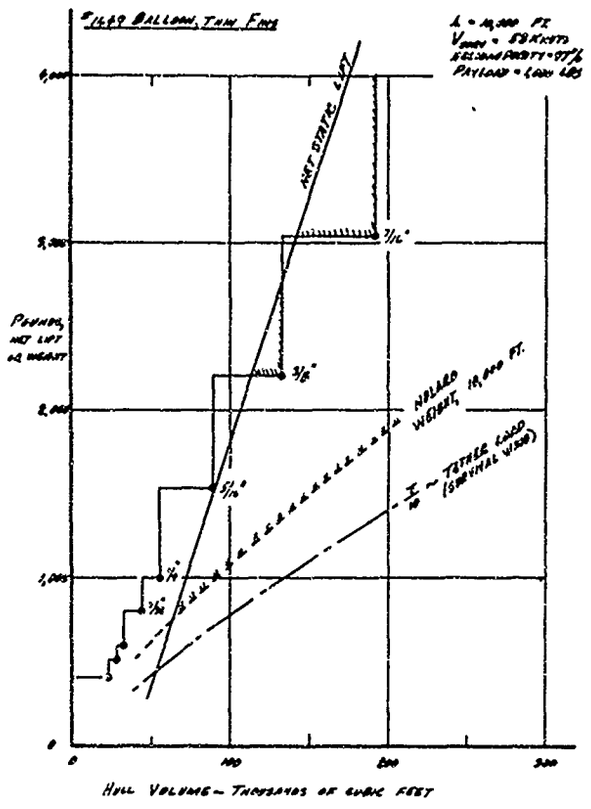

Figure 39. GAC No. 1649 Balloon System, Static Solution for 10,000 Feet Altitude

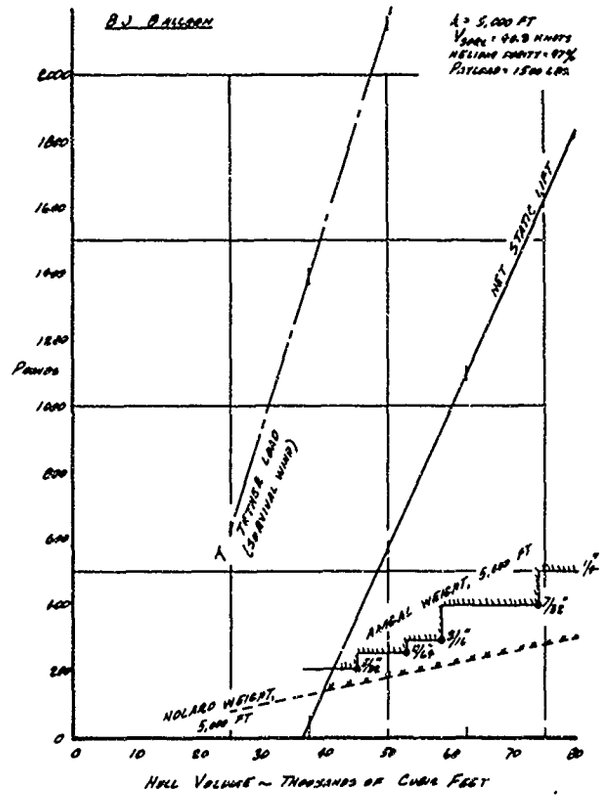

Figure 40. BJ Balloon System, Static Solution for 5,000 Feet Altitude

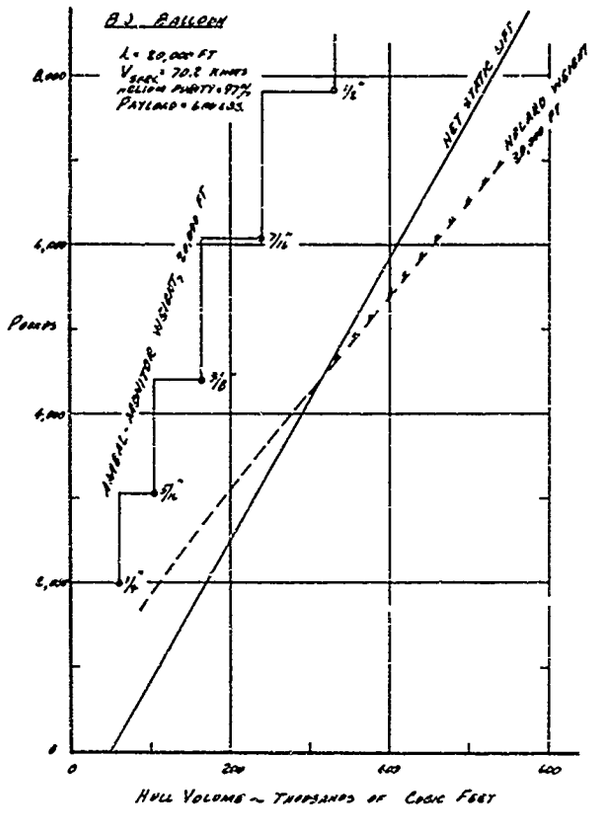

Figure 41. BJ Balloon System, Static Solution for 20,000 Feet Altitude

Table XII summarizes the balloon/cable systems of the several balloon configurations. The BJ shape has been selected and sized for the 5,000 and 20,000 foot altitudes as representing the lightest and thus the smallest possible system of those investigated.

For all single hull balloons (BJ and No. 1649) only the hull was assumed helium inflated; i.e., hull volume is total helium volume at design altitude, and with helium purity of 97 percent.

With the Vee-balloon, the empennage is helium inflated and adds 6.7 percent volume to the reference hull volume (see Table II, Section II). Unless otherwise stipulated, the Vee-balloon volumes quoted in this report are hull volume only.

Table XII includes balloon weight, net static lift, and operational and survival aerodynamic loads developed by the balloon. Tethers are sized with a factor of safety of 1.50 for Amgal-Monitor and 2.00 for NOLARO. Despite these factors the NOLARO permits smaller total systems throughout the design range.

2. DESIGN LOADINGS

Tether loading is the vector sum of L_s, net static lift; L_a, aerodynamic lift; and, D, aerodynamic drag. $L_s + L_a = L_N$, or total lift. Tether angle from the vertical is the angle defined by L_N/D.

Table XII loadings for operational wind are applied to the selected cables with results presented in Section VII.

Table XII. Summary of Balloon/Cable Systems

Balloon Type	h	Hull Volume (ft^3)	Gross Static Lift (lb)	W_B (lb)	P (lb)	L_s (lb)	Survival				Operational				Tether		
							L_a (lb)	D (lb)	L_N (lb)	T (lb)	L_a (lb)	D (lb)	L_N (lb)	T (lb)	Type	O.D. (in)	B.S. ①(lb)
BJ	5,000	46,000	2,534	635	1,500	399	1,391	656	1,790	1,906	659	351	1,058	1,115	NOLARO	0.321	3,813
Vee-Balloon	10,000	80,000 (85,363)[1]	4,029	1,541	1,000	1,488	6,427	2,422	7,916	8,278	4,437	1,514	5,925	6,116	NOLARO	0.585	16,600
		144,000 (153,654)[1]	7,253	2,712	1,000	3,541	9,509	3,583	13,050	13,533	6,564	2,239	10,105	10,350	AMGAL	7/16	20,000
BJ		60,000	2,832	1,031	1,000	801	2,706	1,219	3,507	3,713	1,391	651	2,192	2,287	NOLARO	0.410	7,540
		75,000	3,540	1,276	1,000	1,264	3,140	1,414	4,405	4,626	1,614	755	2,878	2,975	AMGAL	1/4	6,750
#1649 w/ Thin Fins		80,000	3,776	1,548	1,000	1,228	4,963	1,346	6,191	6,336	2,508	757	3,736	3,812	NOLARO	0.320	12,700
		133,000	6,278	2,511	1,000	2,767	6,965	1,887	9,732	9,913	3,519	1,061	6,286	6,376	AMGAL	3/8	14,800
BJ	20,000	500,000	17,037	8,933	600	7,504	15,420	6,785	22,924	23,907	7,571	3,577	15,075	15,494	NOLARO	0.993	47,814

( )[1] Total Helium Volume

① Reference Table XI and Figures 35 and 36

SECTION VII

TETHER CABLE PROFILE PARAMETERS

The profile parameters chosen for representation are the angle between the cable and the vertical at the bottom end of the cable (θ_B), the top end excursion or downwind displacement relative to the bottom end (d), and the total weight of the cable segment (W_c). A supplemental factor is presented in conjunction with θ_B to define the altitude (h_1) at which θ_B occurs. These parameters are illustrated in Figure 42.

Occasions arise where the cable segment becomes horizontal at a point above mean sea level, in which case the factor h_1 is used to define altitude at which a second balloon must be added.

Float altitudes were selected as 5,000, 10,000 and 20,000 feet above MSL. Wind profile is presented in Section I. Cable types are based on the information presented in Sections V and VI.

Flexibility of the cable design solution is made possible by use of the equations given in Reference 15. GAC's IBM S/360, Model 40, digital computer was used for solutions of these equations. The computer program is flexible in that specific values of cable weight and diameter can be assumed, or cable weight, diameter, and breaking strength can be assumed to be a function of cable tension. Any float altitude, wind profile, and cable strength/weight/diameter relation may be specified. Design curves are then obtained by specifying particular values of L_N and L_N/D.

Results of these profile calculations show comparative performance. Derivation of the difference equations and equations defining cable properties are given in Appendix I.

Table XIII presents a typical computer printout, the NOLARO cable for the 46,000 cubic foot BJ balloon, h = 5,000 feet. F_Z and F_X are L_N and D from Table XII, Section VI, for the operational wind.

In the printout:
- x is downwind displacement (ft)
- z is distance down from design altitude (ft)
- PHI is tether angle to the vertical (deg)
- T is tether tension (lb)
- Length is running summation of tether length (ft)
- Velocity is windspeed at that altitude (fps)
- Diameter is tether diameter (ft)
- Weight is tether weight (lb/ft)

Table XIV is a summary of the cable solutions for the eight specific balloon/cable systems.

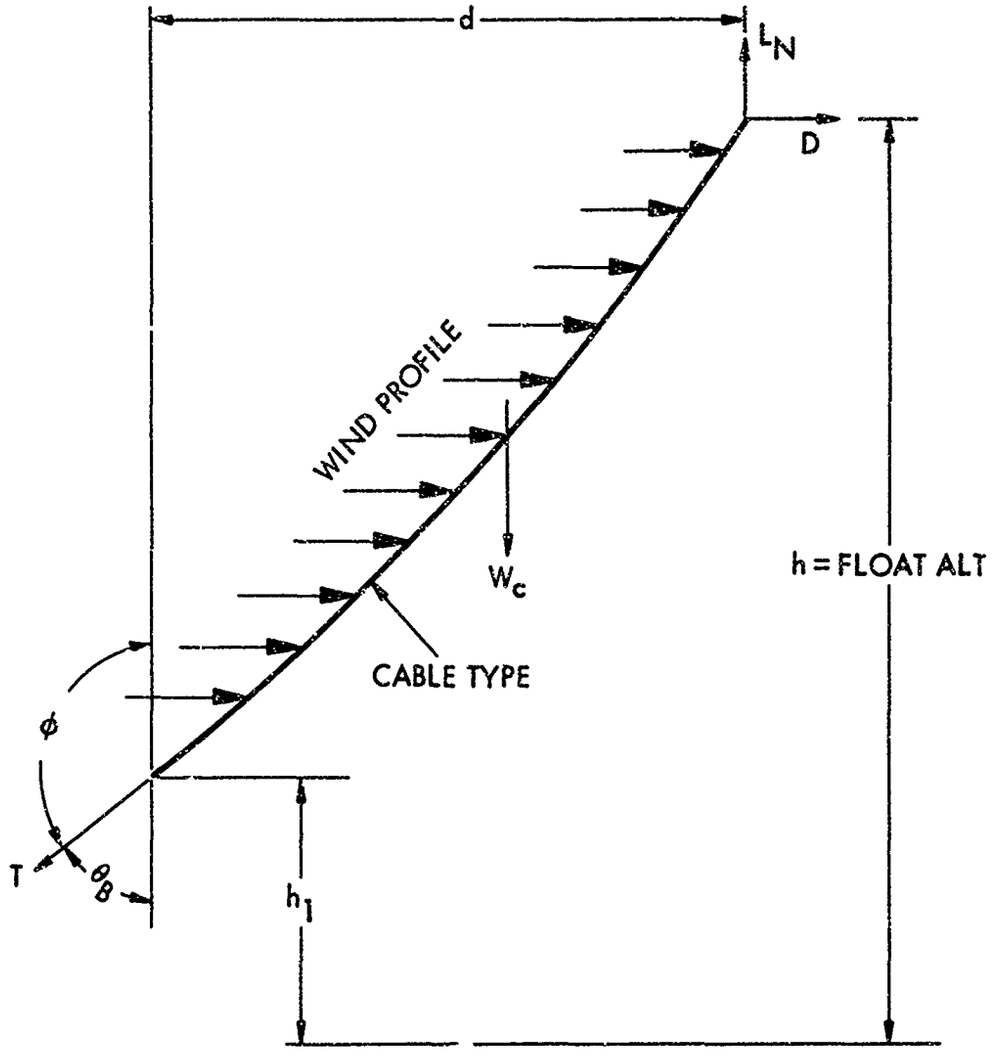

Figure 42. Tether Cable Profile Parameters

Table XIII. Cable Solution for NOLARO Cable For 46,000 Ft^3 BJ Balloon in Operational Wind

NOLARO .32 3813 LBS 8.S

EA626

X	Y	Z	THETA	PHI	T	LENGTH	ALPHA	VELOCITY	DIAMETER	WEIGHT
0.	0.	0.	180.0	161.6	1115.	0.	0.0	52.37	0.02679	0.03211
-63.	0.	-190.	180.0	160.8	1109.	200.	-0.0	51.55	0.02679	0.03211
-129.	0.	-379.	180.0	159.9	1103.	400.	-0.0	50.74	0.02679	0.03211
-198.	0.	-567.	180.0	159.1	1097.	600.	-0.0	49.93	0.02679	0.03211
-269.	0.	-753.	180.0	158.3	1091.	800.	-0.0	49.12	0.02679	0.03211
-343.	0.	-939.	180.0	157.4	1085.	1000.	-0.0	48.32	0.02679	0.03211
-420.	0.	-1124.	180.0	156.7	1079.	1200.	-0.0	47.45	0.02679	0.03211
-499.	0.	-1307.	180.0	155.9	1074.	1400.	-0.0	46.54	0.02679	0.03211
-581.	0.	-1490.	180.0	155.1	1068.	1600.	-0.0	45.64	0.02679	0.03211
-665.	0.	-1671.	180.0	154.4	1062.	1800.	-0.0	44.74	0.02679	0.03211
-751.	0.	-1852.	180.0	153.7	1056.	2000.	-0.0	43.85	0.02679	0.03211
-840.	0.	-2031.	180.0	153.0	1051.	2200.	-0.0	42.94	0.02679	0.03211
-930.	0.	-2209.	180.0	152.3	1045.	2400.	-0.0	41.89	0.02679	0.03211
-1021.	0.	-2386.	180.0	151.7	1039.	2600.	-0.0	40.84	0.02679	0.03211
-1118.	0.	-2563.	180.0	151.0	1034.	2800.	-0.0	39.80	0.02679	0.03211
-1215.	0.	-2738.	180.0	150.4	1028.	3000.	-0.0	38.77	0.02679	0.03211
-1314.	0.	-2912.	180.0	149.8	1023.	3200.	-0.0	37.74	0.02679	0.03211
-1414.	0.	-3084.	180.0	149.3	1017.	3400.	-0.0	36.58	0.02679	0.03211
-1516.	0.	-3256.	180.0	148.7	1012.	3600.	-0.0	35.26	0.02679	0.03211
-1620.	0.	-3427.	180.0	148.2	1006.	3800.	-0.0	33.95	0.02679	0.03211
-1726.	0.	-3597.	180.0	147.7	1001.	4000.	-0.0	32.65	0.02679	0.03211
-1833.	0.	-3766.	180.0	147.2	995.	4200.	-0.0	31.36	0.02679	0.03211
-1941.	0.	-3934.	180.0	146.7	990.	4400.	-0.0	30.08	0.02679	0.03211
-2051.	0.	-4101.	180.0	146.2	985.	4600.	-0.0	28.29	0.02679	0.03211
-2162.	0.	-4268.	180.0	145.8	979.	4800.	-0.0	26.18	0.02679	0.03211
-2275.	0.	-4433.	180.0	145.4	974.	5000.	-0.0	24.08	0.02679	0.03211
-2389.	0.	-4598.	180.0	145.0	969.	5200.	-0.0	21.99	0.02679	0.03211
-2503.	0.	-4762.	180.0	144.7	964.	5400.	-0.0	19.91	0.02679	0.03211
-2618. 2672	0.	-4925. 5000'	180.0	144.3	144.2° 958.	956# 5600.	5692' -0.0	17.84	0.02679	0.03211
-2735.	0.	-5087.	180.0	144.0	953.	5800.	-0.0	15.78	0.02679	0.03211

ALTITUDE IS BELOW LOWER LIMIT

183#

TOTAL CABLE WEIGHT 186.23792

Table XIV. Summary of Cable Solutions

Balloon Type	Altitude (ft)	Hull Volume (ft^3)	Tether Type	B.S. (lb)	O.D. (ft)	Wt/Ft (lb/ft)	X (ft)	ϕ (deg)	T (lb)	Length (ft)	Total Tether Weight (lb)
BJ	5,000	46,000	NOLARO	3,813	0.02679	0.03211	0	161.6	1,115	0	--
h = 5,000 ft P = 1,500 lb	S.L.						2,672	144.2	956	5,692	183
Vee-Balloon	10,000	80,000	NOLARO	16,600	0.04875	0.11400	0	165.7	6,115	0	--
	5,000						1,775	154.7	5,552	5,314	606
h = 10,000 ft P = 1,000 lb	S.L.						4,594	146.6	4,991	11,060	1,260
	10,000	144,000	ANGAL	20,000	0.03642	0.30400	0	167.5	10,350	0	--
	5,000						1,389	160.8	8,836	5,193	1,580
	S.L.						3,452	153.9	7,300	10,605	3,230
BJ	10,000	60,000	NOLARO	7,540	0.03420	0.05600	0	163.4	2,287	0	--
	5,000						2,456	143.6	2,036	5,600	314
h = 10,000 ft P = 1,000 lb	S.L.						7,377	127.7	1,761	12,639	708
	10,000	75,000	ANGAL	6,750	0.02083	0.09970	0	165.3	2,975	0	--
	5,000						1,643	153.2	2,482	5,340	532
	S.L.						5,072	140.3	1,989	11,305	1,128
#1649 w/Thin Fins	10,000	80,000	NOLARO	12,700	0.04330	0.0900	0	168.5	3,812	0	--
	5,000						1,702	153.0	3,374	5,298	476
h = 10,000 ft P = 1,000 lb	S.L.						4,950	141.1	2,930	11,274	1,015
	10,000	133,000	AMGAL	14,800	0.03125	0.22000	0	170.4	6,375	0	--
	5,000						1,193	161.8	5,281	5,145	1,132
	S.L.						3,253	152.7	4,187	10,559	2,325
BJ	20,000	500,000	NOLARO	47,814	0.08281	0.32427	0	166.7	15,494	0	--
	15,000						1,646	155.9	13,897	5,272	1,710
	10,000						4,495	143.7	12,171	11,039	3,580
h = 20,000 ft P = 600 lb	5,000						9,106	130.2	10,702	17,856	5,790
	S.L.						17,231	112.0	9,107	27,436	8,900

APPENDIX I

CABLE PROFILE ANALYSIS[1]

1. MATHEMATICAL ANALYSIS

The mathematical analysis of a cable-balloon system subjected to a wind-vector profile involves techniques similar to those used in the solution of related cable studies arising in a variety of engineering disciplines. These studies include problems on towing cables, mooring lines, supporting cables in bridges, cable-car lines, electric power lines, submarine cables, etc. Problems of this type in their greatest generality involve determination of cable tension as well as three-dimensional cable shape for a transient condition, i.e., time-dependent cable configuration; while reduced problems involve determination of above parameters in two dimensions for transient as well as steady-state condition and also three-dimensional steady-state configuration.

Many problems have been worked out in two dimensions for a flexible cable for a steady as well as transient motion of a cable. The shape and tension of a cable subjected to a fluid flow have been studied by H. Glauert (Reference 16) for a steady condition on the assumption that the cable is uniform and the speed of the fluid is the same at every point of the cable. In this study, only the normal component of cable drag was considered, neglecting tangential or a frictional component; while a study which incorporates both the normal and the tangential components was performed by L. Landweber and M. H. Protter (Reference 17). A transient cable motion has been studied by F.O. Ringleb (Reference 18) and by T.S. Walton with H. Polacheck (Reference 19). In the former work, the change in cable tension was investigated due to a sudden impulse, while in the latter, an extensive analysis has been performed on cable tension due to a periodic motion of one end of the cable with the other end fixed.

The techniques developed for the above two-dimensional problems are useful for the three-dimensional problem at hand. The prime objective of these studies is to select appropriate balloon-cable designs such that they will be operable at a desired altitude under a variety of wind vector profiles, as well as to determine the "operative envelope", i.e., to indicate the optimum configuration of different parameters for various operative conditions.

2. STEADY CONDITION

The problem for a steady-state condition is to determine the tension in a cable as well as the shape, with one end of the cable attached to a free balloon at a given altitude and the other end fixed at the ground. From this then, it is possible to determine the elevation required at tether site. In the solution of the problem, the variation of the following parameters is considered:

(1) Wind-vector profile in the operating range
(2) Wind-vector at float altitude
(3) Float altitude
(4) Terrain height at tether side (determined parameter)
(5) Cable geometry - diameter as function of cable length
(6) Cable weight/length as function of cable length
(7) Cable weight
(8) Balloon buoyancy and drag at float altitude.

To evaluate the effect of these parameters on cable form and tension, a mathematical model is developed incorporating these quantities.

[1] Subsections 1 through 4 of this appendix are excerpts from Reference 15, pages 3-93 through 3-99.

3. MATHEMATICAL MODEL

In developing a mathematical model for the steady-state condition, a set of assumptions are imposed so as to make the problem tractable. It is assumed that the only forces acting on a cable element are the gravity force, pressure drag force, and tension. The gravity is assumed to be uniform in the operating range in the light of the fact that the change is approximately 1.0 percent. The skin-friction drag is neglected due to the fact that the skin-fraction drag coefficient is smaller by two orders of magnitude as compared to basic drag coefficient (see Reference 14) and the fact that the cable is nearly vertical. The buoyancy on the cable is negligible compared to other forces and also is not taken into account. It is assumed that the moments are not transmitted in the cable, thus implying that the cable is perfectly flexible. A physical assumption made is that the drag force on the cable element normal to the element can be determined using the wind vector component normal to the element. This is so-called cosine or sine principle, depending on the definition of angle of attack.

Selecting the origin of the coordinate system at the balloon (see Figure 43) and equating the sum of the forces on an infinitesimal cable element to zero, three equations are obtained.

$$\left.\begin{aligned} &(ds)\ F'_{unx} - (T \sin \phi \cos \theta)_s + (T \sin \phi \cos \theta)_{s+ds} = 0 \\ &(ds)\ F'_{uny} - (T \sin \phi \sin \theta)_s + (T \sin \phi \sin \theta)_{s+ds} = 0 \\ &(ds)\ F'_{unz} - (T \cos \phi)_s + (T \cos \phi)_{s+ds} - \omega(ds) = 0 \end{aligned}\right\} \quad (1)$$

where

T is cable tension

s is length of cable from the origin to the element

ds is infinitesimal cable length

ϕ and θ are spherical coordinates that determine the direction of tangent vector to the cable at position s

ω is weight of cable/length as function of s

u is magnitude of wind-vector as function of z

α is direction of wind-vector horizontally as function of z (the vertical is neglected)

F'_{unx} is drag force on cable element/length in x direction

F'_{uny} is drag force in y direction

F'_{unz} is drag force in z direction.

To evaluate the drag forces, a normal component of the wind-vector has to be computed (as mentioned above) from which the drag force normal to the element can be evaluated, leading thus to the desired results, which become:

$$\left.\begin{aligned} F'_{unx} &= D\,[\cos \alpha - \sin^2 \phi \cos \theta \cos (\theta - \alpha)] \\ F'_{uny} &= D\,[\sin \alpha - \sin^2 \phi \sin \theta \cos (\theta - \alpha)] \\ F'_{unz} &= -D\,[\sin \phi \cos \phi \cos (\theta - \alpha)] \end{aligned}\right\} \quad (2)$$

with

$$D = 1/2\, \rho C_D d \left| [1 - \sin^2 \phi \cos^2 (\theta - \alpha)]^{1/2} \right| u^2,$$

where

u is wind speed

ρ is air density as function of z

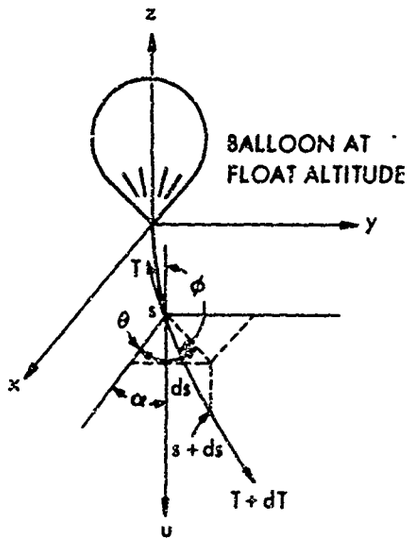

Figure 43. Coordinate System

C_D is cable drag coefficient

d is diameter of cable as function of s.

Dividing each of the equations in set 1 by (ds) and in the limit as ds$\longrightarrow$0, the following differential equations are obtained:

$$\left.\begin{aligned} \frac{d}{ds}\ (T \sin\phi \cos\theta) + F'_{unx} &= 0 \\ \frac{d}{ds}\ (T \sin\phi \sin\theta) + F'_{uny} &= 0 \\ \frac{d}{ds}\ (T \cos\phi) + F'_{unz} - \omega &= 0 \end{aligned}\right\} \qquad (3)$$

with the boundary conditions $T = T_o$, $\theta = \theta_o$, and $\phi = \phi_o$ at $s = s_o$. It is of interest to note at this point that for u = o everywhere (except at float altitude) and ω independent of s, the above three differential equations simplify to a simple equation, which is the equation of a catenary:

$$A\ \frac{d^2y}{dx^2} = \omega\sqrt{1 + \left(\frac{dy}{dx}\right)^2}$$

where A is arbitrary.

To find an analytical solution to the three differential equations is an extremely difficult, if not impossible, task since the diameter of a cable and the linear density are arbitrary functions of s as well as wind-vector profile and air density are both functions of z. In the light of these facts, an approximate technique has to be developed. This is accomplished by representing the differential equations by a set of difference equations which can easily be evaluated by means of a digital computer. Denoting the position s on a cable by i and the position s + ds by i + 1, the following set of equations result from set 3:

$$\theta_{i+1} = \theta_i + \arctan\left[\frac{(ds)\ F'_{unxi} \sin\theta_i - (ds)\ F'_{unyi} \cos\theta_i}{T_i \sin\phi_i - (ds)\ F'_{unxi} \cos\theta_i - (ds) F_{unyi} \sin\theta_i}\right]$$

$$\phi_{i+1} = \phi_i + \arctan$$

$$\left\{ \frac{\left[T_i \sin\phi_i \sin\theta_i - (ds)F'_{unyi}\right] - \sin\theta_{i+1} \tan\phi_i \left[T_i \cos\phi_i + \omega_i(ds) - (ds)\,F_{unzi}\right]}{\sin\theta_{i+1}\left[T_i \cos\phi_i + \omega_i\,(ds) - (ds)F'_{unzi}\right] + \tan\phi_i\left[T_i \sin\phi_i \sin\theta_i - (ds)\,F_{unyi}\right]} \right\}$$

$$T_{i+1} = \frac{\omega_i\,(ds) + T_i \cos\phi_i - (ds)\,F'_{unzi}}{\cos\phi_{i+1}}$$

$$z_{i+1} = (ds) \sum_{k=0}^{i} \cos\phi_k$$

$$x_{i+1} = (ds) \sum_{k=0}^{i} \sin\phi_k \cos\theta_k$$

$$y_{i+1} = (ds) \sum_{k=0}^{i} \sin\phi_k \sin\theta_k$$

This set of six equations together with boundary conditions are used to compute cable form as well as the tension for a given wind-vector profile and a given cable hence known d = d(s) and $\omega = \omega(s)$. It is of importance to get an approximate error resulting from the difference equations. An estimate of this is presented below.

4. ERROR ANALYSIS

The errors in the cable form and tension resulting from approximate computing technique depends, of course, on the magnitude of cable increment chosen for the computation - the smaller the increment the greater the accuracy in the two quantities. However, with decreasing increment the computation time increases, thus leading to a trade-off between accuracy and cost. Preliminary analysis indicates that the ratio (ds) (cable length) in the range 1/200 to 1/240 is quite satisfactory to satisfy the two requirements.

The comparison of the approximate solutions is possible with an exact one in special cases, i.e., when the differential equations can be solved analytically. Such a comparison has been made with the result that the errors in cable position and tension increase with cable length, as would be expected, with maximum errors of 0.75 and 0.45 percent, respectively, at approximately half of the required length. The maximum error for the entire cable would be nearly double these numbers.

5. SOLUTIONS OF DIFFERENCE EQUATIONS

The differential equations in subsection C lead to difference equations in unknowns θ, σ, and T. The difference equations were derived as follows:

$$T_{i+1} \sin\phi_{i+1} \cos\theta_{i+1} - T_i \sin\sigma_i \cos\theta_i + F'_{unx}\,\Delta S = 0$$

$$T_{i+1} \sin\phi_{i+1} \sin\theta_{i+1} - T_i \sin\sigma_i \sin\theta_i + F'_{uny}\,\Delta S = 0$$

$$T_{i+1} \cos\phi_{i+1} - T_i \cos\phi_i + F'_{unz}\,\Delta S - \omega\,\Delta S = 0.$$

Solutions for unknowns θ, ϕ, and T are found sequentially.

$$\tan \theta_{i+1} = \frac{T_i \sin \phi_i \sin \theta_i - F'_{uny} \Delta S}{T_i \sin \phi_i \cos \theta_i - F'_{unx} \Delta S}$$

$$\tan \phi_{i+1} = \frac{T_i \sin \phi_i \sin \theta_i - F'_{uny} \Delta S}{(T_i \cos \phi_i - F'_{unz} \Delta S + \omega \Delta S) \sin \theta_{i+1}}$$

For small values of θ_{i+1} where $\sin \theta_{i+1} \rightarrow 0$, an alternate equation is used.

$$\tan \phi_{i+1} = \frac{T_i \sin \phi_i \cos \theta_i - F'_{unx} \Delta S}{(T_i \cos \phi_i - F'_{unz} \Delta S + \omega \Delta S) \cos \theta_{i+1}}$$

Then to avoid angle adjustment due to quadrant variations, the solutions for θ and ϕ are changed to difference equations by the identity

$$\tan (a - b) = \frac{\tan a - \tan b}{1 + \tan a \tan b}.$$

Tan $(\theta_{i+1} - \theta_i)$ and tan $(\phi_{i+1} - \phi_i)$ are therefore computed before solving for θ_{i+1} and ϕ_{i+1}. Then

$$T_{i+1} = \frac{T_i \cos \phi_i - F'_{unz} \Delta S + \omega \Delta S}{\cos \phi_{i+1}}$$

unless $\phi_{i+1} \rightarrow$ 90 degrees where $\cos \phi_{i+1} \rightarrow 0$. But if $\phi_{i+1} \rightarrow 90$ degrees, the computation is terminated, since at ϕ_{i+1} = 90 degrees, the cable is parallel to the ground plane.

APPENDIX II

DETAILED ANALYSIS OF TETHERED AERODYNAMICALLY SHAPED BALLOONS

1. GENERAL

This appendix contains additional information on the physical dimensions, stress analysis, and weight analysis of the aerodynamically shaped balloons.

2. PHYSICAL SHAPE

For geometrically similar balloons, the linear dimensions are proportional to the one-third power of balloon volume, and the surface area is proportional to the two-thirds power of balloon volume. Therefore, the various lengths and surface areas for various balloon shapes can be obtained by determining the appropriate proportionality constants. These scaling factors (proportionality constants) were based on wind tunnel models or actual balloon designs.

Table XV, which contains scaling factors, and the relationships listed below were used in the computer program to determine the physical size for each balloon shape.

Hull Length (ft)

$$L = K_1 \forall^{1/3} \tag{4}$$

Maximum Hull Diameter (ft)

$$D = \frac{1}{f} L \tag{5}$$

Wetted Hull(s) Area (ft^2)

$$A_h = K_3 \forall^{2/3} \tag{6}$$

Projected Area of One Horizontal Tail (ft^2)

$$A_{pht} = K_4 \forall^{2/3} \tag{7}$$

Projected Area of One Vertical Tail (ft^2)

$$A_{pvt} = K_5 \forall^{2/3} \tag{8}$$

Location of Maximum Diameter (ft)

$$L_{max\ d} = K_L L \tag{9}$$

Wetted Area of One Horizontal Tail (ft^2)

$$A_{wht} = K_h A_{pht} \tag{10}$$

Wetted Area of One Vertical Tail (ft^2)

$$A_{wvt} = K_v A_{pvt} \tag{11}$$

Table XV. Proportionality Constants for the Physical Dimensions of Various Aerodynamically Shaped Balloons

Proportionality Constant	Symbol	Used in Eq	Balloon Type			
			Vee-Balloon	BJ	GAC Single Hull	
					Thin Fin	Thick Fin
Hull Length	K_1	4	2.56	2.35	2.67	2.67
Fineness Ratio	f	5	4.00	2.49	3.00	3.00
Wetted Hull(s) Area	K_3	6	6.97	5.412	5.795	5.795
Projected Area of One Horizontal Tail	K_4	7	0.707	0.23	0.37	0.37
Projected Area of One Vertical Tail	K_5	8	0.0785	0.36	0.37	0.37
Location of Maximum Diameter	K_L	9	0.45	0.287	0.300	0.300
Wetted Area of One Horizontal Tail	K_h	10	2.21	2.33	2.16	2.44
Wetted Area of One Vertical Tail	K_v	11	2.32	2.33	2.16	2.44
Tail Thickness	K_t	12	0.191	0.374	0.163	0.432
Number of Horizontal Tails	n_{ht}	16	1	2	2	2
Number of Vertical Tails	n_{vt}	16	2	1	1	1
Hull Intersect Area	K_{int}	20	0.336	0	0	0
Gas Leakage Rate Constant	K_{le}	21	← 0.00639 $ft^3/ft^2/day$ →			
Ratio of Temp Difference over Avg Temp at Altitude	K_{temp}	22	0.1	0.1	0.1	0.1

Average Thickness of Horizontal Tail (ft)

$$h_{hta} = K_t \sqrt{A_{pht}} \tag{12}$$

Average Thickness of Vertical Tail (ft)

$$h_{vta} = K_t \sqrt{A_{pvt}} \tag{13}$$

Volume of One Horizontal Tail (ft^3)

$$\forall_{ht} = h_{hta} A_{pht} \tag{14}$$

Volume of One Vertical Tail (ft^3)

$$\forall_{vt} = h_{vta} A_{pvt} \tag{15}$$

Volume of Total Balloon (ft^3)

$$\forall_{tot} = \forall + n_{ht} \forall_{ht} + n_{vt} \forall_{vt} \tag{16}$$

Ballonet Volume (ft^3)

$$\forall_{bnt} = \left(1 - \frac{\rho_{alt}}{\rho_0}\right)\forall_{tot} \tag{17}$$

Diameter of Spherical Ballonet (ft)

$$D_{bnt} = 1.24\left(\forall_{bnt}\right)^{1/3} \tag{18}$$

Wetted Area of Spherical Ballonet (ft^2)

$$A_{bnt} = 4.84\left(\forall_{bnt}\right)^{2/3} \tag{19}$$

Hull Intersect Area (ft^2)

$$A_{int} = K_{int}\,\forall^{2/3} \tag{20}$$

Volume of Gas Lost by Leakage (ft^3/day)

$$\forall_{leak} = K_{le}\left(A_h + n_{ht}A_{wht} + n_{vt}A_{wvt}\right) \tag{21}$$

Volume due to Temperature Change at Float Altitude per Day (ft^3/day)

$$\forall_{temp} = K_{temp}\,\forall_{tot} \tag{22}$$

3. STRESS ANALYSIS

a. General

As noted in the text of the report, the design stress used in the balloon analysis was the sum of the stresses caused by the internal pressure, buoyant lift, hull bending moment and aerodynamic load with the appropriate factor of safety.

$$N_{des} = F.S.\left(N_i + N_b + N_{bm} + N_a\right)$$

where

N_{des} is design stress for selection of balloon material (lb/ft)

F.S. is factor of safety

N_i is stress due to internal pressure (lb/ft)

N_b is stress due to buoyant lift (lb/ft)

N_{bm} is stress due to hull bending moment

N_a is stress due to aerodynamic loads (lb/ft).

Maximum stresses on the balloon due to internal pressure and buoyant lift occur at the maximum diameter of the balloon. Maximum stresses due to aerodynamic loads occur somewhat forward of the maximum diameter, but for this analysis, were conservatively assumed to act at the maximum diameter. Therefore, the location of maximum stress occurs at the maximum diameter just above the attachment points of the balloon suspension (bridle) system, which were assumed to be attached near the equator of the balloon. The calculations given in the following paragraphs determine the stresses in the balloon skin at the equator.

b. Stress due to Internal Pressure

The required balloon internal pressure at altitude, as explained in Section V, was selected to be 15 percent greater than the dynamic pressure at altitude, or 1.4 in. H_2O = 1.3 lb/ft^2, whichever is greater. Therefore, P_i = 1.15q or 1.30 lb/ft^2, whichever is greater. This pressure was assumed to be at the bottom of the balloon.

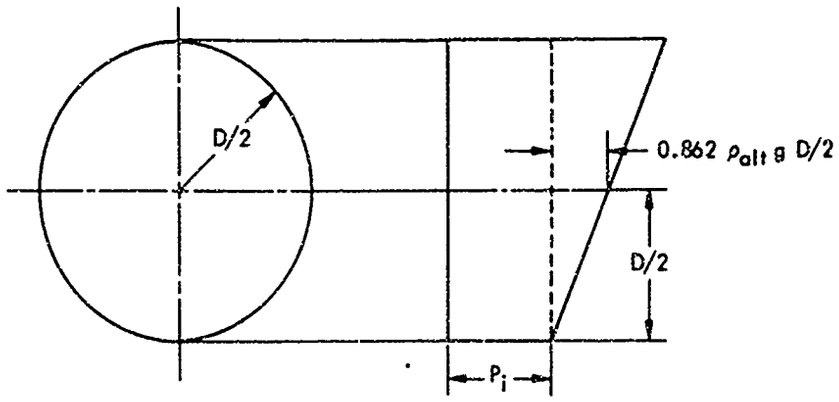

Figure 44. Internal Pressure Occurring in the Balloon at the Maximum Diameter

Referring to Figure 44, the pressure at the balloon equator is

$$P_{eq} = P_i + 0.862\,\rho_{alt}\,g\,\frac{D}{2}\,.$$

The second term represents the helium pressure head at altitude between the bottom of the balloon and the equator.

The maximum internal pressure stress is

$$N_i = P_{eq}\,\frac{D}{2}$$

$$= \left(P_i + 0.862\,\rho_{alt}\,g\,\frac{D}{2}\right)\frac{D}{2}\ \text{lb/ft.} \qquad (24)$$

c. Stress due to Buoyant Lift

From Figure 45, the maximum stress due to buoyant load at altitude acting on a one-foot section of the hull is

$$N_b = \frac{1}{2}\left[L_b(\text{one-foot section})\right]$$

where

L_b = buoyant lift of helium at altitude

= b x volume of the section.

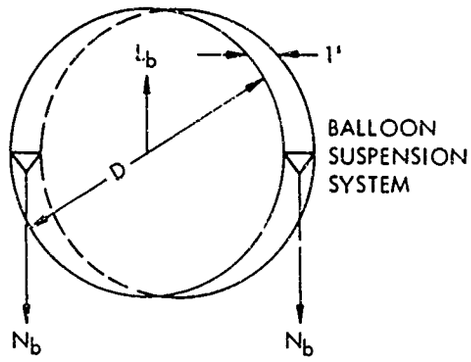

Figure 45. Buoyant Force on Balloon at the Maximum Diameter

Therefore,

$$N_b = \frac{1}{2}\left[(0.862\,\rho_{alt}\,g)\left(\pi\,\frac{D^2}{4}\right)\right]\text{lb/ft.} \qquad (25)$$

d. Stress due to due to Hull Bending Moment

The stress due to aerodynamic bending moment for design q at altitude for the typical hull/suspension arrangements is:

$$N_{bm} = 0.123q\,\forall^{1/3}\ \text{(lb/ft) for all single hulls} \qquad (25a)$$

$$N_{bm} = 0.185q\,\forall^{1/3}\ \text{(lb/ft) for Vee Balloon} \qquad (25b)$$

e. Stress due to Aerodynamic Loads

From wind tunnel tests on the General Mills Aerocap Model Balloon (Reference 20), the maximum local pressure was determined to be approximately

$$x = 0.1q\alpha$$

where

x is maximum local pressure (lb/ft^2)

q is dynamic pressure (lb/ft^2)

α is angle of attack (degrees).

This occurs at approximately 30 percent aft of the balloon nose However, for this analysis, it was assumed to act at the maximum diameter (see Figure 46).

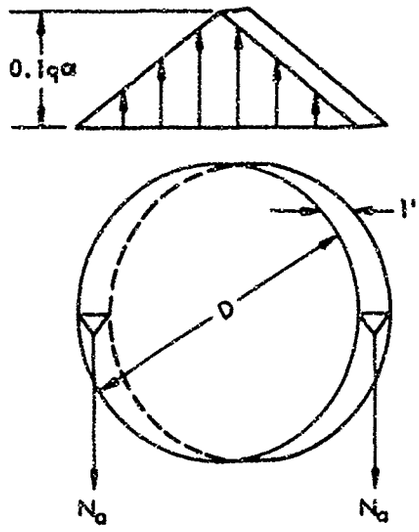

Figure 46. Assumed Aerodynamic Loading on the Maximum Diameter of the Balloon

Therefore, the total aerodynamic force acting on the one-foot section (assuming a linear load distribution) is

$$F = (x)\left(\frac{D}{2}\right) = 0.1q\,\alpha\,\frac{D}{2} \text{ lb.}$$

This load is reacted by the suspension lines of the balloon. Therefore, the stress in the fabric directly above the suspension lines is

$$N_a = \frac{1}{2} F = 0.05q\,\alpha\left(\frac{D}{2}\right) \text{ lb ft.} \qquad (26)$$

4. BALLOON WEIGHT

a. Balloon Material

Once the design stress has been determined, the unit fabric weight can be determined to be

$$w = 0.0111 + 0.344 \times 10^{-4} N_{des} \text{ lb/ft}^2 \qquad N_{des} = < 2{,}000 \qquad (27)$$

or

$$w = 0.0327 + 0.236 \times 10^{-4} N_{des} \text{ lb/ft}^2 \qquad N_{des} = > 2{,}000$$

This is the equation of the curve of Figure 21. Due to ground-handling problems, a minimum weight material of 4.7 oz/yd^2 (.0327 lb/ft^2) was assumed to be the lightest material from which an aerodynamically shaped balloon would be fabricated.

b. Hull, Tail, and Ballonet Weights

Based on the necessary unit material weight and the various physical dimensions that were calculated in the previous sections of this appendix, the hull and tail weights can be determined. However, since little differential pressure acts across the ballonet, a 4.7 oz/yd^2 (0.0327 lb/ft^2) ballonet material was assumed for all sizes of all balloon types.

Proportionality constants for the weights of components of various aerodynamically shaped balloons are given in Table XVI. The equations used in the computer solution are as follows:

Weight of Hull Fabric (lb)

$$W_{hf} = wA_h \qquad (28)$$

Table XVI. Proportionality Constants for the Weights of the Components of Various Aerodynamically Shaped Balloons

Proportionality Constant	Symbol	Used in Eq	Balloon Type			
			Vee Balloon	B J	GAC Single Hull	
					Thin Fin	Thick Fin
Factor of Safety on Fabric Stress	F.S.	23	4	→	→	→
Seam Weight	K_s	29	0.10	→	→	→
Unit Weight of Tail Fabric-Horizontal	w_{th}	32	w	.5w	.5w	.5w
Unit Weight Tail Fabric-Vertical	w_{tv}	35	w	.75w	.75w	.75w
Unit Weight of Partition Material	w_p	34	$2w_t$	→	→	→
Unit Weight of Ballonet Material	w_b	38	.0327	lb/ft^2	→	→
Power Density of Battery	K_{bat}	45-47	3600 watt minutes/lb		→	→
Miscellaneous Equipment Weight	K_{me}	48	0.5	→	→	→
Total Balloon Weight	K_{tb}	54	1.193	→	→	→
Suspension Line Weight	K_{sus}	55	0.0007	→	→	→
Handling Line and Catenary	K_{hl}	56	0.336	→	→	→
Tail Attachment Weight	K_a	33&36	0.330	0.330	0.330	0.330
Misc. Fabric Parts Weight	K_{mf}	39a	0.050	0.050	0.050	0.050
Air Valve Weight	K_{av}	53	0.01445	0.01445	0.01445	0.01445

Weight of Hull Seams (lb)

$$W_{hs} = K_s W_{hf} \tag{29}$$

Intersect Weight (lb)

$$W_{int} = w\, A_{int} \tag{30}$$

Weight of Intersect Attachments (lb)

$$W_{int\ a} = W_{int} \tag{31}$$

Weight of One Horizontal Tail (lb)

$$W_{ht} = w_{t_h} A_{wht} \tag{32}$$

Weight of Attachments of One Horizontal Tail (lb)

$$W_{hta} = K_a W_{ht} \tag{33}$$

Weight of Interior Partitions of One Horizontal Tail (lb)

$$W_{iha} = w_p A_{pht} \tag{34}$$

Weight of One Vertical Tail (lb)

$$W_{vt} = w_{t_v} A_{wvt} \tag{35}$$

Weight of Attachments of One Vertical Tail (lb)

$$W_{vta} = K_a W_{vt} \tag{36}$$

Weight of Interior Partitions of One Vertical Tail (lb)

$$W_{iva} = w_p A_{pvt} \tag{37}$$

Weight of Ballonet (lb)

$$W_{bnt} = w_b A_{bnt} \tag{38}$$

Weight of Ballonet Seams and Attachment (lb)

$$W_{bnt,s} = K_s W_{bnt} \tag{39}$$

Weight of Miscellaneous Fabric Parts

$$W_{mf} = K_{mf} (W_{hf} + W_{hs}) \tag{39a}$$

c. Blower, Battery, and Exit Valve Analysis

(1) Volume and Volume Flow Rate of Air through an Exit Valve or Blower. The volume of air to be expelled through an exit valve of a balloon during ascent or to be filled by a blower during descent may be determined by the expressions given below. It is assumed that the total volume of the balloon remains constant and that the weight of a given mass of air is constant throughout the elevations considered.

The weight of a certain volume (V) of air at an altitude (h) is given by

$$W_h = \gamma_h V_h \text{ lb}$$

where γ_h is the weight density (lb/ft^3) of air at float altitude h. Also, at altitude h - dh,

$$W_{h-dh} = (\gamma_h + d\gamma) V_{h-dh},$$

but

$$W_h = W_{h-dh}.$$

Therefore,

$$\gamma_h V_h = (\gamma_h + d\gamma) V_{h-dh}$$

or

$$V_{h-dh} = \left(\frac{\gamma_h}{\gamma_h + d\gamma} \right) V_h .$$

Let Qt be the volume filled during the change in altitude from h to h-dh. Therefore,

$$\begin{aligned} d(Qt) &= V_h - V_{h-dh} \\ &= V_h \left(1 - \frac{\gamma_h}{\gamma_h + d\gamma} \right) \\ &= V_h \frac{d\gamma}{\gamma_h + d\gamma} \end{aligned}$$

Neglecting second-order effects,

$$d(Qt) = V_h \frac{d\gamma}{\gamma_h} .$$

However, V_h = constant = V_{tot}.

Therefore,

$$Qt = V_{tot} \int_{h}^{0} \frac{d\gamma}{\gamma_h}$$

$$Qt = V_{tot} \ln \frac{\gamma_0}{\gamma_h} ft^3 \tag{40}$$

where

Qt is volume filled by blower (ft^3)

V_{tot} is total volume of balloon (ft^3)

γ_0 is weight density of air at sea level launch altitude (lb/ft^3)

γ_h is weight density of air at float altitude (lb/ft^3).

To determine the volume flow rate (Q) through the exit valve or blower, an ascent and descent rate of 400 ft/min was assumed.

$$Q = Qt \left(\frac{400}{h}\right) ft^3/min \tag{41}$$

or

2000 ft^3/min, whichever is greater. (h is again the float altitude of the balloon.)

(2) Blower and Check Valve Weight. An empirical relation based on information listed in a blower catalog (Reference 21) is given in Figure 47. The plot contains blower weight versus differential pressure for blowers rated at 4000 ft^3/min. Blowers used in this plot include rated flow rates from 500 to 4000 ft^3/min, which were modified to an equivalent rate of 4000 ft^3/min by use of the following relation:

$$W_{blo} = W_{actual} \left(\frac{4000}{Q_{rated}}\right)$$

where

W_{blo} is blower weight equivalent (lb)

W_{actual} is blower weight listed in catalog (lb)

Q_{rated} is flow rate of blower, as listed in catalog (ft^3/min).

Ratings for these blowers are for standard atmospheric conditions. The resulting expression based on Figure 47 is

$$W_{blo} = \frac{Q}{4000} (7.5\ P_{io} + 17.8)\ lb$$

where

P_{i0} is the differential pressure at sea level in in. H_2O.

Use of this blower at higher altitudes will result in differential pressures that vary with the density of the air being blown. That is,

$$P_i = \frac{\rho_{alt}}{\rho_0} P_{io} \frac{1}{0.1922}\ lb/ft^2 \tag{42}$$

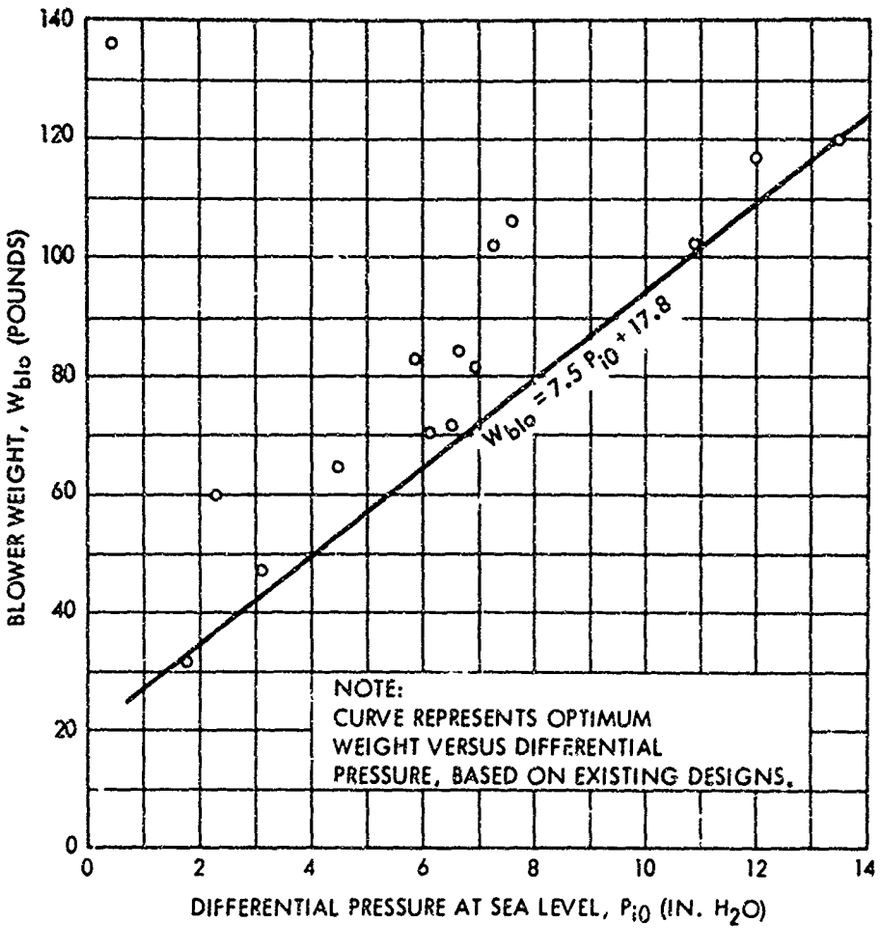

Figure 47. Blower Weight versus Differential Pressure for Volume Flow Rate of 4000 Ft^3 Min

where

P_i is differential pressure at altitude

$\frac{\rho_{alt}}{\rho_0}$ is ratio of air density at altitude to sea level.

Thus,

$$W_{blo} = \frac{Q}{4000}\left(1.442\ \frac{\rho_0}{\rho_{alt}}\ P_i + 17.8\right) \text{lb} \tag{43}$$

where Q is the desired flow rate of the blower (ft^3 /min).

The check valve is mounted on the blower, and therefore its weight was assumed to be proportional to the blower weight. Previous experience has shown that this constant of proportionality is approximately 1/2. Therefore, the weight of the check valve is

$$W_{chk} = \frac{1}{2}\ W_{blo} \text{ lb.} \tag{44}$$

(3) Battery Weight. Battery power is required to operate the blower at altitude to account for daily temperature changes and leakage losses and to operate the blower during descent to maintain a full ballonet. The typical equation for battery weight is

$$W_{bat} = \frac{Pt_{oper}}{K_{bat}}$$

where

W_{bat} is the battery weight (lb)

P is the power required (watts)

t_{oper} is the operating time of the blower (minutes)

K_{bat} is the power density of the battery (watt min/lb).

By plotting battery power versus sea level differential pressure for equivalent 4000 ft^3 min blower capacity, an empirical relation for power required to operate the blowers can be determined to be

$$P = 1000\ P_{lo} \text{ watts}$$

where P_{lo}, as previously defined, is the differential pressure at sea level in in. H_2O (see Figure 48).

Battery weight required at altitude is that required to operate the blower at an equivalent sea level pressure of

$$P_i = \frac{\rho_{alt}}{\rho_0} P_{lo} \frac{1}{0.1922},$$

as defined in Equation 42. Thus, the power required is

$$P' = 1000\ (0.1922)\ \frac{\rho_0}{\rho_{alt}} P_i \text{ lb ft}^2.$$

However, this power would operate the blower at sea level, whereas the power required at altitude varies directly with the density of the air being blown. Thus, the actual power required for the battery is

$$P = \frac{\rho_{alt}}{\rho_0} P'$$

$$P = \frac{\rho_{alt}}{\rho_0} (1000)\ (0.1922) \frac{\rho_0}{\rho_{alt}} P_i$$

$$= 192.2\ P_i \text{ watts.}$$

The battery weight was analyzed as that required while at float altitude and that required during descent. Therefore,

$$W_{bat} = W_{bat,a} + W_{bat,d} \text{ (lb)}$$

where

$W_{bat,a}$ is amount of batteries required at altitude (lb)

$W_{bat,d}$ is amount of batteries required during descent (lb).

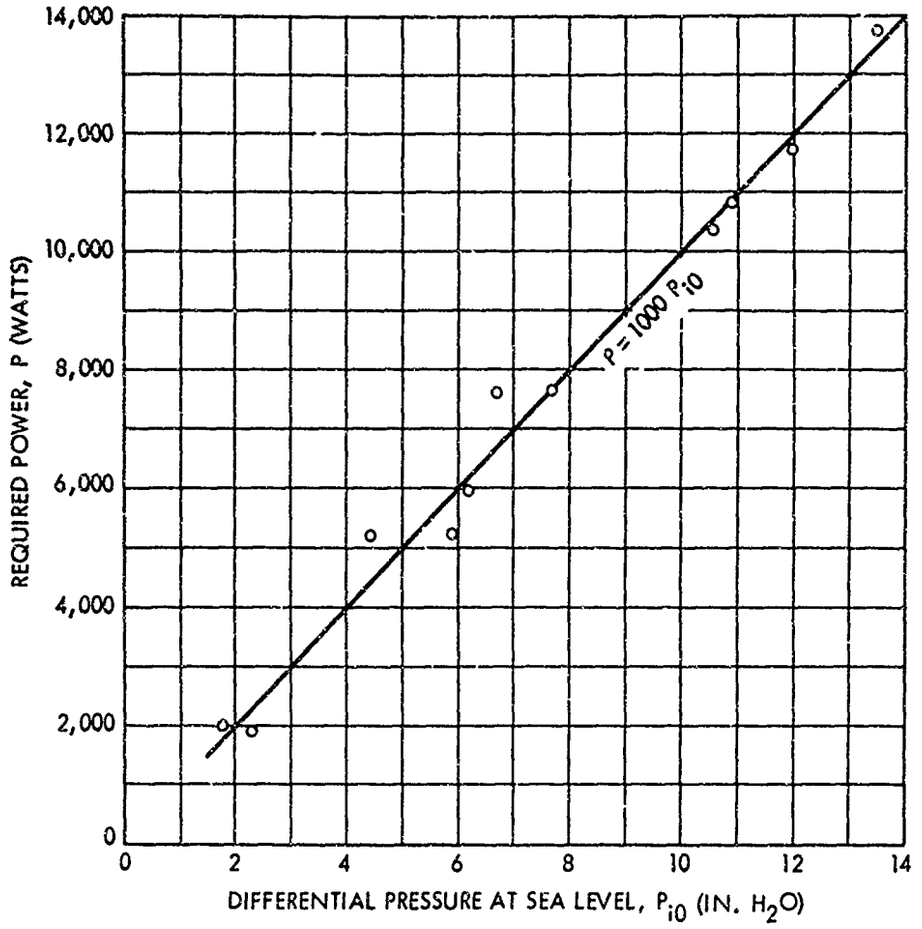

Figure 48. Required Blower Power versus Differential Pressure for Volume Flow Rate of 4000 Ft^3/Min

The equivalent time of operation of the blower at altitude is equal to the volume of air to be replaced each day (V_{repl}) divided by the 4000 ft^3/min blower rate and multiplied by the number of days at float altitude (t/24). Thus, the battery weight required at altitude is

$$W_{bat,a} = \frac{192.2 P_i \ (V_{repl}) \ (t/24)}{K_{bat} \ (4000)} \text{ pounds.} \tag{45}$$

Note that V_{repl} is modified in the computer program to provide a factor of safety of 2.

The work done on the gas during descent is equivalent to the work done on the gas if entirely filled at sea level. It will be assumed that the differential pressure to be maintained in the balloon at all times is P_i, the pressure that was required at altitude. This assumption neglects the fact that dynamic pressure at lower altitudes will probably be greater than that designed at altitude.

However, the fabric in the balloon is also designed for conditions at altitude while neglecting conditions below so that the assumptions are consistent. Thus,

$$P_{i0} = P_i \ (0.1922) \ lb/ft^2,$$

which is identical with Equation 40 when

$$\rho_{alt} = \rho_0.$$

The operating time of the blower during descent is that time required for a 4000 ft^3/min blower to fill the ballonet, or ($\forall_{bnt}/4000$).

Therefore, with a safety factor of 2,

$$W_{bat,d} = (2)\frac{192.2P_i \frac{\forall_{bnt}}{4000}}{K_{bat}}$$

$$= (2)\frac{192.2P_i \forall_{bnt}}{K_{bat}(4000)} \text{ lb.} \tag{46}$$

The total battery weight is

$$W_{bat} = W_{bat,a} + W_{bat,d}$$

$$W_{bat} = \frac{192.2P_i}{K_{bat}(4000)}\left[\forall_{repl}\left(\frac{t}{24}\right) + 2\forall_{bnt}\right] \text{lb} \tag{47}$$

where

P_i is differential pressure at altitude (lb/ft^2)

$\forall_{repl}$ is volume of air that blower has to replace at altitude (ft^3/day)

t is float time at altitude (hr)

$\forall_{bnt}$ is balloon ballonet volume (ft^3).

The weight of the miscellaneous equipment for the blower and battery is

$$W_{me} = K_{me} W_{bat}, \tag{48}$$

which was included to cover the weight of the battery heater, wiring, etc. See Table XVI for the values of K_{bat} and K_{me}.

(4) Weight of Exit Valve. The volume rate of flow through an orifice is given in any fluid mechanics book (e.g., Reference 22) as

$$Q = CA\sqrt{2gZ}$$

where

Q is volume rate of flow through orifice (ft^3/min)

C is discharge coefficient

A is exit area of orifice (ft^2)

Z is pressure head on the fluid at the orifice (ft).

The pressure head (Z) may be written as

$$Z = \frac{p}{\gamma}$$

where

p is pressure head (lb/ft^2)

γ is weight density of the fluid (lb/ft^3).

Therefore,

$$Q = CA\sqrt{2g\frac{p}{\gamma}}$$
$$Q = CA\sqrt{2\frac{p}{\rho}}. \tag{49}$$

For purposes of scaling the weight of the valve, assume that the weight is proportional to its exit area. That is,

$$\frac{W_1}{W_2} = \frac{A_1}{A_2} . \tag{50}$$

Solving Equation 49 for A_1, and adding the subscripts 1, we have

$$A_1 = \frac{1}{C}\frac{Q_1}{\sqrt{2\frac{p_1}{\rho_1}}} \tag{51}$$

However, the value of the discharge coefficient may be obtained using data from an existing valve, since C is a constant for a particular orifice type. Thus,

$$C = \frac{Q_2}{A_2\sqrt{\frac{2p_2}{\rho_2}}} \tag{52}$$

Substituting Equations 51 and 52 into Equation 50,

$$\frac{W_1}{W_2} = \frac{A_2\sqrt{\frac{2p_2}{\rho_2}}}{Q_2}\ \frac{Q_1}{A_2\sqrt{\frac{2p_1}{\rho_1}}}$$

or

$$W_1 = W_2\sqrt{\frac{p_2}{\rho_2}}\sqrt{\frac{\rho_1}{p_1}}\ \frac{Q_1}{Q_2} .$$

Values for a typical exit valve are as follows:

Size = 28 inch in diameter

A_2 = 4.24 ft^2

Q_2 = 8500 ft^3/min

p_2 = 3 in. H_2O = 15.62 lb/ft^2

W_2 = 31.0 lb (aluminum)

ρ_2 = ρ_0 at sea level

$$W_1 = (31.0)\sqrt{\frac{15.62}{\rho_0}}\sqrt{\frac{\rho_1}{p_1}}\ \frac{Q_1}{8500}$$

$$W_1 = 0.01445\sqrt{\frac{\rho_1}{\rho_0}}\ \frac{Q_1}{\sqrt{p_1}}\ .$$

To compute the weight of a valve required at float altitude, note the following changes in notation:

$\rho_1 = \rho_{alt}$

$p_1 = p_i$.

Therefore,

$$W_{aval} = W_1 = K_{av}\sqrt{\frac{\rho_{alt}}{\rho_0}}\ \frac{Q_1}{\sqrt{p_i}}\ . \tag{53}$$

(5) Suspension (bridle) System Weight. The weight of the suspension system is proportional to the length of the balloon and the tether tension in the bridle.

$W_{sus} \propto LT$,

or from Equation 4,

$W_{sus} \propto V^{1/3} T$.

However, to obtain the tether tension, the weight of the balloon (which we are trying to estimate) has to be known. Therefore, an initial estimate of the total weight is made by summing the already estimated parts of the balloon, which include everything except the suspension system, handling line, and catenary weights, and multiplying by an appropriate factor.

The initial estimate of the tether tension is

$$T_{lb} = \left\{\left[L_a + L_b - P - (K_{tb})\, W_{i(tot)}\right]^2 + D_b^2\right\}^{1/2} \tag{54}$$

where

L_a, aerodynamic lift, = $C_L q V^{2/3}$ (lb)

L_b, buoyant lift, = $0.862 g V_{tot}\ \rho_{alt}$ (lb) (helium 97% purity)(lb)

P is payload package weight (lb)

K_{tb} is the factor to obtain total balloon weight

$W_{i(tot)}$ is the initial estimate of weight, which includes all weight except the suspension, handling line, and catenary weight (lb)

D_b, aerodynamic drag on balloon, = $C_D q V^{2/3}$ (lb).

Therefore, the weight of the suspension system is

$$W_{sus} = K_{sus}\, T_{lb}\, (\forall_{tot})^{1/3} \text{ lb.} \tag{55}$$

The weight of the handling line and catenary is

$$W_{hl} = K_{hl} W_{sus} \text{ lb.} \tag{56}$$

See Table XVI for the values of K_{tb}, K_{sus} and K_{hl}.

(6) Total Balloon Weight. The total balloon weight can be obtained for a particular balloon type (Vee-Balloon, BJ, #1649) from the previous equations by inputing the following information:

Payload weight, P (lb)

Float altitude, h (ft)

Wind velocity, v (knots)

Angle of attack, α (degrees)

Hull volume, $\forall$ (ft^3)

Operating Time at altitude, t (hr)

The total balloon weight is equal to the following:

$$\begin{aligned} W_{tot} = {} & W_{hf} + W_{hs} + W_{int} + W_{int\,a} \\ & n_{ht}(W_{ht} + W_{hta} + W_{iha}) + n_{vt}(W_{vt} \\ & + W_{vta} + W_{iva}) + W_{blo} + W_{bat} \\ & + W_{aval} + W_{chk} + W_{bnt} + W_{bnt,s} \\ & + W_{me} + W_{sus} + W_{hl} \text{ (pounds)} + W_{mf} \end{aligned} \tag{57}$$

REFERENCES

1. Design Data and Reports, letter LCB (Major Young/3030/S 30) to J. Vorachek, Goodyear Aerospace Corporation, 29 December 1970.

2. Logging Vee-Balloon Model Wind Tunnel Test, GER-13432, Goodyear Aerospace Corporation, August 1967.

3. Wind Tunnel Test of a 35° Vee-Balloon for Directional Stability, T-6898, Goodyear Aerospace Corporation, internal memorandum, September 27, 1966.

4. Reevaluation of Wind Tunnel Data for the TVLF Vee- Balloon Model ARD 11,265, Goodyear Aerospace Corporation internal memorandum, 15 January 1968.

5. Wind Tunnel Test of a Single Hull Balloon Model, GER-12972, Goodyear Aerospace Corporation, December 1967.

6. Forces and Moments on Kite Balloon Models Fitted with Various Types of Fins, T 3295, Aeronautical Research Committee, H. Bateman and L. Jones, 9 August 1932.

7. Ballonet Kite Balloons Design, Construction, and Operation, M.E. 24, Royal Aircraft Establishment, I.S.H. Brown and L. A. Speed, July 1962.

8. Low Speed Wind Tunnel Tests on a Kite Balloon Model, C.P. No. 643, Ministry of Aviation Aeronautical Research Council, M. H. Simonds, 1963 (Replaces R.A.E. Tech. Note No. Aero. 2799-A.R.C. 23,692.)

9. Data for 100,000 Cubic Feet British Balloon, letter LCB (Major Young/ 3030/S30) to J. Vorachek, Goodyear Aerospace Corporation, 21 January 1971.

10. Operation and Maintenance Instructions for Mobile LTA Vehicle (TVLF) Model GZ 349, GER-12586, Goodyear Aerospace Corporation, 31 January 1966.

11. Lamb, Sir Horace: Hydrodynamics, 6th Edition, The University Press, Cambridge, England, 1932.

12. Munk, Max: Fundamentals of Fluid Dynamics for Aircraft Designers, Ronald Press Company, New York 1929

13. Perkins, Courtland D and Hage, Robert E: Airplane Performance, Stability, and Control. Wiley, New York, 1949

14. Hoerner, Sighard F. Fluid-Dynamic Drag published by the Author, 1958.

16. Glauert, H.: The Form of a Heavy Flexible Cable Used for Towing a Heavy Body Below An Aeroplane. Reports and Memoranda 1952. British Advisory Committee for Aeronautics, February 1934.

17. Landweber, L., and Protter, M.: "The Shape and Tension of a Light Flexible Cable in a Uniform Current. Journal of Applied Mechanics. June 1947, pp. A-121 to A-126.

18. Ringleb, F.O.: "Motion and Stress of an Elastic Cable due to Impact." Journal of Applied Mechanics. March 1957, pp. 417-425.

19. Walton, T.S., and Polacheck, H.: Calculation of Nonlinear Transient Motion of Cables. David Taylor Model Basin Report 1279, 1959. A condensed paper is given in Mathematics of Computation (The Siam Review) No. 69-72, 1960, pp. 27-46.

20. Wind Tunnel Tests of the General Mills Aerocap Model, Part 1. University of Detroit, Project 314, March 1960.

21. Aircraft and Electronic Fan Catalog (Revised). Joy Manufacturing Company.

22. Mark's Mechanical Engineers' Handbook. 6th Edition. 1958, p. 3-62.